MULTIUSER DETECTION EMPLOYING RECURRENT NEURAL NETWORKS FOR DS-CDMA SYSTEMS

Navern Moodley

April 2006

Submitted in fulfilment of the academic requirements for the degree of MScEng
in the School of Electrical, Electronic and Computer Engineering,
University of KwaZulu-Natal, Durban, South Africa.

Abstract

Over the last decade, access to personal wireless communication networks has evolved to a point of necessity. Attached to the phenomenal growth of the telecommunications industry in recent times is an escalating demand for higher data rates and efficient spectrum utilization. This demand is fuelling the advancement of third generation (3G), as well as future, wireless networks. Current 3G technologies are adding a dimension of mobility to services that have become an integral part of modern everyday life.

Wideband code division multiple access (WCDMA) is the standardized multiple access scheme for 3G Universal Mobile Telecommunication System (UMTS). As an air interface solution, CDMA has received considerable interest over the past two decades and a great deal of current research is concerned with improving the application of CDMA in 3G systems. A factoring component of CDMA is multiuser detection (MUD), which is aimed at enhancing system capacity and performance, by optimally demodulating multiple interfering signals that overlap in time and frequency. This is a major research problem in multipoint-to-point communications. Due to the complexity associated with optimal maximum likelihood detection, many different sub-optimal solutions have been proposed.

This focus of this dissertation is the application of neural networks for MUD, in a direct sequence CDMA (DS-CDMA) system. Specifically, it explores how the Hopfield recurrent neural network (RNN) can be employed to give yet another sub-optimal solution to the optimization problem of MUD. There is great scope for neural networks in fields encompassing communications. This is primarily attributed to their non-linearity, adaptivity and key function as data classifiers. In the context of optimum multiuser detection, neural networks have been successfully employed to solve similar combinatorial optimization problems.

The concepts of CDMA and MUD are discussed. The use of a vector-valued transmission model for DS-CDMA is illustrated, and common linear sub-optimal MUD schemes, as well as the maximum likelihood criterion, are reviewed. The performance of these sub-optimal MUD schemes is demonstrated. The Hopfield neural network (HNN) for combinatorial optimization is discussed. Basic concepts and techniques related to the field of statistical mechanics are introduced and it is shown how they may be employed to analyze neural classification. Stochastic techniques are considered in the context of improving the performance of the HNN.

A neural-based receiver, which employs a stochastic HNN and a simulated annealing technique, is proposed. Its performance is analyzed in a communication channel that is affected by additive white Gaussian noise (AWGN) by way of simulation. The performance of the proposed scheme is compared to that of the single-user matched filter, linear decorrelating and minimum mean-square error detectors, as well as the classical HNN and the stochastic Hopfield network (SHN) detectors. Concluding, the feasibility of neural networks (in this case the HNN) for MUD in a DS-CDMA system is explored by quantifying the relative performance of the proposed model using simulation results and in view of implementation issues.

Preface

The research work presented in this dissertation was performed by Navern Moodley, under the supervision of Professor S. H. Mneney, in the Centre of Radio Access Technologies situated in the School of Electrical, Electronic and Computer Engineering at the University of KwaZulu-Natal, Howard College Campus.

Parts of this dissertation have been presented at and published in the conference journals of the SATNAC 2004 (Stellenbosch, SA), AFRICON 2004 (Gaborone, Botswana) and ICT 2005 (Cape Town, SA) conferences. Some of the work has also been accepted for publication in the transactions of the SAIEE.

This dissertation is completely the own work of the author and has not otherwise been submitted in any form, for any other degree or diploma, to any other tertiary institution. Where use has been made of the published or unpublished work of others it is duly acknowledged in the text.

Acknowledgements

I would like to express my sincerest gratitude to my supervisor, Professor S.H. Mneney, for his guidance, time and effort throughout my studies. Thank you for being so accommodating, for having confidence in me, and for always taking time to sit down and problem solve, no matter how big or small my concern was. I acknowledge Telkom S.A. LTD. and Alcatel S.A. for their financial assistance and for providing the equipment necessary for the completion of this research.

To my family, thank you for putting up with the mood swings of a sometimes frustrated student, for your relentless encouragement and for the thoughtful, yet sometimes tiresome, questions. It certainly spurred me on. I am, undoubtedly, most indebted to my mother and father for giving me the opportunity to learn and for supporting me during my studies; and to my grandmother, for always being there.

To my friends, your advice, in both work and life, was invaluable. I will miss our talks about all things concerned. Indeed, it helped relieve the stresses of work. I am grateful to have met and studied in the company of such diverse, intelligent minds. I also extend my appreciation to the pleasant secretarial staff in the School of Electrical, Electronic and Computer Engineering, for kindly assisting me with both postgraduate and work-related issues, always without hesitation.

This dissertation has been printed with the consoling thought that it has been proof read and formatted to a fairly acceptable degree. For that, I thank my friends and family, in particular, Kumaran, for all his editing skills and insight, Jayesh, for his invaluable assistance, as well as Prebantha, Catherine and especially Karusha, all of whom kindly helped to proof-read various parts of this work.

It has been a memorable and rewarding experience. For that and more, I thank God.

Contents

List of Acronyms

2G	Second Generation Systems
3G	Third Generation Systems
AF	Activation Function
AMPS	Advanced Mobile Phone System
AWGN	Additive White Gaussian Noise
BER	Bit Error Rate
BP	Back Propagation
BPSK	Binary Phase Shift Keying
CAM	Content Addressable Memory
CDMA	Code Division Multiple Access
COP	Combinatorial Optimization Problem
DECT	Digital Enhanced Cordless Telecommunications
DS	Direct Sequence
DS-CDMA	Direct Sequence CDMA
DS-SS	Direct Sequence Spread Spectrum
EDGE	Enhanced Data Rates for GSM Evolution
ETSI	European Telecommunications Standard Institute
FDD	Frequency Division Duplexing
FDMA	Frequency Division Multiple Access
FH	Frequency Hopping
FH-CDMA	Frequency Hopping CDMA

FH-SS	Frequency Hopping Spread Spectrum
GPRS	General Packet Radio Service
GSM	Global System for Mobile Communications
HNN	Hopfield Neural Network
IC	Interference Cancellation
IMT-2000	International Mobile Telecommunications 2000
ISI	Inter-symbol Interference
ITU	International Telecommunications Union
LDD	Linear Decorrelating Detector
LPI	Low Probability of Intercept
MAI	Multiple Access Interference
MC-CDMA	Multi-carrier CDMA
MLP	Multi-layer Perceptron
MLS	Maximum Likelihood Sequence
MLSE	MLS Estimation
MSE	Mean-square Error
MMSE	Minimum Mean-square Error
MSD	Multi-stage Detector
MUD	Multiuser Detection
NN	Neural Network
NP	Non-deterministic Polynomial
OCDMA	Orthogonal CDMA
OFDM	Orthogonal Frequency Division Multiplexing
OMD	Optimum Multiuser Detector

PHN	Probabilistic Hopfield Network
PHN-SA	Probabilistic Hopfield Network with Simulated Annealing
PIC	Parallel IC
PN	Pseudonoise
PSK	Phase Shift Keying
RBF	Radial Basis Functions
RNN	Recurrent Neural Network
SHN	Stochastic Hopfield Network
SA	Simulated Annealing
SIC	Serial IC
SNR	Signal-to-Noise Ratio
SS	Spread Spectrum
SSA	Stochastic SA
SUMF	Single-User Matched Filter
TDD	Time Division Duplexing
TDMA	Time Division Multiple Access
TD-SCDMA	Time Division Synchronous CDMA
TSP	Travelling Salesman Problem
UMTS	Universal Mobile Telecommunications System
UTRA	UMTS Terrestrial Radio Access
UWC	Universal Wireless Communications
WCDMA	Wideband CDMA
WLAN	Wireless Local Area Network

List of Notations and Mathematical Symbols

Common Notations

$(\cdot)^*$	Complex conjugate
$(\cdot)^T$	Transpose
Bold capital	Matrix
Bold lower case	Column vector
Capital superscript	Refers to the model under discussion, unless otherwise stated

Mathematical Symbols

α_{kl}	Attenuation of the *k*th signal due to *l*th path
β_k	Leakage coefficient
$\delta(t)$	Delta function
ε	Error vector (between transmitted and estimated symbols)
$\phi_k(t)$	Convolution of the *k*th user's impulse response and spreading waveform
$\mathbf{\Phi}(t) = \{\Phi_{ij}\}$	Continuous correlation matrix of dyadic convolutions between $\phi_i(t)$ and $\phi_j(t)$
η	Load parameter in the HNN
η_c	Critical point of loading in the HNN
$\lambda(k)$	Annealing/Cooling function
$\hat{\lambda}$	SHN cooling factor

$\Lambda(k)$	SHN annealing/cooling function
$\mathbf{\Pi}[i]$	*i*th normalized discrete-time correlation matrix
θ_k	Delay associated with the *k*th user
ρ_{jk}	Synchronous cross-correlation between the *j*th and *k*th user
σ^2	Variance of AWGN with single sided power spectral density
τ_{kl}	Delay of the *k*th user due to the *l*th path
$\upsilon(k)$	Internal random noise variable in the SHN
ω	Weight vector in the OMD
$\Omega(\cdot)$	OMD objective function
$\xi_{u,i}$	*i*th bit of the *u*th fundamental pattern/memory
A_k	Amplitude of the *k*th user's signal
$\mathbf{A}$	Diagonal matrix of all user amplitudes
$b_k(t)$	Binary baseband information signal of the *k*th user
$\mathbf{b}[i]$	$K \times 1$ Column vector of the *i*th transmitted symbol of all users
$\hat{b}_k$	Estimated symbol of the *k*th user
$\mathbf{b}$	$KM \times 1$ Column vector of transmitted symbols of all users
$\hat{\mathbf{b}}$	$KM \times 1$ Column vector of estimated symbols of all users
B	Bandwidth of information signal
B_S	Bandwidth of spread signal
c_k	Discrete spreading sequence of the *k*th user
C_{eq}	Criterion for reaching (possible) equilibrium

$e(t)$	Chip pulse-shaping waveform function
erf	Error function
E	Hopfield energy function
f_i	External bias associated with the *i*th neuron
$F(\cdot)$	Neuron activation function
$h_k(t)$	Channel impulse response of the *k*th user
H	Un-normalized correlation matrix
$\mathbf{I}_{k\times k}$	Identity matrix of dimension $k\times k$
k_B	Boltzmann constant
K	Number of users in DS-CDMA system
L_p	Number of paths associated with a multipath fading channel
L	Number of layers in a neural network
m	Length of a linear feedback shift register
M	Symbol packet size per user per frame
$\mathbf{M}$	Linear transformation
$\hat{M}$	Total number of neurons in the network
$n(t)$	AWGN random variable
$\tilde{\mathbf{n}}[i]$	Discrete filtered AWGN vector of the *i*th symbol of all users
$\tilde{\mathbf{n}}(t)$	Vector of filtered AWGN from all K matched filters
N	Length of spreading sequence (Processing gain)
$P_{e,k}$	Probability of error for the *k*th user
$q_k(t)$	Transmitted DS-CDMA signal of the *k*th user

Q	Q-Function
$r(t)$	Received signal at the input to the DS-CDMA receiver
$\mathbf{R}$	Packet channel cross-correlation matrix
R_c	Chip Rate
$s_k(t)$	Spreading waveform of the kth user
T_b (or T)	Symbol (bit) duration
T_c	Chip duration
$T_{p,k}$	Pseudo-temperature at the kth iteration ($k = 0 \Rightarrow$ initial value)
U	Number of fundamental patterns in the HNN
v_i	Effective input to the ith neuron
w_{nm}	Weight between output of neuron m and input of neuron n
$\mathbf{W}$	Hopfield weight matrix
x_i	State *of* ith neuron (or input from neuron i)
$y_k(t)$	Output of the kth user's matched filter
$\mathbf{y}[i]$	$K \times 1$ Column vector of the ith estimated bit of all users
$\mathbf{y} = \{\mathbf{y}[i]\}$	$KM \times 1$ Column vector of all estimated bits of all users
y_i^N	Final output of ith neuron

List of Figures

1 Introduction

The field of wireless communications is emerging as one of the fastest growing industries in the world. This phenomenon is demonstrated by the statistics of mobile consumer subscription and usage, in recent times. Economic and political implications aside, it is evident that the rapid growth in wireless subscribers is greatly helping to fuel the research and development of enhanced wireless services.

Since its inception, wireless communications has clearly evolved to a point of necessity, where many more people have come to rely on some basic wireless service in their day-to-day work or personal life. Telecommunications, in general, is becoming a pivotal part of the societal infrastructure. A clear example of this may be found in the South African mobile telecommunication industry, which boasts almost 23 million subscribers (2005) since 1994. In Africa the average annual subscriber growth was estimated around 60 percent, which was twice the global average [1]. Worldwide, mobile telephony is dominated by the second generation (2G) GSM standard. It accounts for 1.6 billion subscribers and is growing, with a recorded 28 percent increase in subscribers over the last year [2]. Currently, the technology of public interest and the focus of activity of the wireless research community is the third generation (3G) of mobile networks. Collective statistics (for 2G and 3G) revealed that approximately 285 million of the total mobile phone usage constituted CDMA-based network subscriptions, increasing by 26 percent, in 2005 [3]. On its own, the 3G standard (3GSM) has grown by a staggering 226 percent over 2005 [2].

The full picture indicates that, with a world population of about 6.5 billion, at least 1 in 5 people communicate wirelessly, which is up from 1 in every 12, three years ago [4]. The explosive growth of GSM and the telecommunications industry in general, has intensified the demand for higher data rates, accessibility to flexible multimedia services and convenience of use. These demands are explicit and expected. It is easy to see that this is the general direction for progression of cellular networks, as history has shown; these requirements outline basic evolutionary steps, in this case, from an era dominated by 2G networks towards a new age of 3G networks and beyond.

The objective of fully commercialized 3G systems is to achieve these demands. In the process it is laying the foundation for future generation networks, to which the term 4G now refers to. The 3G statistics are a global reflection of places like Japan and USA, where 3G networks have been in operation for over two years. Research is well into 4G systems and it is predicted that future mobile and wireless applications will require significantly higher speeds and lower costs.

In South Africa, mobile users are still accustoming themselves to concepts such as video conferencing and broadband internet access, due to the fact that 3G services have only recently been introduced by the respective service providers. Nevertheless, the popularity of combined wireless internet, high data rate services and mobile telephony is on the rise and soon we will completely evolve to a stage where "wireless" will exceed "wired" services. Since 2002, the number of mobile subscribers has exceeded fixed-line subscribers, worldwide [4]. This has significantly impacted on public access to basic telecommunication services and to information and communication technologies (ICT); it is now seen as a tool for creating opportunities for social and economic development. From a business point of view, the development of new technology applicable to telecommunications, particularly mobile telephony, creates opportunities for developing existing services further and for introducing completely new ones. This benefits customers and network operators. This is the task of current 3G and future 4G systems.

1.1 3G and Beyond

In simple terms, 3G services combine high speed mobile access with internet protocol (IP)-based services. The list of official targets for 3G systems is long and diverse. These targets are collectively aimed at enhancing and extending mobility through a simple concept of "anywhere, anytime" access. In addition to voice and data, 3G offers high-speed access to the internet, entertainment, information and e-commerce services, all at a supposed convenience. Hence, mobile devices like cellular phones, multimedia devices, personal digital assistants and laptop computers are targeted for 3G services. 3G allows for an always-online connection, and the costs incurred depend on the amount of information transferred and not the length of time of the connection. It is an agreement among industry that 3G systems must be affordable to encourage interest by operators and consumers, world over. Other targets include spectrum efficiency, seamless roaming and a global standard with a high degree of commonality [5]. Beyond spectrum usage, mobility and interoperability, the flexible introduction of new services and applications is a key target for these networks, so as to attract new users and satisfy existing ones.

The standardization for 3G radio networks is overseen by the International Telecommunication Union (ITU). The ITU is located within the United Nations and is responsible for the coordination and planning of global telecommunication services, including standardization and spectrum regulation. Together with industry bodies from around the world, ITU defines and approves technical requirements, standards and frequency allocation for 3G systems under the IMT-2000 (International Telecommunication Union-2000) program. It is also concerned with tariffs and billing, technical assistance and studies on regulatory and policy aspects.

IMT-2000 allows for the provision of value-added services (e.g. entertainment, information and location-based services) and applications on the basis of a global standard for 3G wireless communications, as defined by a set of inter-dependent ITU recommendations. It provides the platform for distributing converged fixed and mobile services for voice, data, internet and multimedia. The IMT-2000 standard accommodates five radio interfaces as part of the ITU-R (Radiocommunications) recommendation, which is responsible for the frequency spectrum and system aspects of IMT-2000. These interfaces are based on three different access technologies, namely frequency division, time division and code division multiple access (i.e. FDMA, TDMA and CDMA, respectively).

There are several reasons why this so-called family of 3G systems is composed of the different radio interfaces that fall under IMT-2000. First, it benefits operators worldwide that employ any one of the various 2G standards and that have to make provision for 3G services using the available infrastructure, at least temporarily. This concept ensures ease of convergence, i.e. the smooth introduction and growth of 3G systems in different locations, by maintaining backward compatibility with existing 2G standards. The different access technologies are based on the proposals of several international standard bodies, namely ETSI (European Telecommunications Standard Institute) in Europe, ARIB (Association of Radio Industry Board) in Japan, TIA (Telecommunications Industry Association) in the USA, and TTA (Telecommunication Technology Industry) in Korea.

Universal Mobile Telecommunications System (UMTS) is the ETSI proposal to answer the IMT-2000 requirements for 3G systems. It is one of several in the family of 3G mobile radio technologies that is identified by the ITU. It is managed by the Third Generation Partnership Project (3GPP) which is also responsible for managing GSM, GPRS and EDGE. UMTS is a successor to GSM. It is also known as 3GSM, emphasizing the combination of the 3G nature of the technology and GSM. In keeping with 3G network specifications, UMTS is an integrated solution for mobile voice and data with wide area coverage and represents an evolution in terms of capacity, data speeds and new service capabilities from 2G mobile networks. This is achieved by employing WCDMA as the air interface standard.

Most of the underlying technological aspects of UMTS are common among all WCDMA variants. WCDMA (as per the definition of IMT-2000) is the air interface. However, it is frequently used to refer to the family of 3G standards that employ WCDMA, in particular UMTS. The ETSI 3G network solution, known as UTRA (UMTS Terrestrial Radio Access), is based on the UMTS standard. It is divided into two WCDMA modes for paired and unpaired frequency bands. The result is UTRA TDD (time division duplex) and UTRA FDD (frequency division duplex).

Today, UMTS is commercially available in 25 countries through 60 network operators [4]. Current work within 3GPP is aimed at increasing speeds of the WCDMA radio access network through standardized high speed downlink packet access (HSDPA) and high speed uplink packet access (HSUPA) technologies. Trials have commenced. In Japan it is predicted that by 2006 the move from 2G to 3G will be completed, allowing for the implementation of the 3.5G (HSDPA) stage to get underway. Even faster (downlink) speeds, as high as 14.4 Mbps, will greatly help to position UMTS as a true "mobile broadband" provider.

The other significant 3G standard is CDMA2000, proposed by TIA. It is derived from the 2G CDMA IS-95 standards, known as cdmaOne. It is employed mainly in the USA and Korea and is managed by 3GPP2, which is separate and independent from 3GPP. CDMA2000 now represents a family of technologies. It shares a common CDMA air interface with UMTS. However, unlike UMTS, which employs direct sequence WCDMA, CDMA2000 is based on multi-carrier CDMA (MC-CDMA). Figure 1.1 provides a summary of the IMT-2000 global standard for 3G services. An overview of multiple access air interface for IMT-2000 can be found in [5]. An overview of WCDMA and its viability for 3G systems is provided in [6].

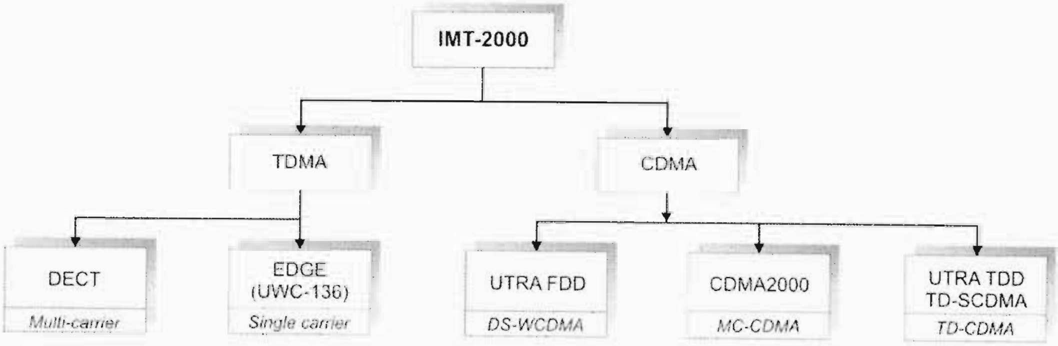

Figure 1.1 Overview of 3G technologies under the ITU IMT-2000 standard, including their respective air interface schemes.

1.2 Problem Formulation

CDMA is the standardized multiple access scheme for UMTS and CDMA2000 systems. Among the different proposed air interfaces, it has attracted a great amount of research. A key area of design of the WCDMA air interface is the receiver. To achieve the capacity requirements of CDMA-based systems, the suppression of multiple access interference (MAI), which is the sum of interference resulting from multiple transmissions in a cell and from neighbouring cells, is required. By reducing MAI, the amount of users that can be supported theoretically increases.

Interference suppression can be achieved through the use of signal processing techniques which attempt to jointly detect multiple users that are transmitting simultaneously in the same noisy channel. This joint detection technique is known as multiuser detection (MUD) and it is an important topic in multiple access communications. In addition to interference suppression and the theoretical capacity increase, MUD increases spectral efficiency and reduces the need for tight and accurate power control that is needed in the conventional matched filter receiver, or the RAKE receiver in the case of a multipath channel.

The conventional receiver for DS-CDMA is interference limited. As the number of users increases, the MAI increases, which lowers the bit error rate (BER) performance of the receiver. Furthermore, the performance degrades when users transmit with different powers; users near the base station are more powerful than those far away and add to the interference that is encountered during the detection of the weaker user. This is known as the near-far effect. It is a severe problem that is usually combated by employing some form of power control. The optimum near-far resistant receiver for MUD, proposed by Verdú [7], is achieved by the minimization of an integer quadratic objective function. However, this is a computationally intensive task, i.e. minimizing the optimal objective function is a combinatorial hard problem. These concepts are revisited in the proceeding chapters, although the point to note is that the optimum detector is far too complex for practical implementation.

Various research studies into sub-optimal detection strategies are aimed at offering a trade-off between practical implementation and performance. Sub-optimal detectors, which exhibit good near-far resistance properties with low computational complexity and BER performance comparable to that of the optimum multiuser detector, have been proposed. Numerous attempts have been based on linear and non-linear detection algorithms. This research explores how neural networks may be employed to give yet another sub-optimal solution to the MUD optimization problem.

Neural networks are not unfamiliar to the communications field. They have been successfully applied to the area of channel equalization in communications as non-linear adaptive filters [8], [9]. There are several characteristics of neural networks that justify their application in multiuser receivers for CDMA communications. Neural networks perform a non-linear form of statistical signal processing. The feedback types, which we are concerned with, are useful for pattern classification and association. In addition, they have been used extensively in optimization problems. Multiuser detection encompasses both these problem fields and it has been demonstrated that feedback-type neural networks are able to efficiently solve the famous Travelling Salesman Problem (TSP) [10], which is a combinatorial optimization problem (COP). Multilayered networks are capable of solving for arbitrary (non-linear) decision boundaries in classification problems [11]; it has been shown that the optimum MUD decision boundary is non-linear.

The various network topologies share the feature of being massively interconnected and capable of parallel distributed processing. This affords the property of robustness, which is desirable for solving a complex task like (optimum) MUD that depends on several parameters, some of which may or may not be known. The very nature of a neural network is adaptive; it has the ability to learn dynamical mappings and track changes in the surrounding environment, which is appropriate for use in a typically time-varying communication channel. There are, as it will be shown, several works that have identified neural-based techniques for MUD, and the results of which substantiate the efficiency of neural networks for such a task.

This thesis investigates the use of a recurrent neural network (RNN), based on the Hopfield model, for sub-optimal MUD in a DS-CDMA system. In particular, the research investigates the feasibility of employing the Hopfield neural network (HNN), and variations thereof, for MUD by comparing it to other popular sub-optimal MUD schemes. Although preventative measures exist, which bypass some of the cost and complexity of using signal processing techniques to cancel out multiuser interference at the receiver, the aim of this research is to provide a neural-based sub-optimal solution and to demonstrate the usefulness of neural networks in such a field. This is best illustrated by assuming that no preventative measures (advanced signal processing techniques or otherwise) have been employed at the transmitter.

The HNN is structured and operates in a manner that makes it applicable to combinatorial optimizations problems (like optimal MUD); its success is evident in the TSP [10]. It is primarily used for pattern association, i.e. it stores patterns and recalls them, individually, when presented with a suitable input pattern. This is like the human memory, e.g. a student learning for a test and then recalling the studied material based on the questions posed to him. In that respect, the HNN is also able to correct errors in the input pattern when it is noisy. It achieves its overall functionality by way of feedback connections in a vastly interconnected structure. Correction of errors in the input pattern is comparable to some sub-optimal MUD schemes that work to suppress multiuser interference present in a received DS-CDMA signal. It is therefore an attractive and appropriate alternative solution to optimal MUD.

The problem of MUD is tackled by firstly presenting a method of mapping a classical HNN to a conventional DS-CDMA receiver. Techniques related to the field of statistical mechanics, which greatly improve the performance of the HNN, are introduced. The underlying process in the HNN is that of optimization, of the Hopfield energy function. The HNN is able to address and reduce the complexity of optimizing the optimal MUD objective function through the optimization of its own Hopfield energy function, which is a much simpler task. This parallel problem of optimization is then addressed using concepts from statistical mechanics. Thus unlike the typical MAI cancellation techniques, the signal processing that occurs within the HNN is directly related to solving the optimal objective function.

1.3 Dissertation Outline

The introductory chapter provides an overview of mobile radio standards and attempts to illustrate the role of DS-CDMA in 2G and 3G networks. It presents the framework on which this research is based and, in formulating the problem of optimal MUD, it motivates the use of neural networks for near-optimal multiuser demodulation in DS-CDMA communications.

Chapter 2 introduces basic multiple access techniques and the standards which incorporate them. The view taken is in terms of the evolution of the mobile communication industry and multiple access techniques, from the first generation networks to the current 3G networks. The chapter proceeds to focus on CDMA. It discusses spread spectrum techniques in general and provides motivation for DS-CDMA. Fundamental concepts and properties of this multiple access technique are reviewed since it is the air interface for the proposed MUD scheme.

Chapter 3 presents the generalized vector-valued transmission model for the uplink of a DS-CDMA system in an AWGN channel. The central topic is multiuser detection and some important concepts and performance criteria, that are used to quantify the quality of sub-optimal solutions, are reviewed. The conventional matched filter receiver is described and the fundamental problems surrounding (optimal) demodulation in multipoint-to-point communications are highlighted. The use of sub-optimal methods, which offer a trade-off between performance and complexity, is discussed. In particular, the linear decorrelating detector (LDD) and the minimum mean-square error (MMSE) detector are reviewed. The chapter concludes with an overview of optimum multiuser detection.

Chapter 4 focuses on the topic of neural networks. The basic neural network (NN) types are discussed briefly and the general NN architecture is viewed in terms of the simple processing unit (neuron). The recurrent-type Hopfield neural network (HNN), which is the basis of the MUD proposal in this research, is investigated. Fundamental properties and functionality (namely, auto-association and optimization) exhibited by the dynamic HNN are provided, in the context of its intended application. Simulation results illustrate the associative properties and the optimization pitfall of the classical HHN. Attention is drawn to the HNN energy function and the inherent process of energy optimization that occurs during pattern retrieval. The network capacity and conditions necessary for stability (in terms of convergence) are also considered.

Chapter 5 describes the method of mapping the classical HNN to the conventional receiver, for developing a Hopfield neural-based MUD scheme. Basic concepts from statistical mechanics are introduced and simulated annealing (SA) for combinatorial optimization is reviewed. Stochastic techniques, that help to combat the problem of localized optimization in the HNN, are discussed. The stochastic Hopfield network (SHN) detector is reviewed. Thereafter, a stochastic HNN, based on SA techniques analogous to statistical mechanics, is proposed for MUD. A SA algorithm is developed in conjunction. The proposed receiver is compared, via simulations, to the sub-optimal linear and neural-based MUD schemes. These simulations are based on the uplink of a DS-CDMA system operating in an AWGN channel. The simulation results are used to quantify the relative performance of the proposed model and the feasibility of employing a HNN (and stochastic SA techniques) to obtain a sub-optimal solution to the MUD (combinatorial) optimization problem is explored.

Chapter 6 concludes the dissertation with a summary of the work that has been presented and some remarks to confirm the objectives of the research. It also discusses concerns and ideas which may be addressed in future work. Appendix A discusses some basic properties of spreading sequences, utilized in the simulation of the DS-CDMA system. In Appendix B, the formula for the Gaussian approximation of the error probability of the conventional receiver is provided. Appendix C discusses the issue of pattern stability and stable points in the HNN. It also provides a sample demonstration of pattern association, using relevant equations. Appendix D describes the Logistic distribution. Appendix E discusses the software and simulation environment. It outlines the basic program structure, parameters and functions.

1.4 Original Contribution

In this study, a sub-optimal MUD scheme based on a recurrent HNN technique is proposed. The HNN has been employed in several previously proposed DS-CDMA receivers, the results of which justifies its use for MUD in DS-CDMA systems, and therefore further research into HNN-based multiuser detectors. One drawback of the HNN is that it suffers from localized optimization. In this research, we investigate the use of a HNN for MUD and develop a new HNN-based detection strategy which utilizes stochasticity to overcome the inherent problem of the classical HNN.

Stochastic search techniques are commonplace in optimization problems, in which globally optimum solutions need to be found. By adding stochasticity to the classical HNN, its performance as a multiuser receiver is greatly improved. There are a handful of methods with which stochasticity may be introduced into the HNN. In this work, we propose using a probabilistic firing mechanism in the neuron model with which to construct the HNN. This serves to introduce randomness in the Hopfield model and thus prevent it from getting stuck in local minima.

This new approach combines simple well-known statistical and neural-based techniques, namely the stochastic neuron model and simulated annealing (SA). It draws on a thermodynamic metaphor from statistical physics, i.e. the stochastic neuron model simulates the effects of temperature in a thermodynamic system; specifically it is linked to random perturbations which result in energy changes in the system. As such, application of SA is plausible. SA is a heuristic optimization technique used to locate optimal or near-optimal solutions to large-scale optimization problems. It likens solving an optimization problem to finding the low temperature state of a physical system. In the case of minimization, the idea is to avoid local minima by permitting fluctuations that may not always lower the cost function, while in search of a global minimum. The thermodynamic metaphor is appropriate as the underlying process in an HNN is optimization and the cost function is an energy function. Together with the development of a probabilistic Hopfield network that utilizes SA (PHN-SA), an efficient annealing algorithm is derived to search for a globally optimum solution. It is shown to be independent of the SA cooling factor, which has been a point of concern in other stochastic-based NN proposals.

Collectively, this study has resulted in several research papers in contribution to the field of neural-based multiuser receivers. The proposed ideas and results, discussed above and contained in these papers, constitute some parts of the work presented in this dissertation. These papers have been presented at, and published in the proceedings of, national and international conferences, and one work has been submitted for publication in the transactions of the SAIEE.

- N. Moodley and S. H. Mneney, "Neural network-based multiuser detection in a simple AWGN CDMA environment", presented at South African Telecommunications, Networking and Applications Conference (SATNAC'04), Stellenbosch, Western Cape, SA, Sept. 6–8, 2004.
- N. Moodley and S. H. Mneney, "Recurrent neural network techniques for multiuser detection," in *Proc. IEEE AFRICON 2004*, Gaborone, Botswana, Sept. 2004, vol. 1, pp. 89–94.
- N. Moodley and S. H. Mneney, "Simulated annealing for multiuser detection employing a recurrent neural network," presented at 12*th* International Conference on Telecommunications (ICT), Cape Town, SA, May 3–6, 2005.
- N. Moodley and S. H. Mneney, "Recurrent neural networks for sub-optimal multiuser detection," *Transactions of the SAIEE: Towards next generation communications*, accepted for publication, April, 2006.

2 Multiple Access Systems and Standards

2.1 Introduction

A multiple access system refers to any system in which multiple users simultaneously access a common channel to transmit information. The basis of current and future wireless communication networks is determining how the common transmission medium is shared between users. In mobile radio communications the available channel bandwidth is a limited resource. Efficient sharing of this resource is necessary to achieve higher network capacity. This represents a challenge in any air interface design which must meet the ever-increasing demands of today's technologically-accustomed society.

Multiple access techniques[1] refer to the various ways in which resource-sharing may be achieved; they define the manner in which the wireless medium is distributed amongst the users of the system. When spectrum utilization is considered, these techniques may be classified as either narrowband or wideband. In terms of RF assignment, they can also be designated as fixed assignment, random access or demand assignment [12]. A common distinction is based on the most fundamental dimensions that may be allocated to provide multiple access, namely space, time and frequency. In context of this research, only time and frequency allocations warrant a discussion. FDMA, TDMA and CDMA are the three most common multiple access techniques that are used to share the available spectrum between users in a radio network. These schemes are the foundation for understanding the several extensions and hybrid techniques, such as orthogonal CDMA (OCDMA), hybrid CDMA/TDMA and orthogonal frequency division multiplexing (OFDM). The

[1] Multiple access techniques may also be referred to as multiple access schemes. In this dissertation, both terms are used interchangeably.

following sections provide an overview of the common access techniques, briefly showing their development and usage. The focus is on CDMA and the basic DS-CDMA process, as well as the general advantages of using spread spectrum methods.

2.2 Frequency Division Multiple Access

FDMA is the most classic of the basic multiple access schemes. It has been in use since the early days of telecommunications in first generation mobile systems which used analog transmission for speech services. Today, it is employed in satellite, cable and radio networks to multiplex analog and digital signals [13]. In FDMA (Figure 2.1), the available system bandwidth is subdivided into non-overlapping frequency channels which are assigned to different users of the system. When a user is allocated a unique band in which to transmit or receive on, no other user can utilize that same frequency band. In practice, a sufficient guard band is left between adjacent spectra to compensate for imperfect filters, frequency shifts and inter-channel interference.

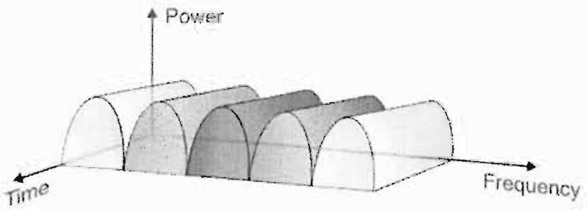

Figure 2.1 Multiple access achieved by frequency division of the available bandwidth into individual frequency channels (FDMA).

FDMA is intrinsically narrowband since each user is provided with a single narrowband channel. An example of a FDMA system is the Advanced Mobile Phone Service (AMPS) in the United States, which has a total bandwidth of 50 MHz. This is shared between the reverse and forward channels, occupying the bands from 824 – 849 MHz and 869 – 894 MHz, respectively. FDMA is used to divide these two bands into 30 KHz channels for FM transmission, of which the usable bandwidth is limited to 24 KHz, due to guard bands. In an effort to increase performance, AMPS was replaced first by the IS-54 standard (D-AMPS) and later by the fully digital IS-136 standard. To ensure backward compatibility with AMPS, the carrier spacing is also 30 KHz. The advantage of these narrowband channels is that each channel experiences flat fading and so there is a low overhead in combating inter-symbol interference (ISI). Also, since transmission is continuous (i.e. channels are used on non-time-sharing basis), fewer bits are required for control as compared to TDMA.

There are, however, several areas of concern in pure FDMA systems. One is the excessive cost and complexity involved in modulation and demodulation if a network is to support hundreds or thousands of users, which is currently the situation in cellular networks. The existence of guard bands, while necessary, lowers the utilization of the available spectrum and in some cases only a subset of the channels is used so as to reduce inter-cell interference. Second generation networks basically targeted higher spectrum efficiency and better data services to succeed FDMA analog transmission systems. Among the proposed 2G multiple access solutions were TDMA and CDMA, both of which are utilized 2G and 3G networks (e.g. GSM, IS-95 and UMTS). Even so, frequency division is still employed in TDMA and CDMA-based networks to divide large allocated frequency bands into smaller channels.

2.3 Time Division Multiple Access

With the advent of digital radio transmission in the late 1980's, TDMA was seen as the likely successor to FDMA. Today it is a prevalent multiple access technique that is employed in several international cellular standards and proprietary systems. It is the standard technology for a wide range of second generation networks (GSM, PDC, IS-136), of which GSM is the most popular network standard overall. Beyond radio networks, it has found application in satellite and security systems, as well as in technical specifications of international forums such as the Digital Video Broadcasting (DVB) project [13].

TDMA can be implemented either as a narrowband or wideband system, in which the bandwidth is shared in the time domain. This is shown below in Figure 2.2. In TDMA-based cellular networks, time is divided into frames and each frame is divided into multiple non-overlapping time slots. A single time slot, within a frame, is allocated to each user to transmit or receive information. Accordingly, the carrier frequency is shared by multiple users, with each using the carrier in separate time slots. The number of time slots per carrier depends on a combination of factors, such as available bandwidth, modulation scheme and synchronization information.

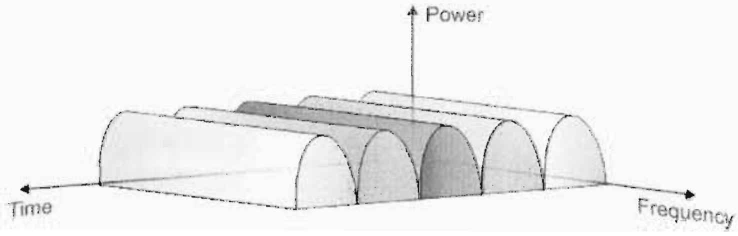

Figure 2.2 Multiple access achieved by time division of the available bandwidth into individual time slots (TDMA).

The allocation of time slots (shown in Figure 2.3) occurs in a round robin fashion, characterizing the buffer-and-burst communication inherent to TDMA. Once a user accesses a carrier, transmission or reception occurs during the time slot assigned to that user, within that frame. On the next frame, each user waits for its allotted time slot to transmit again. In dynamic TDMA schemes, slots are assigned according to traffic demands so that the time slot assigned to a specific user changes each frame.

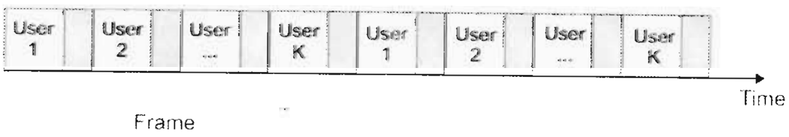

Figure 2.3 TDMA scheme showing frames divided into non-overlapping time slots with guard times inserted between slots.

Since transmission is discontinuous, a user's information is buffered over the previous frame and burst transmitted at a higher rate during the next time slot for that user. The high data rates in TDMA result in high ISI, thus equalization is of greater concern than in FDMA. To protect against inter-slot interference due to different propagation paths, guard times are inserted between adjacent slots (Figure 2.3) [12], to help negate the adverse effects of the channel and receiver. The short slot duration imposes strict synchronization between transmitters and receivers as opposed to asynchronous transmission in FDMA [14]. Thus, there is a significant overhead for allocating guard times and control information for synchronization purposes.

An advantage of TDMA is that, due to the burst-type communication, a user only needs to listen and broadcast for its own timeslot. The idle time allows safe handoffs (when a mobile moves between cells) without any perceptible interruption. However, the mostly empty time slots at any given time results in only a fraction of the bandwidth being utilized. This 'dead-time' between slots limits the potential bandwidth of a TDMA channel. This explains why early efforts to incorporate time slots into 3G CDMA-based systems (which is now WCDMA) failed, leaving WCDMA as a purely CDMA technology.

In current second generation networks, TDMA is most often used alongside FDMA and FDD. This is the case in both GSM and IS-136. In the GSM900 uplink (890 – 915 MHz) the available bandwidth is split into 124 carriers (using FDMA), each 200 kHz wide. Each carrier is divided in the time domain, using TDMA, into 26 frames of 8 slots and these carrier frequencies are then assigned to base stations of the GSM network as required.

The GSM system and its sibling systems operating at 1.8 GHz and 1.9 GHz (which are known as DCS1800 and GSM1900, respectively) are regarded as the first approach towards a true personal communication system. The success of these GSM systems is attributed to the robust TDMA air interface. It ensures interoperability and together with international roaming and support for a variety of services including data transfer, short message service and supplementary services, GSM comes close to fulfilling the requirements for a personal communication system. Notably, it is the basis for Enhanced Data Rates for GSM Evolution (EDGE), which is the only TDMA-based 3G standard and that is also backward compatible to GSM/IS-136. EDGE was developed for the purposes of migration from 2G to 3G networks. Although it has been incorporated into IMT-2000, its capabilities are far exceeded by WCDMA, and emerging requirements for higher rate data services and better spectrum efficiency is the main driver for employing spread spectrum techniques in third generation networks.

2.4 Code Division Multiple Access

Although CDMA was first proposed in the early 1950's, relative to FDMA and TDMA, it has not shared the same popularity within the telecommunication society. It was only in the 1970's when CDMA was first introduced into military and navigational systems, for which it was being developed [6]. It was only considered for possible commercial cellular applications 10 years later. At that time (1985) the European telecommunications body, *Conference Européenne des Postes et des Télécommunications* (CEPT), which was responsible for establishing the GSM standard, disregarded it as a proposed multiple access solution for GSM [15].

CDMA development and trial testing was first carried out by a North American company called Qualcomm in the early 90's. In 1993, the first second generation narrowband CDMA-based network standard, known as IS-95, was completed. Thus it took nearly two decades of technology-pushing by industry and governments before CDMA was seen as the appropriate choice of technology to meet the objectives of the third generation of mobile radio networks; to ultimately provide the average mobile user with high speed "anytime, anywhere" access encompassing a wide range of multimedia services. CDMA is now established as the standardized multiple access scheme for 3G wireless personal communication systems.

In CDMA each user in the system has access to the same available bandwidth all of the time. Independent information signals may be transmitted simultaneously and, by concurrently sharing the bandwidth, these individual transmissions overlap in time and frequency. This is illustrated in Figure 2.4.

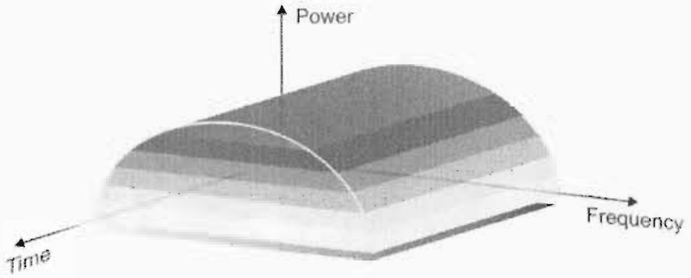

Figure 2.4 CDMA with signals superimposed in time and frequency.

In current CDMA implementations, each user is assigned a unique pseudorandom[2] codeword to distinguish them from other users. The bandwidth of the codeword is much greater than that of the information-bearing signal so that when superimposed onto the information signal, the resulting signal is spread in bandwidth and appears noise-like to every other user during transmission. Hence they are also termed as spreading codes[3]. They possess appropriate correlation properties that minimize the multiple access interference (MAI). By using well designed codes, message privacy is maintained between users and from other sources of interference. In addition, these sequences are known only to the respective transmitter and receivers.

Through the use of high-bandwidth sequences, CDMA spreads the bandwidth of the information-bearing signal over a bandwidth in excess of the minimum bandwidth required to transmit the signal. Therefore, understanding CDMA in the context of

[2] It is also known as pseudonoise (PN) sequences, owing to their noise-like properties.

[3] The terms "spreading codes", "codewords" and "sequences" all refer to the pseudorandom bit sequences. These terms are used interchangeably in this dissertation.

mobile radio communications requires some insight into its origins, namely spread spectrum (SS) communications. Today, CDMA is often used to refer to one specific SS technique, namely direct-sequence spread spectrum (DS-SS), which was briefly described above. DS-SS dominates spread spectrum research. It is employed in all 3G CDMA-based networks [12] and is also the method used in this research.

Technically speaking, however, CDMA refers to a collection of spread spectrum techniques that employ pseudorandom sequences to achieve multiple access communications. The manner in which frequency and time resources are utilized and shared is determined by how the sequences are employed.

2.4.1 Origins

Spread spectrum communication systems have been in existence for several decades, although, up until the last decade or two, most of these systems have been predominantly used for military communications [6]. These systems were developed during World War II, when it was necessary to avoid jamming or interception by enemy systems. Thus, they were typically designed to be wideband.

Spread spectrum signals are characterized by having a transmission bandwidth W that is much greater than the information rate R (in bits/s). This type of transmission has several benefits. Firstly, by spreading the information signal over a much larger bandwidth using random-like sequences, the spread signal has a noise-like appearance and a low power spectral density, which makes it difficult for a hostile listener to detect and intercept in the presence of background noise. This property is known as low-probability-of-intercept (LPI). These systems provide narrowband interference rejection and anti-jamming capabilities; jamming refers to the intentional introduction of interference into the system, while other interference may arise from the channel or from other users. Spread spectrum modulation also mitigates the effects of ISI due to multipath propagation. However, its effectiveness depends on the type of modulation that is employed [15].

Spectral spreading is achieved by using high rate sequences. The combination of spectral spreading, interference rejection and unique spreading sequences gives to SS its multiple access capability. As mentioned before, there are several spread spectrum techniques, each that has a unique method of employing these sequences to spread the system bandwidth and which are applicable in mobile radio communications. The two methods discussed herein are DS-SS and frequency-hopping spread spectrum (FH-SS), with emphasis on the former method due to its pertinence in this research.

2.4.2 Frequency Hopping Spread Spectrum

In FH-SS the carrier frequency of the information signal changes every signaling interval by hopping from one frequency to another. The available bandwidth is divided into a large number of contiguous narrowband channels. During a symbol interval, the transmitted signal may occupy one or more of these channels, but on the next interval the carrier randomly changes, i.e. a short burst of data is transmitted and then the transmitter tunes to another frequency and transmits again. The choice of the frequency slot/carrier is determined by a pseudorandom sequence. The random changes in the carrier frequency constitute the hopping pattern.

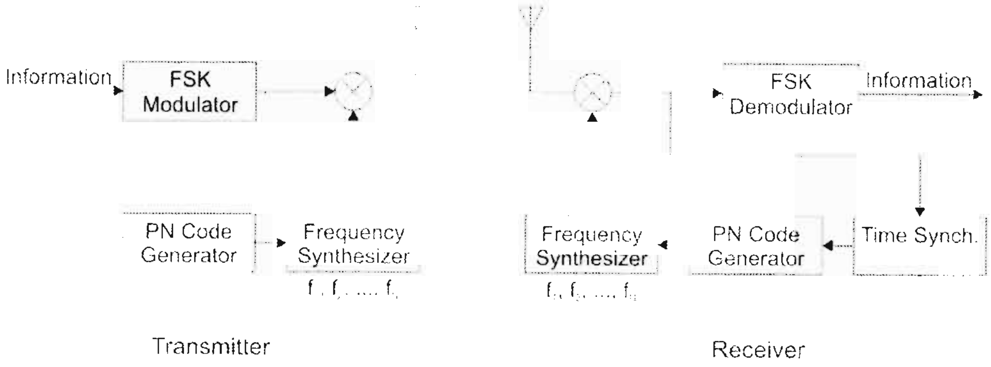

Figure 2.5 Block diagram of a basic FH-SS system.

A typical FH-SS system is shown in Figure 2.5 above. The information signal is baseband modulated and then up-converted to a transmission frequency that is derived using a frequency synthesizer. The synthesizer is controlled by a PN sequence generator [15]. At the receiver, locally generated sequences ensure that the received signal is correctly despread; the receiver must lock on to the PN sequence and then use a frequency synthesizer to demodulate the narrowband signal at the appropriate carrier. For this purpose, the hopping patterns need to be synchronized to that of the received signal. Demodulation is usually non-coherent since it is difficult to maintain phase coherence as the signal hops from one frequency to another.

The spreading of the transmission bandwidth occurs discretely since only a small portion of the total bandwidth is used during transmission, at any particular time. For a signaling interval, all transmitted power is concentrated on one channel. Although transmission may be regarded as being instantaneously narrowband (for M-FSK modulation), on average it is wideband because (over many hops) the signal is spread across the total available bandwidth. On average, DS-SS and FH-SS transmit the same power in the frequency band.

The occupied bandwidth depends also on the shape of the hopping signal and the rate at which the carrier frequency changes. The latter, known as the hopping frequency, dictates the performance that is achievable using FH-SS. Fast frequency hopping occurs when the hopping rate is greater than the information symbol rate so that the carrier frequency changes more than once during the transmission of a symbol. In slow frequency hopping a single symbol or multiple symbols are transmitted over a single frequency before hopping occurs. In this case, the hopping rate is equal to or smaller than the symbol rate. Slow frequency-hopping is better suited for cellular systems since it averages out interference from other cells.

In general, FH-SS is well suited for military and anti-jamming communications [16]. An unintended listener on any narrowband channel will only be able to receive a small part of the transmission and since the signal is transmitted over several carrier frequencies the probability of being intercepted is lowered. FH-CDMA is the multiple access solution based on FH-SS in which each transmitter-receiver pair is assigned its own pseudorandom hopping pattern. If interfering users transmit in the same frequency slot, error correcting codes are used to recover the transmitted information. Synchronization is easier than in DS-CDMA and higher SS bandwidths can be employed leading to a greater possible reduction in narrowband interference. However, this comes at the cost of employing complex frequency synthesizers to achieve the larger spread bandwidth. FH-CDMA is not commonly used in radio networks for multiple access control. It is an option in the physical layers of wireless personal and local area networks (LAN), like IEEE 802.11 WLAN and Bluetooth [12]. FH is also easily combined with narrowband signaling techniques, as in GSM.

2.4.3 Direct Sequence Spread Spectrum

DS-SS is a technique in which a pseudorandom sequence directly modulates a modulated data-bearing signal and thus spreads the spectrum. While in principle any modulation technique can be used [17], the most widespread form is phase shift keying like BPSK or QPSK. These are employed in WCDMA. In the case of digital signaling it is convenient to use baseband notation. Typically then, data modulation is omitted and the binary (antipodal) information signal is directly multiplied to the PN sequence before modulating a wideband carrier. This basic process is shown below in Figure 2.6. The process of direct multiplication gives DS-SS its name. In some circle it is also called direct-spread (DS) spread spectrum.

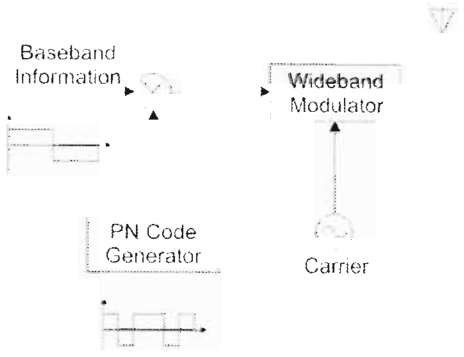

Figure 2.6 Block diagram of a basic DS-SS transmitter.

At the receiver (Figure 2.7), the spread signal is translated back to baseband by multiplying it with a locally generated sequence. The receiver requires knowledge of the sequence; sequence generation must be synchronized with the received signal. There is greater difficulty in acquiring and maintaining synchronization, as compared to FH-SS, since it has to be kept within a fraction of T_c.

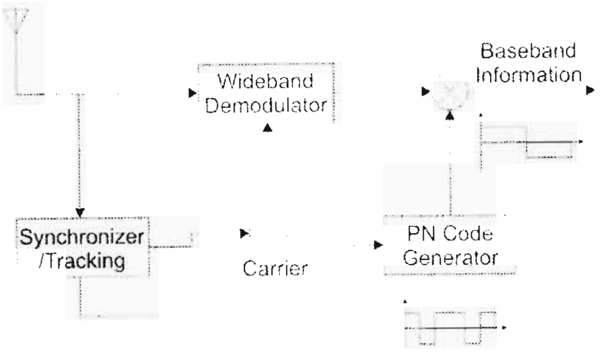

Figure 2.7 Block diagram of a basic DS-SS receiver.

While spectral spreading is the target of DS-SS, there are several ways of modelling the transmitter and receiver, each varying mostly in modulation and demodulation. In this dissertation, the DS-SS transmitter and receiver (in Figure 2.6 and Figure 2.7, resepectivley) illustrates a rudimentary system for BPSK baseband communications.

Spectral spreading is possible by choosing the bit rate, R_c, of the PN sequence to be much greater than the rate, R_b, of the information-bearing signal. The bit duration of the information signal is defined as $T_b = 1/R_b$ and is a multiple N of the spreading code bit duration, $T_c = 1/R_c$. Given that T_c is a fraction of T_b, the spreading sequence bits are appropriately referred to as 'chips' where R_c and T_c denote the chip rate and chip duration, respectively. Therefore, N refers to the number of chips per information bit. By multiplying the wideband sequence with the narrowband information signal, the spectrum of the information-bearing signal is spread. The new wideband spread signal occupies a bandwidth equal to that of the spreading sequence (under ideal conditions). In this context, N represents the gain achieved in processing the spread spectrum signal over the unspread signal. It is formally defined as the processing gain, which is the ratio of the bandwidth of the spread signal B_S to the bandwidth of the unspread information-bearing signal B. For a fixed duration of the spreading waveform, the bandwidth is proportional to N. In practical systems, the processing gain is an integer and is expressed as

$$N = \frac{B_S}{B} = \frac{T_b}{T_c}. \tag{2.1}$$

The processing gain accounts for many spread spectrum properties. During despreading of the *k*th user, the interfering signals that are either narrowband or wideband (such as all other users) will be spread when multiplied by the *k*th user's wideband sequence. The interference power in the information bandwidth is thus reduced by a factor of N. For the same reason, the LPI property of a SS signal is enhanced with increasing N, which contributes to the privacy of the system. Consider that in the absence of background noise, a narrowband interferer with power up to $10\log_{10} N$ dB above the spread signal will induce no errors [14].

2.4.4 DS-CDMA

Multiple access capability is an inherent property of spread spectrum systems, which is exploited by using spreading sequences. DS-CDMA is a SS spectrum multiple access technique that employs direct-sequence (DS) techniques. By assigning a different sequence to each user, it is possible to allow many users to occupy the same channel bandwidth. Users can transmit simultaneously over the channel and their individual signals can be separated at the receiver using their own unique sequence.

In a simple synchronous DS-CDMA system with K users, each user's baseband information signal $\{\, b_i(t), i = 1, 2, \ldots, K \,\}$ is spread by multiplication with an assigned sequence $\{\, s_i(t), i = 1, 2, \ldots, K \,\}$. The signals simultaneously pass through the channel in which noise is modeled as AWGN. The received signal[4] is the sum of the wideband spread signals $(b_i(t)\times s_i(t)\ \forall\, i=1,2,\ldots,K)$ and Gaussian noise $n(t)$, i.e.

$$r(t)=\sum_{i=1}^{K} b_i(t)s_i(t)+n(t). \tag{2.2}$$

At the receiver, the jth user's information signal is obtained by multiplying the received signal with the jth user's spreading sequence $s_j(t)$. Despreading results in the signal of interest $b_j(t)$ plus interference and noise, given by $y_j(t)$.

$$\begin{aligned} y_j(t)&=s_j(t)\left[\sum_{i=1}^{K} s_i(t)b_i(t)+n(t)\right] \\ &=s_j^{\,2}(t)b_j(t)+s_j(t)\left[\sum_{i=1,i\neq j}^{K} s_i(t)b_j(t)+n(t)\right]. \end{aligned} \tag{2.3}$$

For transmission privacy to be maintained some level of orthogonal signaling must be employed i.e. reception of the jth user, free from interference due to other users, is a consequence of the cross-correlation properties of the spreading sequences. Thus, there is an (approximate) orthogonality constraint on the pseudorandom sequences to guarantee acceptable performance. Ideally, fully orthogonal codes are preferred. If the users are not totally separable then they appear as (multiple access) interference to other users, as indicated by the second term in (2.3).

As the number of users increases, the MAI accumulates and this in turn reduces the BER performance of the receiver. This is the behaviour of an interference-limited system. The number of users that can be supported depends on several factors. Unlike TDMA and FDMA, this is a soft limit, which typically depends on the processing gain, the signal-to-noise ratio, correlation between spreading sequences

[4] The complete mathematical derivation of the transmission model for a DS-CDMA system is provided in Chapter 3.

and the type of receiver. The spreading gain theoretically represents the maximum number of users that can be supported in a synchronous orthogonal CDMA system.

The importance of the type of spreading sequences is evident. However, while orthogonal sequences ensure that interfering signals are transparent at the receiver during the recovery of a specific signal, orthogonality is not imperative [14]. Even so, it is practically impossible to maintain orthogonality because the channel introduces imperfections that result in a loss of orthogonality. It is sufficient to employ sequences with low cross-correlation. This provides several benefits in multiuser communications.

2.4.5 Spreading Sequences

Coding and pseudorandomness are two important elements in the design of CDMA systems. Coding allows for bandwidth expansion and is an efficient way of introducing redundancy to help overcome the severe levels of interference that may be experienced during transmission. However, if a digital signal is only encoded, say, using a type of block or convolutional code, then it may still be possible for a sophisticated interferer to mimic or decode the signal and disrupt transmission. Spread spectrum systems employ high rate spreading sequences to lower the probability of interception and even circumvent this possibility.

Spreading sequences[5] have several purposes. It has been discussed that due to their relatively high chip rate, they spread the bandwidth of the (encoded) information waveform. They possess noise-like properties which, after spreading, allow the transmitted signal to be virtually hidden in the background noise. They also increase the robustness of the transmitted signal to interferers (intentional or otherwise). Technically, spreading sequences may be classified as being either pseudonoise or orthogonal. This classification is inherited by the non-orthogonal (PN-CDMA) and

[5] Unless otherwise stated, spreading sequences is also used to imply PN sequences, within the text.

orthogonal (OCDMA) systems [13], and it has vast implications on the number of users that can be supported as well as the output signal-to-noise ratio (SNR).

A major issue in sequence design is distinguishable spreading sequences. The conventional matched filter receiver exploits the auto- and cross-correlation properties of PN sequences to separate individual signals. Besides randomness and LPI, there are two other desired properties. Firstly, a sequence $s_i(t)$ should be distinguishable from a time-shifted version of itself. This is necessary for acquiring the sequence and for combining signals from different paths, due to multipath fading channels. Secondly, in a sequence set, $s_i(t)$ should be distinguishable from $s_j(t)$ $\forall\ i, j \in [1, K]$ and time-shifted versions of them. This is required for despreading the CDMA signals and it accounts for the fact that (in the reverse link of a cellular system) there is no control over the transmission times of each user. Also, each user experiences different delays due to multipath propagation.

For a normalized sequence set, the continuous-time periodic cross-correlation (which should ideally be zero), calculated over a bit/symbol interval $T = NT_c$, is defined as:

$$\rho_{ij}(\tau) = \int_0^T s_i(t) s_j(t+\tau) dt . \qquad (2.4)$$

In light of this, codes with highly peaked auto-correlation and minimum (zero) cross-correlation are required. Orthogonal codes satisfy these requirements to some extent. However, their out-of-phase correlation properties are worse than maximal-length sequences (m-sequences), except in the case of super orthogonal codes.

An alternative family of sequences is semi-orthogonal Gold codes, which are derived from m-sequences. Their properties make them ideally suited to demonstrate the effects of multiuser interference and thus they are sufficient for the purposes of this study; they are easily constructed and their construction allows for a greater number of codes as compared to pseudorandom m-sequences of the same degree. Although the periodic auto-correlation properties of m-sequences cannot be bettered, gold sequences have better periodic and aperiodic cross-correlation properties, and hence they are more favourable. The reader is referred to Appendix A, which presents basic characteristics and correlation properties of m-sequences and Gold codes.

2.5 Summary

This chapter reviewed the three most basic multiple access schemes. Their current use in mobile radio communications was indicated. While TDMA and FDMA are still employed (to a relatively large extent), they are not suited to meet the demands of future generation systems. Transmission schemes proposed for next generation wireless networks employ spread spectrum techniques, multi-carrier techniques, or a combination of these two. Current 3G networks that have recently been deployed in South Africa are based on wideband DS-CDMA, which is the current standard in Asia, America and Europe. It is evident that DS-CDMA will play a pivotal role in the development of next generation networks; this is in view of the wideband DS-CDMA air interface solution which is fulfilling the key requirements of 3G systems.

CDMA has several advantages over TDMA or FDMA. Spread spectrum technology is inherently resistance to multipath fading. Receivers employing diversity techniques may take advantage of this and improve the signal-to-noise ratio in fading channels that are characteristic of urban areas. DS-CDMA systems, employing pseudorandom (semi-orthogonal) sequences, undergo a gradual degradation in signal-to-noise ratio as the number of users is increased. This soft capacity limit allows the number of active users to be increased beyond the design specifications. Orthogonal systems like FDMA, TDMA and OCDMA do not allow more users beyond a fixed limit but they can guarantee a minimum quality of service for the active users, whereas an overloaded CDMA system will see gradually increasing bit error rates before it begins dropping users. Reception quality is traded for increased capacity thus making DS-CDMA systems interference limited.

3 DS-CDMA and Multiuser Detection

3.1 Introduction

Multiple access interference limits the capacity and performance of DS-CDMA. In a conventional DS-CDMA system, a bank of matched filter detectors (correlators) is employed, in which a user's signal is detected by correlating the received signal with that user's spreading waveform and then performing a simple threshold decision. In MUD literature, this detector is commonly known as the single-user matched filter (SUMF) or conventional detector. Detection of a single desired user is made without regard to other users, i.e. their corrupting influence is not accounted for. In an ideal situation there is zero cross-correlation between user spreading sequences, so this is not an issue. If symbol synchronism is maintained and the waveforms are mutually orthogonal then the channel is decoupled into single-user channels and the SUMF receiver achieves optimal demodulation [18], in the presence of additive Gaussian noise. (The conventional receiver is revisited in greater detail in Section 3.3).

However, in practice the conventional receiver is not optimum, unless in the case of a single user or when orthogonality between spreading sequences is maintained. The first case is an exception in multiuser communications. Furthermore, asynchronous transmission is unavoidable, and depending on the type of coding that is employed, even orthogonal synchronous CDMA transmissions lose their orthogonality once passed through the channel. This research employs semi-orthogonal Gold codes to illustrate the effect of MAI, which in turn is used to verify the performance of the sub-optimal MUD schemes. The finite cross-correlation, resulting from semi-orthogonal spreading sequences and asynchronous transmission, means that users are not transparent to each other. Thus, the output of a desired user's matched filter contains some signal information belonging to other users as well. This constitutes MAI and it is a significant contributor to the total interference seen at the receiver. In the conventional receiver, MAI is regarded as additive noise in the desired user's demodulated signal. So even in the absence of receiver thermal noise or inter-cell interference the error probability of the conventional receiver exhibits a non-zero floor due to MAI. As the number of active users increases, the MAI also increases. This reduces the achievable bit error rate and leads to low bandwidth efficiency.

Another factor greatly affecting (or responsible for) the amount of MAI that is experienced, is relative signal power. Severe performance degradation occurs when the received powers of some users dominate over other users. The conventional receiver is unable to detect weak signals, typically originating far from the receiver, in the presence of strong interferers located closer to the base station/receiver. This is the so-called near-far problem. If some signals are significantly stronger than others their signal energy/information will overshadow that of the desired user's, thus making it difficult to separate the signals.

Several strategies exist to mitigate MAI. For example, in the CDMA-based IS-95 standard, highly redundant error-correcting codes are employed to reliably detect the information in the presence of MAI at the output of the matched filters. To account for a near-far situation, very accurate and fast power control prevents strong interferers from dominating at receiver, with single-user matched filtering. Even so, as with the conventional receiver, second generation systems treat the MAI as background noise and no signal-processing measures are taken to combat it.

However, MAI has considerable structure and is much less random than white Gaussian background noise [19]. Multiuser detection (MUD) is a signal processing technique which exploits the structure of MAI to overcome the limitations of the conventional receiver and enhance the performance of DS-CDMA systems. It performs, what is referred to as, joint detection by taking into account the interference that may result from other users in the system i.e. the information about multiple users is used jointly (for their mutual benefit) to better detect each individual user. Its main objective, therefore, is to reduce/remove the effect of MAI, hence it is also known as co-channel interference suppression. Using MUD algorithms can increase spectral efficiency and capacity (in terms of reducing bit error rates and increase the number of users), and helps to reduce the need for tight power control (the level of which is dependent on the algorithm).

Sergio Verdú proposed the first optimal multiuser detector for the AWGN channel in 1986 [7]. MUD has, ever since, gained enormous interest in academic circles and is a dominant area of research in the field of multiuser communications. There are two notable reasons for this. Firstly, Verdú [14] showed that the optimum multiuser detection problem is combinatorially hard. The optimal detector, which is the maximum likelihood sequence estimator (MLSE), has a computational complexity that grows exponentially with the number of users. The implementation of such a receiver is unfeasible in current DS-CDMA systems. This has inspired research of sub-optimal multiuser detectors to achieve near-optimal performance with reasonable implementation complexity. Secondly, optimum detection of multiple users in multipoint-to-point (and its dual, point-to-multipoint) communications is essential for the growth of personal wireless communications, to satisfy higher data rates, bandwidth-intensive applications and to provide an overall higher level of service.

A general classification of CDMA detectors is shown in Figure 3.1. We differentiate between the conventional receiver containing the bank of matched filters (single-user strategy) and the multiuser detectors that account for MAI. In terms of optimal and sub-optimal solutions, the MLSE is the only optimal solution; some proposed schemes are also referred to as near-optimal. Sub-optimal detectors may be classified as being either linear or interference cancellation (IC) detectors. There are a myriad of detectors that are a combination of basic architectures. Such detectors constitute the family of combined (or hybrid) schemes. Schemes that lie outside the linear/non-linear classification have also been proposed [14], [15], [20], [21]. The field of neural networks is an example of this. However, to date, there has been no classification of neural-based multiuser detectors (e.g. feedback/feed-forward, memory association, soft/hard decisions). In Figure 3.1 a novel classification is presented.

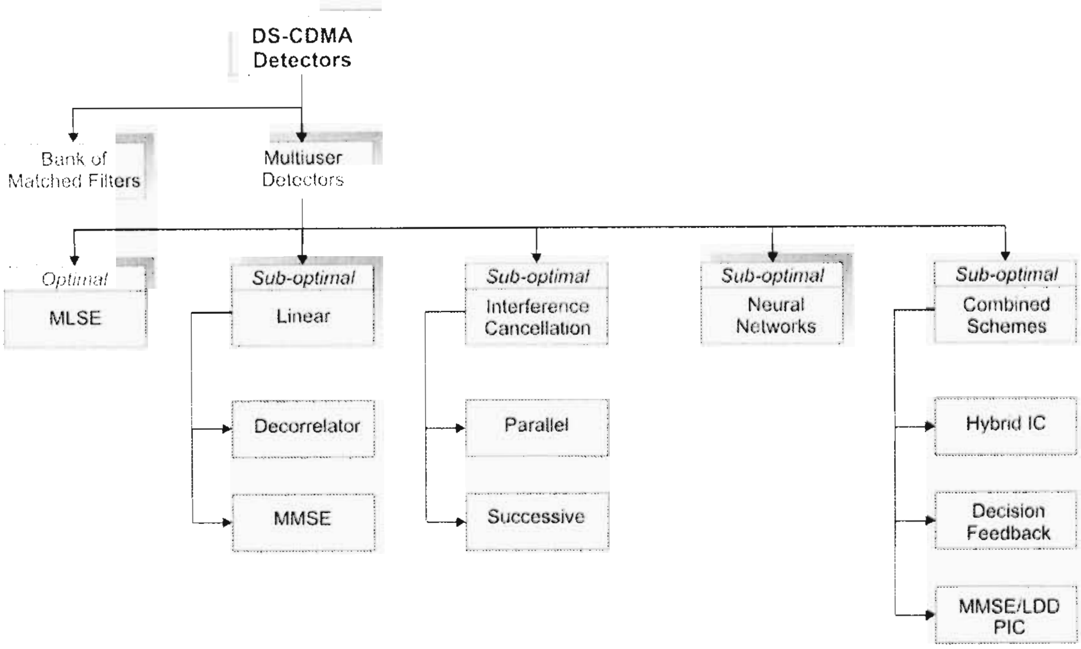

Figure 3.1 Classification of CDMA receivers.

In MUD, the front-end of most receivers is traditionally (but not necessarily) a bank of matched filters followed by filters that perform linear or nonlinear transformations. The sampled signals at the output of the matched filter bank constitute a sufficient statistic of the received continuous-time signal. It is thus possible to derive a receiver that (optimally) demodulates all transmitted signals.

In the linear schemes, a linear mapping is applied to the soft outputs of the bank of matched filters. In non-linear IC schemes, which employ feedback, the MAI and multipath induced interference is estimated from the outputs of the conventional receiver and then subtracted out. The foregoing multiuser detectors depend on various parameters like amplitude, phase and cross-correlations which change over time. This has led to research in adaptive and blind detection schemes [14], [20]–[24]. In this regard, MMSE is very attractive from an implementation perspective because of its natural link to adaptive filtering techniques. Studies have also incorporated space-time processing, which involves use of multiple transmit and receive antennas to mitigate the effects of multipath fading in wireless channels

[25]–[27]. The WCDMA standard supports space-time techniques as a means to increase system capacity.

In this study, we restrict ourselves to linear detection schemes to draw comparisons to the neural-based detectors. These are well known sub-optimal multiuser detectors and serve as a benchmark for many of today's proposed MUD algorithms. The linear class of receivers have the advantage of performing decentralized demodulation [28] i.e. the demodulation of each user can be implemented completely independently. Poor and Verdú [29] showed that the optimum decentralized receiver is a one-shot detector. It need not concern itself with demodulating every user for which it has a spreading code, which is an advantage. We discuss, the LDD, MMSE and the OMD later in this chapter, but first the basic DS-CDMA transmission model is described.

3.2 The DS-CDMA Model

The transmission and reception in a DS-CDMA system can be described by a discrete-time mathematical model. An asynchronous model for the uplink of a mobile radio network is considered. It is based on the vector-valued transmission system, proposed in [30], which has been employed in several neural network-based detectors [30]–[34] and is applicable to the neural network based multiuser detector proposed in this work.

Consider a DS-CDMA channel that is shared by K users, simultaneously. The channel state information is known at the receiver. Each user $k \in \{1, 2, \ldots, K\}$ transmits a packet of M bits. For simplicity, binary antipodal[1] signalling is assumed. The baseband representation of the kth user's transmitted spread signal is given by:

$$q_k(t) = A_k \sum_{i=1}^{M} b_k[i] s_k(t - iT - \theta_k). \qquad (3.1)$$

[1] Binary antipodal refers to BPSK i.e. $b_k[i] \in \{-1, 1\}$.

In (3.1), $b_k[i]$ is the ith transmitted symbol of the kth user taking on the values $\{-1,+1\}$ with equal probability, T is the bit interval, $\theta_k \in [0,T)$ is the uniformly distributed relative delay of the kth user, and A_k and s_k are the kth user's amplitude and signature waveform, respectively. In a synchronous system $\theta_k = 0 \, \forall \, k$. The continuous signature waveform (or spreading signal) of user k is defined as:

$$s_k(t) = \sum_{j=1}^{N} c_k[j] e(t-(j-1)T_c), \tag{3.2}$$

where N is the processing gain, $T_c = T/N$ is the chip duration, c_k is the kth user's spreading sequence consisting of N chips $\{c[j], j = 1, 2, \ldots, N\}$, and $e(t)$ is the pulse shaping waveform of the chip (so as to reproduce simulation results), i.e.

$$e(t) = \begin{cases} 1, & 0 \le t \le T_c \\ 0, & \text{otherwise} \end{cases} \tag{3.3}$$

For short codes, $s_k(t)$ is defined in the interval $0 \le t \le T$. All signature waveforms $\{s_k(t),\ k = 1, 2, \ldots, K\}$ are normalized to have unit energy i.e.

$$\int_0^T s_k^2(t) dt = 1. \tag{3.4}$$

Without loss of generality, it is assumed that the channel is composed of multiple paths and is slowly changing such that it is constant during packet transmission. The kth user's channel impulse response characterizes the adverse effect of the channel on that user. It may be modelled by a sum of simple attenuators and phase shifters,

$$h_k(t) = \sum_{l=1}^{L_p} \alpha_{kl} \delta_k(t - \tau_{kl}), \tag{3.5}$$

where the complex coefficient α_{kl} represents the attenuation and phase shifting due to the lth path, τ_{kl} is the propagation delay experienced by the kth user on the lth path and L_p is the number of multipaths. The signal at the receiver input, $r(t)$, is the summation of all signals corrupted by AWGN and may be expressed as:

$$r(t)=\sum_{k=1}^{K} h_k(t)*q_k(t) + n(t), \tag{3.6}$$

where $n(t)$is zero mean additive Gaussian noise with a constant one sided power spectral density $2\sigma^2 = N_0$, and where the symbol $(*)$ denotes the convolution operator. $n(t)$ models the thermal noise plus noise sources that are unrelated to the transmitted signals [14]. When specifying the discrete-time model, the notation may be simplified by introducing $\phi_k(t)$ [34], which is defined as:

$$\phi_k(t)=s_k(t-\theta_k)*h_k(t). \tag{3.7}$$

By making the substitution of (3.7) into (3.6), then

$$r(t)=\sum_{k=1}^{K}\sum_{i=1}^{M} A_k\phi_k(t-iT)b_k[i] + n(t). \tag{3.8}$$

One way of converting the received signal into a discrete time process is to pass it through a bank of K matched filters. The kth matched filter has an impulse response $\phi_k^*(-t)$ that matches to the kth user's waveform and the channel, where ϕ_k^* denotes the complex conjugate of ϕ_k. The matched filter performs a convolution product on the incoming bit stream and $\phi_k^*(-t)$ resulting in the filter output signal $y_k(t)$, i.e.

$$y_k(t)=\phi_k^*(-t)*r(t). \tag{3.9}$$

It is convenient to define a correlation matrix, $\mathbf{\Phi}(t)$ that contains the correlation between $\phi_k(t)$ and $\phi_j(t)$ $(\forall\, k, j=1,2,\ldots,K)$, such that

$$\Phi_{kj}=\phi_k^*(-t)*\phi_j(t). \tag{3.10}$$

The output of the kth matched filter in (3.9) may then be expanded, using the appropriate substitutions, to arrive at (3.11) below. By making the generalization for all of the K users, the outputs from the bank of matched filters may be expressed in matrix-vector notation, shown in (3.12).

$$y_k(t) = \phi_k^*(-t) * \left(\sum_{j=1}^{K} \sum_{i=1}^{M} A_j \phi_j(t - iT) b_j[i] \right) + \phi_k^*(-t) * n(t) \tag{3.11}$$

$$\mathbf{y}(t) = \mathbf{A} \sum_{i=1}^{M} \mathbf{\Phi}(t - iT) \mathbf{b}[i] + \tilde{\mathbf{n}}(t) \tag{3.12}$$

where

$$\begin{aligned} \mathbf{y}(t) &= [y_1(t),\ \ldots,\ y_K(t)]^T, \\ \mathbf{b}[i] &= [b_1[i],\ \ldots,\ b_K[i]]^T, \\ \tilde{\mathbf{n}}(t) &= \boldsymbol{\phi}^*(-t) * n(t), \\ \mathbf{A} &= \mathrm{diag}[A_1\ ,\ \ldots,\ A_K\ ], \end{aligned} \tag{3.13}$$

with $\boldsymbol{\phi}^*(-t) = \{\phi_k^*(-t),\ k = 1, 2, \ldots, K\}$ denoting the vector of impulse responses of the K channel matched filters; $\mathbf{A}$ is the diagonal matrix of all users amplitudes.

By symbol-sampling the output from the bank of matched filters (every T seconds), the result is a discrete-time model in which $\mathbf{b}[i]$ is mapped to $\mathbf{y}[i]$ in such a way that,

$$\mathbf{y}[i] = \mathbf{A} \sum_{s=-\infty}^{\infty} \mathbf{\Pi}[s] \mathbf{b}[i - s] + \tilde{\mathbf{n}}[i], \tag{3.14}$$

where $\mathbf{\Pi}[i] = \mathbf{\Phi}(iT)$ is the normalized discrete-time cross-correlation matrix, $\mathbf{y}[i] = [y_1[i],\ \ldots,\ y_K[i]]^T$ is a vector of the ith output of all users, and similarly $\mathbf{b}[i]$ and $\tilde{\mathbf{n}}[i]$ are vectors of the ith element of all users. For all $i \in \{1, \ldots, M\}$, these vectors constitute elements of larger vectors of size $KM \times 1$ that are given by:

$$\begin{aligned}\mathbf{y} &= [y_1[1],\ y_2[1],\ \ldots,\ y_K[1],\ y_1[2],\ \ldots,\ y_K[M]]^T,\\ \mathbf{b} &= [b_1[1],\ b_2[1],\ \ldots,\ b_K[1],\ b_1[2],\ \ldots,\ b_K[M]]^T,\\ \tilde{\mathbf{n}} &= [\tilde{n}_1[1],\ \tilde{n}_2[1],\ \ldots,\ \tilde{n}_K[1],\ \tilde{n}_1[2],\ \ldots,\ \tilde{n}_K[M]]^T.\end{aligned} \tag{3.15}$$

Using the above notation, it is convenient to express the channel matched filter output (3.14) in matrix-vector product form:

$$\mathbf{y} = \mathbf{RAb} + \tilde{\mathbf{n}}, \tag{3.16}$$

where $\mathbf{R}$ is the $KM \times KM$ packet channel matrix, which is composed of the discrete-time $K \times K$ sub-matrices $\mathbf{R}[i]$, $i \in \{-M+1, M-1\}$. As such it has a block *Toeplitz* structure and also has the *Hermitian* property; its composition is given by:

$$\mathbf{R} = \begin{bmatrix} \mathbf{R}[0] & \mathbf{R}[-1] & \ldots & \mathbf{R}[-M+1] \\ \mathbf{R}[1] & \mathbf{R}[0] & \ldots & \mathbf{R}[-M+2] \\ \vdots & & \ddots & \\ \mathbf{R}[M-1] & \ldots & \mathbf{R}[1] & \mathbf{R}[0] \end{bmatrix}. \tag{3.17}$$

The number of non-zero elements (sub-matrices) in $\mathbf{R}$ depends on the properties of the signature waveforms and asynchronous characteristics of the users; usually non-zero $\mathbf{R}[i]$ exists for $i \in \{-2, 2\}$. The elements of the matrices $\mathbf{R}[i]$ are obtained by the cross-correlation of the user; that is, consider that for $k, l = 1, 2, \ldots, K$ and $a, b = 1, 2, \ldots, M$, the elements of the arbitrary matrix $\mathbf{R}[a-b]$ may be expressed as:

$$\mathbf{R}_{kl}[a-b] = A_k A_l \sum_{m=1}^{L_p} \sum_{n=1}^{L_p} \alpha_{km}\alpha_{ln} \cdot \int_{-\infty}^{\infty} s_k(t) s_l(t-(a-b)T-D)dt, \tag{3.18}$$

where

$$D = \tau_{ln} + \tau_{km} + \theta_l + \theta_k\,. \tag{3.19}$$

3.3 Conventional Receiver

The objective of the front-end of a multiuser detector is to discretize the received continuous-time waveform. Continuous-to-discrete-time conversion is realized by conventional sampling or generally correlating the received signal with a deterministic signal [14]. The simplest strategy to demodulate CDMA signals is to employ a bank of single-user matched filters (SUMF). This is equivalent to using a bank of correlators [16]. Each filter is matched to a signature waveform of a different user and each user is demodulated without any knowledge of the other users.

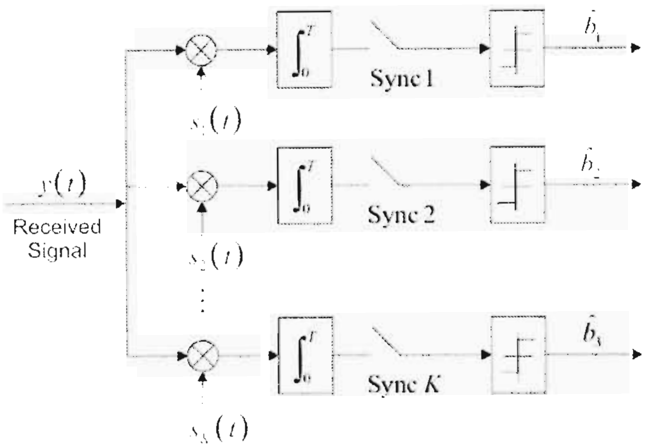

Figure 3.2 A conventional DS-CDMA receiver (Bank of K correlators).

The received signal at the input to a bank of K correlators (SUMF detector), in Figure 3.2, is correlated with each of the K spreading sequences. Sampling occurs at the symbol (or bit) rate i.e. every T seconds. Chip-based receivers are conceptually simpler but sampling is computationally more intensive. Symbol-based receivers employ an additional pre-processing stage to reduce the dimensionality of the received signal by despreading the signal prior to sampling (Figure 3.2). Without loss of generality, the output from the kth user's correlator yields soft estimates of that user's signal. A threshold decision is then made on the output of the kth correlator. The result is antipodal and it represents the kth user's probable transmitted information. The presence of other users is neglected during detection and detection is one-shot in the sense that adjacent bits are not incorporated in the final hard decision. If a bit-synchronous system is assumed then, for the *k*th user, the output of the *k*th correlator, over a bit interval $\left(0 \leq t \leq T\right)$, is given by:

$$y_k = \int_0^T y(t)s_k(t)dt = A_k b_k + \sum_{j=1,j\neq k}^{K} A_j b_j \rho_{jk} + \widetilde{n}_k(t), \tag{3.20}$$

where $\widetilde{n}_k(t)$ is filtered AWGN with variance equal to σ^2, and ρ_{jk} is the synchronous normalized cross-correlation between the *k*th and *j*th users ($\rho_{jk} = 1, \forall\, j = k$). They are defined respectively as:

$$\widetilde{n}_k(t) = \int_0^T n(t)s_k(t)dt \tag{3.21}$$

and

$$\rho_{jk} = \int_0^T s_j(t)s_k(t)dt\,. \tag{3.22}$$

In (3.20), y_k is composed of the transmitted bit $A_k b_k$, the MAI due to non-zero cross-correlations between users (sequences) and AWGN $\widetilde{n}_k(t)$. MAI does not change with SNR. Thus, a BER floor is always exhibited by the SUMF, regardless of whether the system is synchronous or asynchronous (unless the sequences are fully orthogonal and orthogonality is maintained). In the latter case the receiver is more vulnerable to MAI since time offsets can result in higher cross-correlations depending on the spreading codes used. Then, the adverse effect of a near-far situation is enhanced.

Similar to the derivations in Section 3.2, (3.20) is written in matrix-vector form as:

$$\mathbf{y} = \mathbf{RAb} + \mathbf{n}\,, \tag{3.23}$$

where $\mathbf{R}$ is now the $K \times K$ normalized cross-correlation matrix with $R_{ij} = \rho_{ij}$ (for the synchronous case) and $\mathbf{A}$ is the diagonal matrix containing the amplitudes of all users. Unless otherwise stated, this definition of $\mathbf{R}$ is implied henceforth in this chapter. The definitions for $\mathbf{y}$, $\mathbf{b}$ and $\mathbf{A}$ follow closely to those in Section 3.2, with:

$$\begin{aligned} \mathbf{y} &= [y_1, \quad \ldots, \quad y_K]^T, \\ \mathbf{b} &= [b_1, \quad \ldots, \quad b_K]^T, \\ \mathbf{A} &= \mathrm{diag}[A_1, \quad \ldots, \quad A_K]. \end{aligned} \tag{3.24}$$

The noise vector $\tilde{\mathbf{n}}$ in (3.23) is made up of i.i.d. zero mean Gaussian random variables with covariance matrix $E[\tilde{\mathbf{n}}\tilde{\mathbf{n}}^T] = \sigma^2\mathbf{R}$, where T denotes the transpose operation. The output of the conventional receiver is determined by the (symmetrical) hard decision, so the estimated transmitted information is given by:

$$\hat{\mathbf{b}} = \mathrm{sgn}(\mathbf{y}), \tag{3.25}$$

where

$$\mathrm{sgn}(x) = \begin{cases} +1, & x \geq 0 \\ -1, & x < 0 \end{cases} \tag{3.26}$$

For a single-user channel $(K = 1)$ the matched filter method is optimal in the sense that it maximizes the SNR of the decision statistic Y [14], which represents the output of the SUMF. If the noise is Gaussian then it can be shown that the matched filter minimizes the probability of error. Its output is a sufficient statistic to achieve the lowest probability of error [14], given by[2]:

$$P_{e,1} = Q\left(\frac{A_1}{\sigma}\right). \tag{3.27}$$

The error probability is that of a single user employing binary antipodal signalling (BPSK) in an AWGN channel [16]. In synchronous OCDMA ($\rho_{jk} = 0, j \neq k$), the

E_b is different

$= \frac{1}{2}$

$= 1$

[2] $Q(x)$ denotes the Q-function, which is defined as $Q(x) = \frac{1}{\sqrt{2\pi}} \int_x^\infty e^{-\frac{t^2}{2}} dt$

system effectively consists of K non-interfering single-user channels. Thus the same error probability would be obtained by each user, which is ideal. Therefore, in practice the error probability for user k of any multiuser detector is lower bounded by the single-user error probability:

$$P_{e,k} \geq Q\left(\frac{A_k}{\sigma}\right). \tag{3.28}$$

The assumption that the users sharing the channel are transparent to each other is valid only when the spreading sequences are orthogonal and remain so at the receiver. However, orthogonality is lost since the signals that pass through the wireless (fading) channel often arrive at the base station with random delays. In the non-orthogonal case, the error probability of the SUMF detector is affected by the cross-correlations between sequences and its performance degrades as the number of users increases since the MAI increases. This can be seen by considering a simple two-user scenario [14]. In that case, by expanding (3.20), the correlator outputs are:

$$y_1 = A_1 b_1 + A_2 b_2 \rho_{21} + \tilde{n}_1, \tag{3.29}$$

$$y_2 = A_2 b_2 + A_1 b_1 \rho_{12} + \tilde{n}_2. \tag{3.30}$$

Since there are only two synchronous users, it is convenient to adopt the notation in which $\rho_{12} = \rho_{21} = \rho$. The error probability of the conventional receiver for user 1 in the presence of one other interfering user [14] is given as:

$$P_{e,1} = \frac{1}{2}\left[Q\left(\frac{A_1 - A_2|\rho|}{\sigma}\right) + Q\left(\frac{A_2 + A_1|\rho|}{\sigma}\right)\right]. \tag{3.31}$$

By interchanging the roles of user 1 and user 2, the error probability of user 2 can be obtained [14]. The error probability is the same for both users, provided they have equal amplitudes. Since the Q-function is monotonically decreasing, (3.31) is dominated by the term with the smaller argument and so the upper bound is given by,

$$P_{e,1} \leq Q\left(\frac{A_1 - A_2|\rho|}{\sigma}\right). \tag{3.32}$$

This shows that, if the interferer is not dominant, the bound is less than $1/2$ (due to the Q-function) and the SNR for the conventional receiver ($K = 2$) reduces to:

$$SNR_{out} = \left(\frac{A_1 - A_2|\rho|}{\sigma}\right)^2. \tag{3.33}$$

This performance degradation is shown in Figure 3.3 [14], for two equal-power users. The MAI increases the BER of user 1 beyond the single-user bound (3.28). When the relative amplitude of the interferer is greater than the desired user, i.e.

$$\frac{A_2}{A_1} > \frac{1}{|\rho|}, \tag{3.34}$$

then the near-far problem is experienced, as shown in Figure 3.3 (for two users [14]).

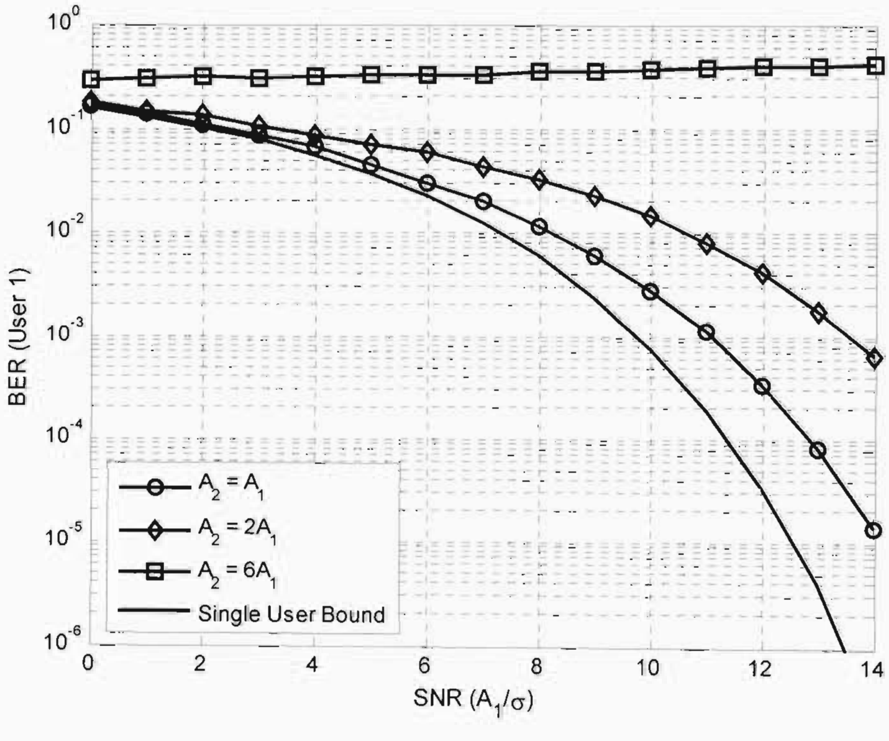

Figure 3.3 BER performance of the conventional detector with 2 synchronous users, for varying powers of the interfering user. $K = 2, \rho_{kl} = 0.2$.

As the strength of the interferer increases, erroneous decisions occur with probability 1/2 (Figure 3.3). It clearly emphasizes the need for tight power control due to the adverse effect that the higher-powered interferer has on the desired user.

The error probability analysis can be extended for K (asynchronous) users [14]. A Gaussian approximation (in Appendix B) is also useful for showing the effect of increasing the number of users, when it becomes difficult to compute the K-user error probability. However they are mostly accurate for low SNR. In DS-CDMA, the error probability in general depends on the relative amplitudes of the received signals, (partial) cross-correlation values between spreading sequences and the noise power. Cross-correlation values are affected by how much one symbol overlaps with another. This, in turn, depends on the transmission instants of the individual users and their distances from the base station, which often are time-varying.

The conventional receiver performs optimally in a synchronous DS-CDMA system with no channel ISI, orthogonal spreading codes, equal-power users and no inter-cell interference. It is a simple detection strategy with low computational complexity and is also capable of decentralized demodulation. However, the SUMF is interference limited i.e. its output is dominated by MAI; a typical mobile radio channel dictates that no matter the type of spreading sequences, there are always random delays and received powers for which errors occur even in the absence of white noise.

Although the synonymous near-far problem may be overcome using power control techniques, such methods come at the cost of complexity. Near-far resistant detectors are required for this very reason. Furthermore, there is still the problem of MAI, which lowers the BER performance of the SUMF receiver. Several methods are aimed at reducing MAI, as well as providing near-far resistance. This includes well designed spreading sequences, use of smart antennas, channel coding, and interference cancellation/data detection techniques [20], [21], [26], [27], [35]. Ideally, and in practice, a combination of these methods is required to provide a near-optimal, near-far resistant solution and hence a successful CDMA implementation.

3.4 Decorrelating Detector

The linear decorrelating detector (LDD), shown in Figure 3.4, was first proposed by Lupas and Verdú [28]. It is a linear detection scheme in the sense that it performs a linear transformation on the received vector of samples (which are the soft outputs of the bank of matched filters). Its objective is to reduce MAI and this is achieved by decoupling the information of the interfering users from the desired user.

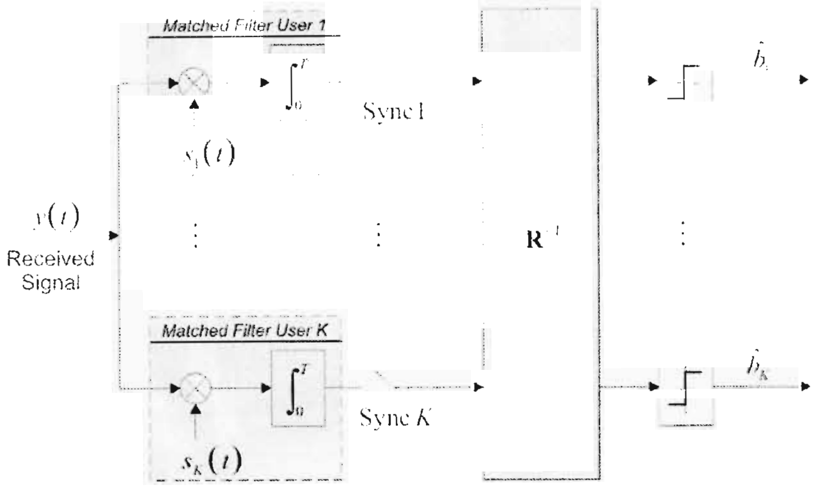

Figure 3.4 Linear decorrelating detector model (synchronous channel).

The non-diagonal terms in the cross-correlation matrix $\mathbf{R}$ are an indication of the amount of MAI that will be experienced at the output of the matched filter. It may be the result of an asynchronous channel, spreading sequences, phase offsets (due to fading) for example, or a combination of all of these.

The LDD effectively cancels out the effect of the non-diagonal terms by applying the inverse of the cross-correlation matrix $\mathbf{R}^{-1}$, as the linear transformation, on the soft outputs of the matched filters (Figure 3.4). In the absence of noise, (3.16) is given by

$$\mathbf{y} = \mathbf{RAb}. \tag{3.35}$$

Then (assuming $\mathbf{R}$ is invertible), it can be shown that the transmitted bits are correctly detected by simply multiplying the matched filter outputs to $\mathbf{R}^{-1}$, i.e.

$$\begin{aligned}\hat{\mathbf{b}}^{DD} &= \operatorname{sgn}\left(\mathbf{R}^{-1}\mathbf{y}\right) \\ &= \operatorname{sgn}\left(\mathbf{R}^{-1}\mathbf{RAb}\right) \\ &= \mathbf{b}\end{aligned} \tag{3.36}$$

The signature waveforms of the users are required to be linearly independent [14] to ensure that $\mathbf{R}$ is invertible. Thus, in the absence of noise, each user is perfectly detected, unlike in the conventional receiver. When the background noise is taken into consideration, then processing the matched filter outputs with $\mathbf{R}^{-1}$ results in:

$$\begin{aligned}\mathbf{R}^{-1}\mathbf{y} &= \mathbf{R}^{-1}\left(\mathbf{RAb}+\tilde{\mathbf{n}}\right) \\ &= \mathbf{Ab}+\mathbf{R}^{-1}\tilde{\mathbf{n}}.\end{aligned} \tag{3.37}$$

The output is still free from MAI and the only source of interference is the background noise. However the noise term $\tilde{\mathbf{n}}$ is now amplified, with the new noise term now equal to $\mathbf{R}^{-1}\tilde{\mathbf{n}}$. Its variance is obtained from

$$E\left\{\left(\mathbf{R}^{-1}\tilde{\mathbf{n}}\right)\left(\mathbf{R}^{-1}\tilde{\mathbf{n}}\right)^T\right\} = \sigma^2\mathbf{R}^{-1}. \tag{3.38}$$

Thus when the background noise is dominant (low SNR), then unless all users are completely orthogonal to each other, it is possible that the LDD performs worse than the conventional receiver since the AWGN is enhanced at its output. This may occur even when the interfering amplitude is small. Furthermore, there exist cross-correlation matrices for which the conventional receiver achieves better performance (in terms of bit errors) than the LDD, irrespective of the SNR [14].

From an implementation standpoint, knowledge of the received amplitudes is not required, so no estimation is involved. When the amplitudes are unknown the LDD is optimal in the sense that it corresponds to the maximum-likelihood sequence (MLS) detector i.e. it yields the joint maximum-likelihood sequence estimation of the transmitted bits and their received amplitudes [20]. The LDD is also capable of optimum near-far resistance [36]. This is evident from the kth user's probability of error, which is given in [28] as:

$$P_{e,k}^{LDD} = Q\left(\frac{A_k}{\sigma}\sqrt{1-\mathbf{a}_k^T\mathbf{R}_k^{-1}\mathbf{a}_k}\right), \tag{3.39}$$

where $\mathbf{a}_k$ is the kth column of $\mathbf{R}$ without the diagonal elements and $\mathbf{R}_k$ is the $(K-1)\times(K-1)$ matrix that results by striking out the kth row and kth column in $\mathbf{R}$. The kth user's probability of error is completely independent of the amplitudes of the interfering users, indicating that the LDD is optimally near-far resistant. Figure 3.5 illustrates the performance of the LDD. The simulation agrees with the bound analysis (3.40) for $K = 2$. Also, the comparatively poor performance at low SNR is verified, but at higher SNR it clearly outperforms the conventional receiver.

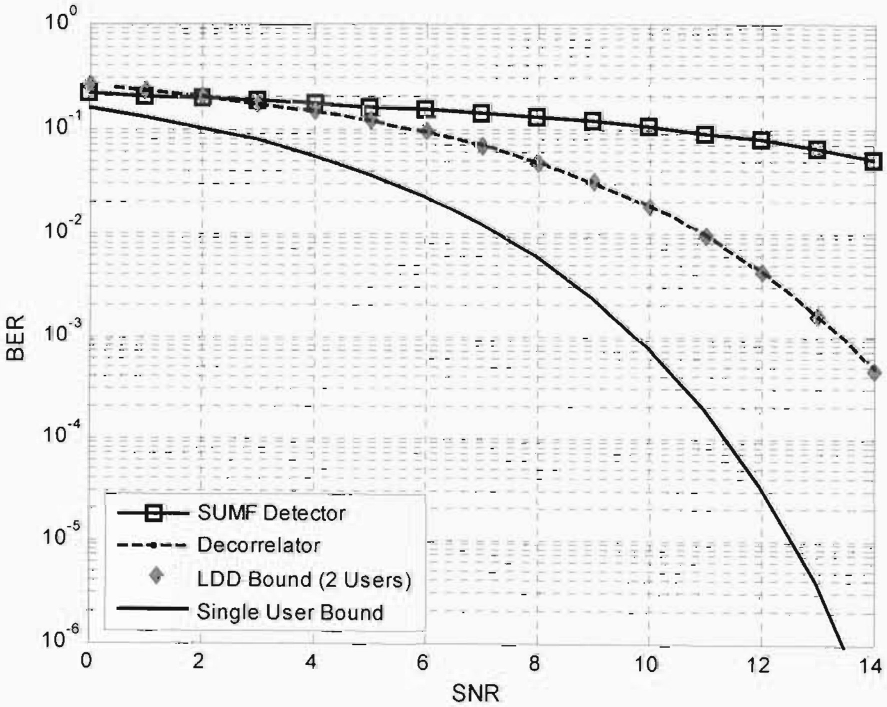

Figure 3.5 Comparative BER performance (for user 1) of the LDD and the SUMF detector for $K = 2$ users, with respective bounds.

One advantage of the LDD is that each user can be detected independently of the other users. Furthermore, demodulation can occur over a single bit interval. It has a lower computational complexity than the MLS detector. However, the computations required for matrix inversion are difficult to perform in real-time, especially for asynchronous transmissions (when $\mathbf{R}$ is of the order NK). Despite this drawback, it generally offers greater benefits (performance/capacity gains) than the conventional receiver and has received relatively more interest than other sub-optimal schemes [20], [21], [35]. Research into the LDD, has provided several methods, including hybrid techniques, which reduce the complexity associated with matrix inversion.

3.5 Minimum Mean-Square Error Detector

The linear minimum mean-square error (MMSE) multiuser detector achieves the balance between the cancellation of MAI and the enhancement of background noise. It does so by utilizing the knowledge of the received signal powers and accounting for the noise. Since the matched filter detector is better than the LDD for low SNR, it makes sense to incorporate the SNR of the different users to achieve better performance. This is the case with the MMSE solution (Figure 3.6).

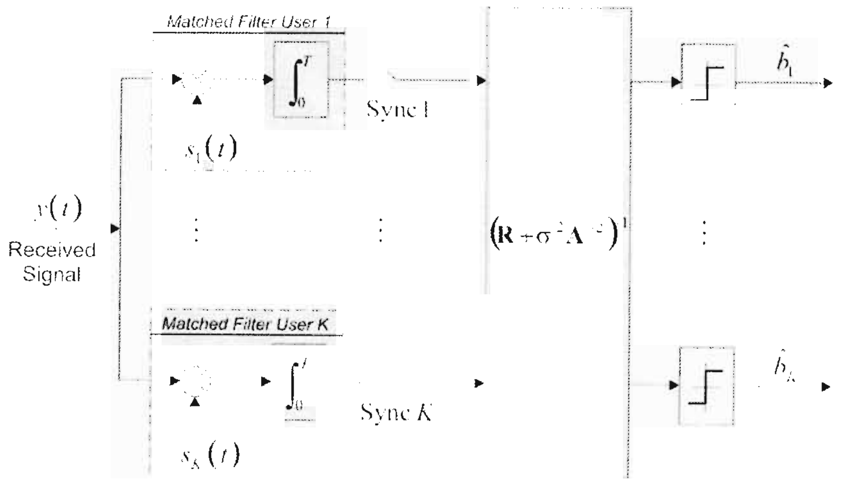

Figure 3.6 Model of the MMSE detector (for the synchronous channel).

This linear detection scheme is based on the MMSE criterion that is used for equalization. The goal is to find a linear mapping which minimizes the mean-square error (MSE) between the transmitted data and the output of the detector,

$$E\left[\left\|\mathbf{b}-\hat{\mathbf{b}}\right\|^2\right]. \tag{3.41}$$

If we define $\mathbf{M}$ as the linear filter which processes the output of the conventional receiver $\mathbf{y}$, then the output of the MMSE detector is

$$\hat{\mathbf{b}}^{MMSE} = \operatorname{sgn}(\mathbf{My}). \tag{3.42}$$

The solution is found by choosing transformation $\mathbf{M}$ that satisfies the MSE criterion:

$$\min_{\mathbf{M}\in R^{K\times K}} E\left[\left\|\mathbf{b}-\mathbf{My}\right\|^2\right]. \tag{3.43}$$

The linear transformation that achieves this minimization [14] is given by

$$\mathbf{M}_{MMSE} = \left[\mathbf{R}+\sigma^2\mathbf{A}^{-2}\right]^{-1}, \tag{3.44}$$

where

$$\sigma^2\mathbf{A}^{-2} = \operatorname{diag}\left[\frac{\sigma^2}{A_1^2},\ \ldots,\ \frac{\sigma^2}{A_K^2}\right] \tag{3.45}$$

The MMSE detector, like the LDD, is capable of decentralized demodulation [37]. For the *k*th user, the output of the linear MMSE detector (in Figure 3.6) is given by:

$$\hat{b}_k^{MMSE} = \operatorname{sgn}((\mathbf{My})_k). \tag{3.46}$$

The compromise that is offered by the MMSE detector can be seen from (3.44); if the received amplitudes are fixed, then for high SNR $(\sigma \to 0)$,

$$\left[\mathbf{R}+\sigma^2\mathbf{A}^{-2}\right]^{-1} \to \mathbf{R}^{-1}. \tag{3.47}$$

Thus, the MMSE scheme converges to the LDD. This means that it is also capable of the same optimum near-far resistance. However, for low SNR $(\sigma \rightarrow \infty)$, the MMSE detector approaches the conventional receiver in the sense that (3.44) becomes a strongly diagonal matrix [14].

The error probability of the MMSE detector is not as simple as that of the LDD. This is because the decision statistic at the output is not Gaussian, but is made up of additive noise plus MAI. To analyze the probability of a bit error we consider, without loss of generality, the linear detection of bit b_1. As shown in [37], for any linear detector of the form (3.46), it follows from the sufficient output (3.23) that this bit is given by the decision on

$$\frac{(\mathbf{My})_1}{B_1} = \left(b_1 + \sum_{k=2}^{K} \beta_k b_k \right) + \frac{\sigma}{B_1} \bar{n}_1 , \tag{3.48}$$

where $\{\beta_1, \ldots, \beta_K\}$ are the leakage coefficients defined as

$$\beta_k = \frac{B_k}{B_1}, \tag{3.49}$$

which quantifies the contribution of the *k*th interferer to the decision statistic, relative to the contribution of the desired user [7], with

$$B_k = A_k (\mathbf{MR})_{1,k} \tag{3.50}$$

and where

$$\bar{n}_1 \sim N\left(0, (\mathbf{MRM})_{11}\right). \tag{3.51}$$

The probability of error is then given by

$$P_{e,1}^{MMSE} = 2^{1-K} \sum_{b_2,\ldots,b_K \in \{-1,1\}^{K-1}} Q\left(\frac{A_1}{\sigma} \frac{(\mathbf{MR})_{1,1}}{\sqrt{(\mathbf{MRM})_{1,1}}} \left(1 + \sum_{k=2}^{K} b_k \beta_k \right) \right). \tag{3.52}$$

The computational complexity that results from (3.52) increases exponentially with the number of users and this complexity is further increased by the calculation of the leakage coefficients. For simplification, a valid approximation is to replace the binomial distribution of the MAI, represented by the summation term in (3.48), with a Gaussian distribution with same variance. The accuracy of this approximation is supported in [37]. Figure 3.7 indicates the gain in BER performance of the MMSE detector over the SUMF receiver, for 8 synchronous equal-power users with equal simulated cross-correlation of $\rho_{jk} = 0.8$ [14]. The single-user AWGN bound (3.27) is also plotted to compare this sub-optimal scheme to the optimal single-user bound.

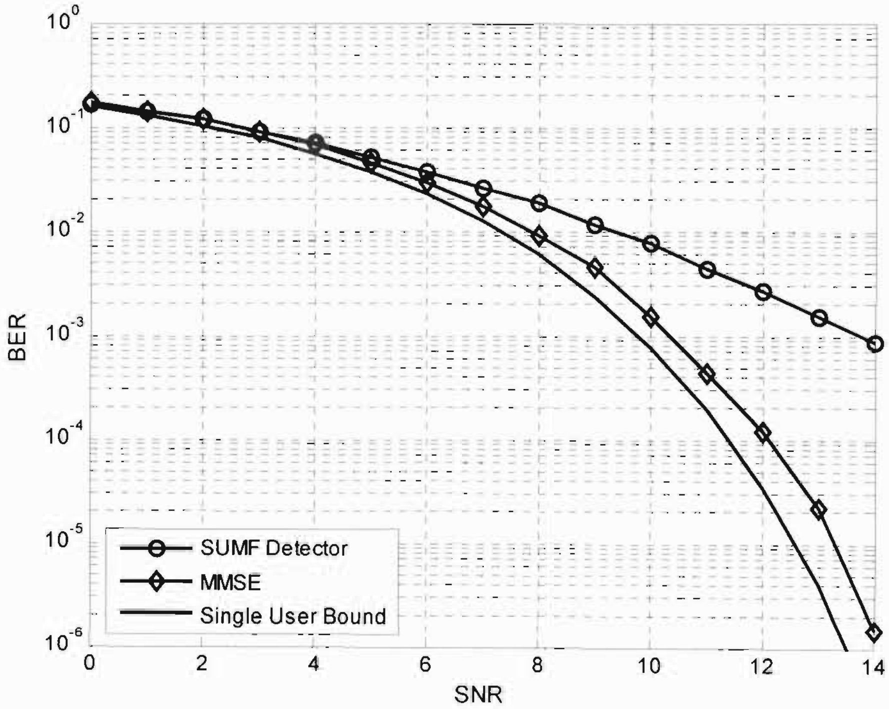

Figure 3.7 BER performance of MMSE detector, in a synchronous AWGN channel, with equal power users. $K = 8$, $\rho_{kl} = 0.1$.

The MMSE receiver compromises between perfect decorrelation and noise amplification. The LDD and SUMF receiver are limiting cases of the MMSE detector [14], [37]. However, while it accounts for noise and MAI, unlike the LDD, it does impose the same computational disadvantages such as matrix inversion. In addition to knowing all the signature waveforms, knowledge of the received powers of the interfering users is required and thus estimation is necessary. For high SNR, if the signature waveforms are linearly independent, the complexity incurred for knowing the received SNR does not justify the performance improvement over the LDD. The MMSE detector is often implemented adaptively, which does not require knowledge of the signature waveforms, channel and that of the received powers [37].

3.6 Optimum Multiuser Detection

The optimum multiuser detector (OMD) for the AWGN channel, proposed by Verdú [7], is based on the criterion of maximum likelihood sequence estimation (MLSE), in which the maximization of a cost function leads to the joint optimum detection of all users. The K-user MLSE detector (Figure 3.8) employs a bank of matched filters followed by the Viterbi linear programming algorithm, which estimates the most likely set of transmitted bits for all the users. Sequence detection has several advantages over one-shot detection strategies since the observation is taken over the entire received waveform to produce a sufficient statistic for any symbol decision.

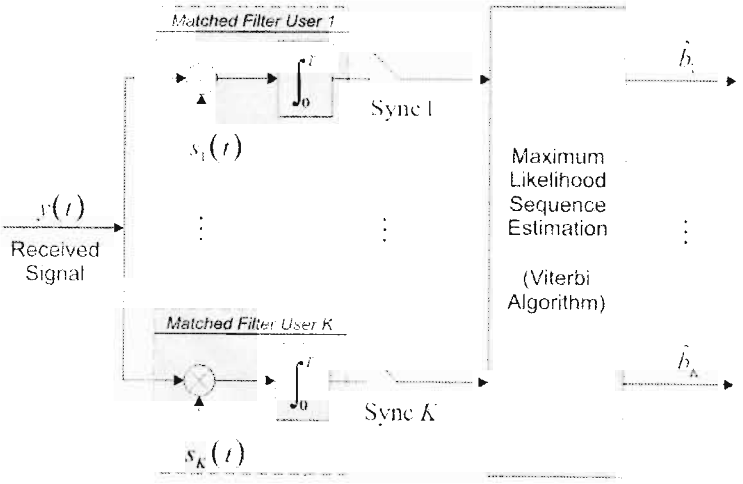

Figure 3.8 Block diagram of the Optimum Multiuser Detector.

The objective of the MLSE detector is to find the input sequence that maximizes the probability conditioned on the given output sequence i.e. $P(\mathbf{b}\,|\,\mathbf{y})$, which is a globally optimum or maximum likelihood sequence. This probability is referred to as the joint *a posterior* probability. If all sequences are equiprobable, then the objective is to choose the most likely transmitted vector, which is the output of the MLSE detector, given by $\hat{\mathbf{b}} = \left[\hat{b}_1, \ldots, \hat{b}_K\right]^T$, such that it maximizes the probability of receiving the signal $\mathbf{y}$ on the condition that vector $\mathbf{b}$ was sent, i.e.

$$\hat{\mathbf{b}}^{\text{Opt}} = \arg \max_{\mathbf{b}\in\{-1,1\}^K} P(\mathbf{y}|\mathbf{b}). \tag{3.53}$$

This is equivalent to maximizing the log-likelihood function [7] given by

$$\Omega(\mathbf{b}) = 2\mathbf{b}^T\mathbf{A}\mathbf{y} - \mathbf{b}^T\mathbf{H}\mathbf{b}, \tag{3.54}$$

where $\mathbf{y}$ is the column of matched filter outputs, $\mathbf{A}$ is the $K \times K$ diagonal matrix of received amplitudes, such that

$$\begin{aligned} \mathbf{y} &= [y_1, \quad \ldots, \quad y_K]^T, \\ \mathbf{A} &= \operatorname{diag}\{A_1, \quad \ldots, \quad A_K\}, \end{aligned} \tag{3.55}$$

and $\mathbf{H}$ is the un-normalized cross-correlation matrix [14] defined as

$$\mathbf{H} = \mathbf{ARA}. \tag{3.56}$$

Equation (3.54) indicates that $\mathbf{y}$ is a sufficient statistic for the optimum detection of the transmitted data $\mathbf{b}$. However, it is solved by performing an exhaustive search through each of the possible sequences until the combination that maximizes the log-likelihood function is found, which is clearly not feasible for large systems.

The issue surrounding the maximization of (3.54) is discussed shortly but first we state the fundamental quantity of interest, which is the minimum error probability.

Optimum performance is attributed to the MLSE detector and the lower bound for the probability of error, which is derived in [7], is given by:

$$P_{e,k}(\sigma) \geq 2^{1-\omega_{k,\min}} Q\left(\frac{d_{k,\min}}{\sigma}\right), \tag{3.57}$$

where $\omega_{k,\min}$ is the smallest weight $\omega(\boldsymbol{\varepsilon})$, of all the error vectors, with $\boldsymbol{\varepsilon} = \mathbf{b} - \hat{\mathbf{b}}$ denoting the error vector and $\omega(\boldsymbol{\varepsilon})$ denoting the number of non-zero components (weight) of an error vector that is given by

$$\omega(\boldsymbol{\varepsilon}) = \sum_{k=1}^{K} |\varepsilon_k|, \tag{3.58}$$

and with $d_{k,\min}$ representing one half of the minimum distance between two multiuser signals that differ in the *k*th bit.

Besides yielding the most likely transmitted sequence, this detector offers optimum asymptotic multiuser efficiency and near-far resistance [7], [14], [18]. Intuitively, the average optimum near-far resistance with synchronous random DS-SS waveforms is a function of the number of users and processing gain. While optimal (near-far resistant) multiuser demodulation can be achieved via the maximization of an integer quadratic function, in context of practical implementation, it has several disadvantages. Besides knowing all the spreading sequences, estimates of the delays, carrier phases and the receiver power of all the users are required. These are not known *a priori* and estimation adds to the overhead incurred during implementation.

The most important issue is the one of computational complexity, since the problem of solving (3.54) is combinatorially hard. It is for this reason that the optimal detector is impractical to use in current DS-CDMA systems. This problem is made clear by considering a K-user system. Over a bit interval, where $b_k \in \{-1, 1\}$ occurs with equal probability, there exists 2^K different combinations of $\mathbf{b}$, one of which is the most likely transmitted sequence. In [7] it was shown that the maximum likelihood sequence receiver, proposed for asynchronous channels, can be implemented using the Viterbi algorithm. In that case, **R** is defined according to (3.17) and a dynamic programming algorithm, such as the Viterbi algorithm, maximizes (3.54). Without it, in the MLS approach, a brute-force maximization of (3.54) would require a complexity of $O(2^{KM})$ [20] i.e. a search through 2^{MK} possible **b** vectors. This is not practical, especially if it is considered that the growth in complexity is exponential in the number of users.

By employing the Viterbi algorithm, the optimal detector has complexity $O(2^{K})$. This complexity makes the optimal detector practical when the number of users in the system is relatively small. Unfortunately, in practice this is seldom the case. No algorithm is known for optimal multiuser detection whose complexity is polynomial in the number of users. In optimization literature this is denoted as an NP-complete problem. It will be shown, in the chapters to follow, that neural networks are well suited to solve combinatorial optimization problems, and their success in the field of optimization (e.g. TSP) justifies their application to MUD.

Due to the resulting complexity issues, research has concentrated on sub-optimal detectors that are near-far resistant, have a relatively low complexity and compare in performance to the optimal detector. The LDD and MMSE schemes, which have been discussed, are examples of such sub-optimal MUD strategies and they also include adaptive and blind detection schemes. Nevertheless, the performance of the OMD serves as a benchmark for the current and future sub/near-optimal schemes.

3.7 Summary

This chapter highlighted the need for multiuser detection in order to reduce MAI and overcome the near-far problem in multiuser communications, particularly in the reverse link (uplink) of a cellular network. The conventional single-user strategy was discussed, the performance of which motivates the need for joint detection techniques. An asynchronous model for a DS-CDMA system was presented, for which synchronous transmission can easily be adopted. A review of two popular sub-optimal receivers for the CDMA channel was provided. Clearly there is a need for sub-optimal joint detection schemes which balance complexity and performance. The linear schemes, discussed herein, have the advantage of being computationally simpler than non-linear IC schemes. Furthermore, they are able to perform decentralized demodulation. They have been shown to outperform the SUMF detector, via simulations, and are capable of near-far resistance.

The benchmark for all sub-optimal schemes is the optimal MUD solution, which due to its prohibitive computational complexity makes it undesirable for current DS-CDMA applications, despite its optimum near-far resistance property and optimum BER performance. This is the main reason for sub-optimal schemes, however even the most popular linear sub-optimal implementations are dependent on information like spreading sequences and channel parameters such as delays and phases. Furthermore, while these schemes offer comparable performance, their main objective is to reduce background noise and MAI. It is possible then that detection strategies which are designed to operate directly on the maximum-likelihood objective function will be capable of near-optimal performance.

4 Neural Networks

4.1 Introduction

Neural networks, or artificial neural networks to be more precise, constitute a major part of the field of distributed artificial intelligence (AI). In the broad sense, AI incorporates several areas of computing that attempt to mimic the signal processing that occurs in the human brain [38]; usually these are the processes that are carried out without much consciousness. In this regard, it may be defined as the intelligence exhibited by any manufactured (artificial) system and thus it is also known as machine intelligence. But this definition begs the question of "what is regarded as intelligence?" Foremost, AI is the scientific investigation into theory and practical application of artificially intelligent systems and learning models, all of which is rooted in the neurosciences [39].

Modern AI research is focussed on application in the engineering fields. While it is concerned with the production of useful machines to automate human tasks requiring intelligent behavior, AI is also the source for providing solutions to a number of diverse underlying engineering problems, especially in research. They find application in business, medical fields, military installations, and even in our homes, on our personal computers. It may be software alone or a meld of software and hardware. Like most sciences, AI is decomposed into a number of sub-disciplines (or techniques) that, while sharing an essential approach to problem solving, are concerned with different applications.

The discipline of AI stemmed from the potential of neural computation models, known as neural networks. Although, it is worth pointing out that neural networks (or connectionist models) are distinguished from classical AI. In general, classical AI research involves symbolic manipulation of abstract concepts [38], and is the methodology used in most expert systems which is one sub-discipline. Expert systems perform domain-specific problem solving by combining a theoretical understanding of the problem and a collection of heuristic problem-solving rules that has shown to be effective. It is likened to a human expert who must use knowledge and experience to solve a problem. Most expert systems have been written for relatively specialized fields that are generally well studied and have clearly defined problem-solving strategies [39]. Problems that depend on a more loosely defined notion of "common sense" have a greater difficulty in being solved by these means.

Parallel to classical systems are connectionist systems. They attempt to evolve or learn using intelligence by building systems and then improving on them through some automatic process rather than systematically designing something to complete the task. Artificial neural networks are the best-known examples.

In its most general form, a neural network (NN) is an adaptive machine that is designed to model the way in which the brain performs a particular task or function of interest [38]. It captures and represents input/output relationships and is able to perform useful computations through the process of learning [40]. The relationships may be linear or complex non-linear and can be learnt from the data being modelled. The network is characterized by the number and the type of connections between the simple computing cells which constitutes it, namely neurons, and its operation is governed mathematically through a set of learning rules. The unique organization and connection of neurons results in different types of neural networks. It is worth noting that the term "neural" is used in the sense that these networks have been inspired by neuroscience (scientific study of the human brain and nervous system) and not necessarily because they are concerned with faithfully modelling biological neural phenomena [39]. NN theory, however, still appeals to biological realism.

It is well known that neural networks are viable computational models for a wide variety of problems. They find application in a diversity of fields such as pattern recognition, image analysis, signal processing (equalization), clustering algorithms, computational neuroscience, statistical physics, and control theory [38], [40]. Consequently, a large variety of mathematical tools and methods are used: statistical mechanics, probability theory, linear algebra, Lyapunov functions and theory of dynamical systems, and combinatorial optimization tools. The technology is rooted in several disciplines, namely engineering, mathematics, physics, statistics, medical (neuroscience), and geology [38]. Their suitability for use in these fields is the result of several important factors. Firstly, their operation is usually free from assumptions; they have the ability to learn and hence generalize. Their inherent distributed nonlinearity is important for accepting non-linear inputs (such as speech signals). They are adaptive and can thus respond to changes in the operating environment. Furthermore, they are able to handle noisy data in difficult non-ideal contexts, even when the available knowledge is regarded as sufficient to use conventional modelling or a statistical approach. This type of robust computation depends on the algorithm that is used to train the network.

The description and ability of a neural network is usually clarified in the context of formal neurons (described in Section 4.2), and the parallel distributed processing that is achieved by a network having a vast composition of interconnected neurons (similar to the human brain). The massive interconnection of these neurons gives to neural networks its characteristics and functionality in the field of machine learning. Based on this, a neural network may be defined as a massively parallel distributed processor with the natural tendency to store knowledge through the process of learning and to make it available for use [38]. Although there is no universal definition, there are several other accepted definitions, which have been proposed by authors and researchers alike, usually expressing the same fundamental idea.

In recent years, neural network research has received a steadily growing interest from different scientific disciplines, like those mentioned above. This multidisciplinary atmosphere has proven to be very inspiring and has led to a fairly deep grounding of neural network theory in classical theoretical approaches as well as to numerous applications, and importantly in industry. The engineering field has definitely benefited. In the field of signal processing and communications, neural networks have been utilized successfully as adaptive equalizers [8], [9], [16] and have progressed considerably in field of MUD in DS-CDMA [11], [31]–[34], [41]–[54]. Although many classical methods are used, their connection and joint application yields a number of new results. In some cases known methodology has to be extended to achieve reasonable results, such as with recurrent type neural networks.

4.1.1 Brief History

The era of neural networks and computational modelling began with work by McCulloch and Pitts in 1943 [40], however, the idea of modelling biological neurons was introduced much earlier. McCulloch and Pitts combined neurophysiology with mathematical logic [39]. In their work, the simple processing unit, called the neuron, was introduced. The formal neurons were presented as models of biological neurons and as conceptual components for circuits. They were designed to operate as switches. The authors showed that, conditioned on a reasonable set of parameters, a network made up of these units, in principle, could perform universal computation. It is generally agreed that this paper herald the birth of AI and neural networks.

Over the years, there were several works on the detailed logic of threshold networks. The robustness of parallel processing was realized and at the same time the significance of statistical mechanics increased in the context of this subject matter. Known as neurodynamics, this approach used differential equations to describe the behaviour of neural activity [40].

A major development (around 1949) was the proposal by Hebb that, biologically, the connections in the brain change to accommodate for learning different tasks [38]. Hebb introduced the learning rule for synaptic modifications in the brain. This is well known as Hebb's *postulate of learning*, which roughly states that the strength of the connection between two neurons increases depending on their states. This inspired the development of models of adaptive (learning) systems.

The idea of artificially intelligent systems that could mimic human behaviour, even in elaborate context, began as an experimental field (known as AI) in the 1950s with such pioneers as Allen Newell and Herbert Simon who founded the first artificial intelligence laboratory at Carnegie Mellon University, and John McCarthy and Marvin Minsky, who founded the MIT AI Lab in 1959 [39], [40]. Minsky's work in 1961 detailed what is now known as neural networks.

The first learning algorithm was proposed by Frank Rosenblatt. He focused on finding appropriate weights for certain tasks [40] and introduced a novel method of supervised learning for pattern recognition, in his work on the perceptron. The perceptron consists of two layers of neurons with feedforward connections. It was introduced as a processing element that produced an output based on a decision taken on the weighted sum of its input signals. Rosenblatt's main contribution was proving the convergence of the learning rule, for ways of updating the NN weights to perform specific computations. This paved the way for classifying tasks. It was proven that if sets of parameters exist for carrying out a task correctly, then the perceptron algorithm finds one set [39]. During this period, neural networks were considered to be capable of brain-like computation. Although this was greatly exaggerated, it resulted in new training algorithms and trainable networks for tasks like adaptive pattern classification and it also opened up research into multi-layered networks.

In 1969, two authors Minsky and Papert showed that the perceptron was flawed and that the convergence theorem only applied to certain tasks. Elementary computations (such as the popular XOR operation) could not be performed by the single-layer perceptron [40]. They further concluded that this problem (of finding the correct weights) would exist in multi-layered perceptrons. This saw the demise of perceptron research, and except for the neurosciences, it is generally the view that neural network research fell into a depression thereafter. However, the idea of (associative) content addressable memory (CAM) was soon revived. In conjunction the field of self-organizing maps, which employs unsupervised competitive learning that is motivated by topological ordered maps in the brain, was introduced.

In the 1980's several major contributions to the NN field revived interest. The work by physicist John Hopfield on the Hopfield neural network (HNN) stands out and now forms the basis for the recurrent neural network (RNN) [55]. His research extended on using statistical mechanics in networks utilizing the McCulloch-Pitts model. He introduced the idea of an energy function and emphasized the notion of memories as dynamically stable attractors in the energy space of the network. Moreover, he established the isomorphism between the RNN with symmetric connections and the Ising model of statistical physics [38], and later drew on spin-glass models. His work drew much interest, as well as some controversy regarding the originality of the ideas. Nevertheless, the principle of storing and retrieving information using a dynamically stable RNN was made explicit in Hopfield's paper.

In the related field of combinatorial optimization, simulated annealing (SA) was introduced by Kirkpatrick *et al.* [56] to solve combinatorial optimization problems. Later, Hinton and Sejnowski (cited in [39]) developed the Boltzmann machine using stochastic neurons. It employs SA and resembles a thermodynamic process. It was the first successful multi-layered network, which aided in dispelling some of the damaging work of Minsky and Papert (cited in [40]). The Boltzmann machine is an extension of the HNN. It helped develop the idea of employing stochastic techniques and concepts from statistical mechanics for solving optimization problems.

Before discussing the HNN, we first consider the basic neural network architecture in terms of two basic structures and the fundamental component, the artificial neuron.

4.2 Conceptual Architecture of Neural Networks

The research in neural networks is largely motivated by the idea of wholly artificial computing networks that have the ability to operate and make decisions without human intervention. Yet, as the term implies, it was originally aimed more at modelling networks of real neurons in the brain [40]. From a neurophysiological viewpoint, the models are very simplified. However, they continue to develop and provide insight into the brain's ability to compute and make decisions based on experience while processing difficult tasks.

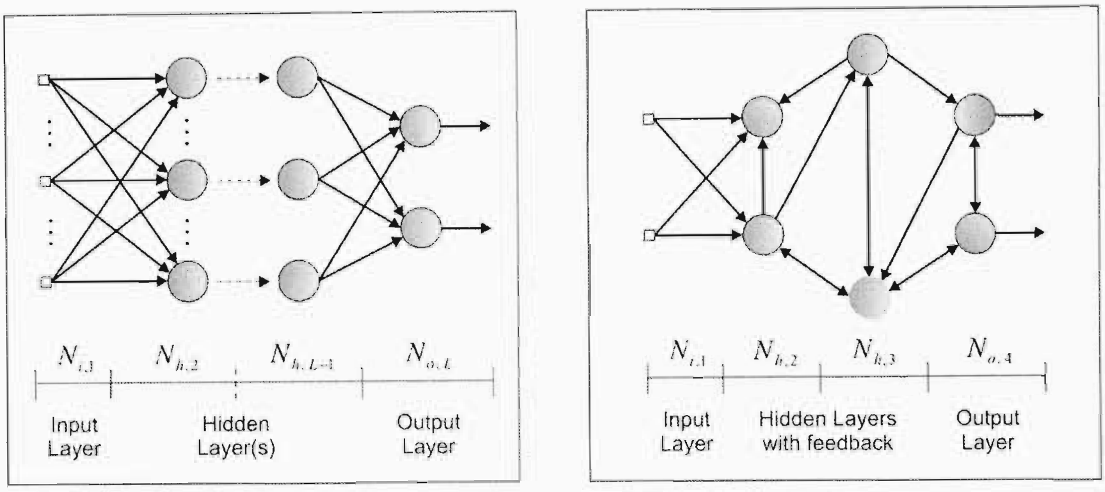

(a) Feedforward based neural network.

(b) Feedback based neural network.

Figure 4.1 Two basic network types with a common structure. Operation is either static (a) or dynamic (b). Data processing may occur over multiple layers.

It is beyond the scope of our work to provide taxonomy of the different neural network models, except that which is of concern and unless a general discussion or comparison is warranted. However, it is noted that a common categorization of neural networks is the feedforward or feedback type (Figure 4.1). This is important, as the ability of a neural network to perform specific computational tasks depends on the organization and interconnection of neurons in the network, to some degree.

In general, a network may be composed of one layer or multiple layers of neurons. A multi-layered network usually has one input layer, one output layer and may have one or more hidden layers. A common, though not universal, naming convention is to denote the set of inputs (source) to the network as the first layer. For a network composed of L layers, the input layer $N_{i,1}$ is thus the first layer. It is non-processing and only supplies input signals to the network. Any intermediate layers $N_{h,i}$ that may exist $(\forall\, i = 2, \ldots, L-1)$, are responsible for processing the inputs and are called hidden layers. This is illustrated in Figure 4.1(a). The hidden and output layer neurons may be connected to all of the units in the preceding layer (fully connected network), or only to some units in the preceding layer (partially connected). For most applications fully-connected networks are well suited.

In a feedforward network, shown in Figure 4.1(a), signal flow from input to output is strictly unidirectional. There is no memory as the output depends only on the current input and it is computed one-shot. Feedforward structures are the most common networks types, and are usually multi-layered. Since the direction of flow is certain, feedforward networks are easier to analyze and to a greater degree than feedback types. It has been shown that they can approximate any given function from static input values to static output values arbitrarily well. Further, experimental results show that they often outperform more traditional methods in non-linear classification, especially in high-dimensional tasks.

Recurrent or feedback networks, shown in Figure 4.1(b), have internal dynamics as a result of feedback loops within the network. Biologically they are more plausible since the human nervous system is composed almost entirely of recurrent networks. These types of networks are mathematically described by a (non-linear) dynamical system given by a first order differential equation. In general it is hard to predict even their qualitative behaviour. Therefore the common RNN in use is the Hopfield network, which is characterized by a symmetric organization of weights. This architecture is widely employed as CAM. Other symmetric architectures have been used to (approximately) solve optimization tasks [57]. Without symmetry the network dynamics are less tractable, but in general any of these networks are considered to transform input functions into output functions.

This perspective is developed in greater detail by starting with some non-formal remarks on the properties of the artificial neuron. The neuron is the basic component of any NN. It is responsible for processing information and is fundamental to the operation and functionality of a NN, through a large interconnection of neurons. It mimics the neurons (nerve cells) in the brain of which there are many different types.

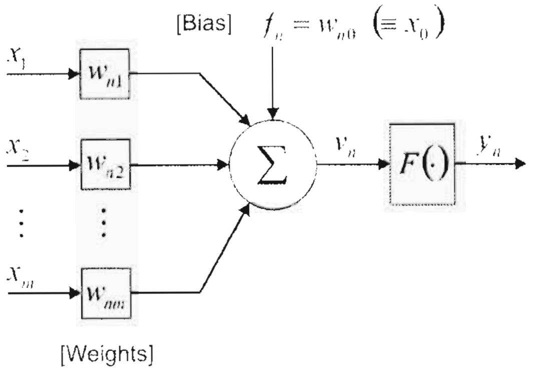

Figure 4.2 Non-linear model of a neuron.

Figure 4.2 illustrates the model of a single neuron. Without loss of generality we consider the operation of the nth neuron, in the presence of $m-1$ neurons, where m denotes an arbitrary number of neurons. Neuron n has a number of weighted connections $\{w_{n1}, \ldots, w_{nm}\}$ over which it is able to communicate with other neurons. Specifically, w_{nj} is the weight associated with the connection between the jth and nth neuron; it determines the effect of the jth unit's signal on the nth unit [38]. These connections represent the synapses of real neurons and the weights represent the strength of the synapse. The weight w_{nj} is positive if the associated synapse is excitatory otherwise it is negative if the synapse is inhibitory.

For now, signals $\{x_1, \ldots, x_m\}$ denote the inputs (from other neurons) to the neuron n and f_n is an externally applied fixed input (bias term) that represents a general inclination of whether the neuron fires or not. A propagation rule determines the effective input v_n of a unit, given its initial inputs and biasing. In most instances, as in this case, the rule is to perform a summation of the weighted inputs.

$F(\cdot)$ is the activation function (AF), which determines the state (or output) y_n^N of the nth neuron. (For clarification, the superscript refers to a NN model). It indicates whether the neuron fires or inhibits; its output is called the activation level of the neuron. The AF is an important function for configuring the NN, as it is the source of non-linearity that is responsible for the approximation capabilities of the network.

So the operation of the nth neuron may be described by

$$v_n = \sum_{j=1}^{m} w_{nj} x_j + f_n \,, \qquad (4.1)$$

and by defining the linear combiner output as u_n, the output is given as

$$y_n^N = F(u_n + f_n), \qquad (4.2)$$

where

$$u_n = \sum_{j=1}^{m} w_{nj} x_j \,. \qquad (4.3)$$

The AF determines how the inputs are interpreted and how changes in the network affect neuron excitation or inhibition, i.e. whether a neuron is firing or non-firing (for two-state neurons, this simply implies being in the on or off state, respectively). The type of AF, therefore, assists in providing the neuron, and the network as a whole, with unique benefits and specific functionality. This may be exploited when soft outputs are required for feedback, which is the case in some MUD schemes.

The first model of a neuron (McCulloch-Pitts) was viewed as a logical gate with two internal states: active (excited) and silent (inhibited), and in which the AF is a threshold function. The McCulloch-Pitts neuron model is the simplest and the most popular, to date. Its output is given by:

$$y_n^N = F(v_n) = \begin{cases} 1, & v_n \geq 0 \\ 0, & v_n < 0 \end{cases} \qquad (4.4)$$

Given the above mathematical description, it can be seen that the bias f_n is the threshold value for the *n*th neuron; the weighted sum of the inputs must reach or exceed this threshold for the neuron to fire.

Though simple, it was proven that a synchronous assembly of neurons of this type is capable of a high level of computation [39]; all logical operations can be implemented using conveniently associated neurons with a suitable set of weights w_{nj}. However it is only since the last 20 years that the true potential of neural computation is being realized.

The McCulloch-Pitts model can also employ the symmetric hard function (3.26). In that case, the neuron's activation level resides in one of two states: $+1$ (firing) or -1 (non-firing). This is conveniently used when analyzing the RNN, as well as for the purposes of antipodal signalling in the DS-CDMA system.

Numerous other AF's may also be employed, but it often depends on the network and the application. One common choice is the hyperbolic tangent function,

$$F(v) = \tanh(v). \tag{4.5}$$

It takes on a continuous range of values in the range $[-1,1]$ and is easily differentiable; this provides analytical benefits in some networks such as those based on back-propagation techniques.

The sigmoid (logistic) function with parameters a and b, indicated in (4.6) below, is another common AF. Notably, it is the standard choice for modelling the stochastic neuron. Appendix D provides an overview of this function.

$$F(v) = \frac{1}{1 + e^{-(v-a)/b}}. \tag{4.6}$$

4.3 Recurrent Hopfield Neural Network

In principle a feedback network can contain any number of layers with a myriad of connections between and within different layers. One well-known and well-researched example is the recurrent Hopfield neural network (HNN), which is composed of a single layer of symmetrically interconnected neurons (Figure 4.3).

The HNN is rooted in the field of neurodynamics, which describes the combined theory of non-linear dynamical systems and neural networks. It is primarily used to perform pattern association (information storage and retrieval) by storing fundamental patterns (memories) as dynamical attractors in a state space [55], [58]. It is commonly employed as auto-associative, content addressable memory (CAM) or as a platform for solving combinatorial optimization problems.

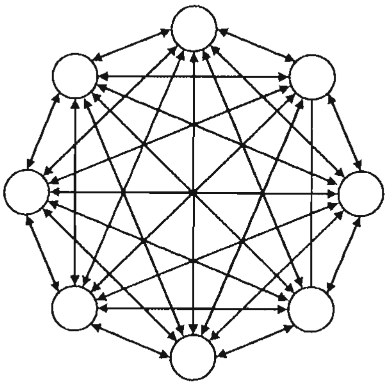

Figure 4.3 Schematic view of the auto-associative HNN. Neurons provide both inputs and outputs. (No self-feedback).

Feedback networks are often described by dynamical systems that evolve in either continuous or discrete time; they can be classified as a discrete or a continuous network. The standard discrete version of the HNN employs the McCulloch-Pitts neuron model, but other versions exist [58]. Learning of a specific input-output association is defined without the use of correct examples, i.e. learning is unsupervised. The only available information is in the correlation of the input data and data that is stored. The HNN is designed to store a number of patterns by distributing their information across the network weights. It uses the correlation information to produce an output associated with the input that is presented to it.

The idea of CAM is to map fundamental patterns to stable points in a state space of a dynamic system. The HNN stores information in a dynamically stable configuration. Associative memory models may be described by a configuration space containing all possible states (Figure 4.4). Within this state space are attractors (stable points) representing stored patterns. Given sufficient information as a starting point in the state space and provided that this point lies in a basin of attraction (near an attractor), the HNN should converge to a stable point, which ideally is the desired pattern. The state space is idealized for the purposes of explanation, i.e. it should be described by a set of discrete points (on a hypercube) and not by a continuous region.

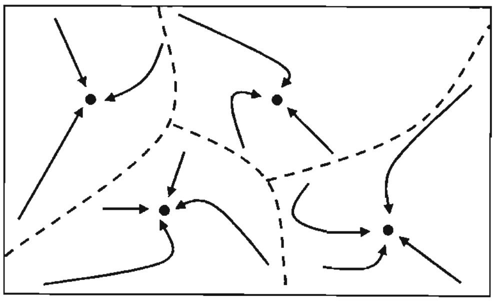

Figure 4.4 Schematic view of a configuration space (with four attractors).

The above process occurs internally and it is conceptual. Externally this translates to the HNN retrieving a pattern when subjected to an initial input, which may be a noisy or incomplete version of a fundamental pattern. An advantage of CAM is its insensitivity to small errors in the initial input. This is particularly useful when detecting signals in the presence of AWGN. The HNN model is shown in Figure 4.5. The HNN employs feedback to iteratively update neuron states, from an initial state, until a stable point is reached or when there are no further state changes. The dynamics of the HNN follows a trajectory to the closest attractor, signifying a stored pattern (as shown in Figure 4.4). Its symmetrical configuration ensures that all trajectories are asymptotically stable and that they reach static equilibrium [58]. The equilibrium state is thus a fundamental pattern, retrieved by applying a suitable input. However, correct association is not always guaranteed. In general, it depends on the initial pattern and on stability conditions which must be met. This is discussed later.

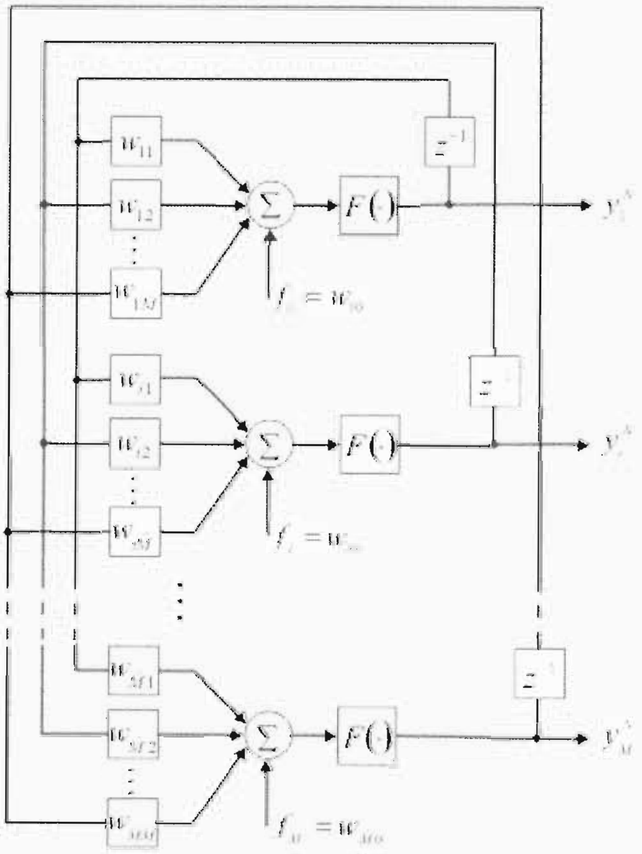

Figure 4.5 The Hopfield architecture, with N neurons.

The formulae that mathematically describe the process of pattern storage and retrieval (as discussed above) are easily derived. Figure 4.5 shows the connection of the classical Hopfield model with unit delay elements. The output of each neuron is fed back to every other neuron. Although self-feedback is indicated here, it is usually avoided in pattern association for stability purposes (See Appendix C).

The operation of the HNN is two-staged, i.e. *storage* and *retrieval.* Storage is a one-shot computation since the network learns and obtains its weights once over. Suppose that a set of U patterns $\{\xi_u, u = 1, 2, \ldots, U\}$ is to be stored. For convenience, each pattern is considered to be made up of independent bits, such that $\xi_{u,i}$ denotes the ith element of ξ_u. If each vector is of dimension $\hat{M}$, then $\hat{M}$ neurons are required, where each neuron state corresponds to one bit.

The one-shot learning rule is a generalization of Hebb's *postulate of learning*, which says that the synapse w_{ij} between neurons i and j should increase if both neurons are simultaneously activated. This is implemented via the outer product of the patterns. Therefore the synaptic weights (between pairs of connected neurons) are defined in the $\hat{M} \times \hat{M}$ synaptic weight matrix which is given by:

$$\mathbf{W} = \frac{1}{\hat{M}} \sum_{u=1}^{U} \xi_u (\xi_u)^T - \frac{U}{\hat{M}} \mathbf{I}. \tag{4.7}$$

In (4.7), $1/\hat{M}$ is employed for the purpose of simplification. The second term indicates that there is no self-feedback by ensuring that $w_{ii} = 0 \, \forall \, i$ with $\mathbf{I}$ denoting the identity matrix. This learning rule is used with the aim of simulating the HNN; however, it will be shown in the subsequent chapter that (4.7) is not explicitly used in the neural-based MUD implementation.

The primary function of CAM is to retrieve a pattern stored in memory in response to a presentation of an inconsistent version of that pattern i.e. incomplete or noisy [55]. As long as it shares a reasonable degree of similarity with any of the stored patterns, the network should be able to find a pattern that most closely resembles the input pattern. For a network made up on $\hat{M}$ neurons, the state vector (at the kth time step) that contains the state of each neuron, may be defined as

$$\mathbf{x}(k) = [x_1(k), \quad x_2(k), \quad \ldots, \quad x_{\hat{M}}(k)]. \tag{4.8}$$

During retrieval an input pattern of dimension $\hat{M}$ is imposed on the HNN as an initial state, i.e. $\mathbf{x}(0)=\xi_{initial}$. Each neuron is then updated (randomly), at a fixed rate, based on a dynamic rule. State updating at each discrete time step k is therefore deterministic and each neuron's state is updated according to the state transition rule:

$$x_j(k+1)=F\left(\sum_{i=1}^{\hat{M}} w_{ji}x_i(k)+f_j\right). \tag{4.9}$$

Normally, the AF is given by $F(\cdot)=\mathrm{sgn}(\cdot)$, but binary decisions or other non-linear functions, like those described earlier, may be employed. If the effective input v_j to neuron j is zero then the state remains the same (See Appendix C). The updating procedure of (4.9) is repeated for k iterations until there are no state changes to report or when a fixed point (stable state) has been reached. Then the HNN outputs a time-invariant state vector, which satisfies (4.9). It is denoted in matrix form as,

$$\begin{aligned}\mathbf{y}^N &= \mathbf{x}_{fixed} \\ &= F\left(\mathbf{W}\mathbf{x}_{fixed}+\mathbf{f}\right).\end{aligned} \tag{4.10}$$

The final state of the neurons that the HNN converges to is given by $\mathbf{x}_{fixed}$ and may be an element of the solution set $\{\xi_u, u=1,2,\ldots,U\}$, and $\mathbf{f}$ is the vector of the externally applied biases. Updating may be done serially, in which case a single neuron is updated at a time and its output is used to update the next neuron. This is known as asynchronous updating; physiologically this is a more natural way. Usually neurons are chosen at random to be updated, or with some constant probability [40], or even sequentially. Parallel updating is also possible, but stability is an issue [38].

A useful examination is the generic problem of storing a random set of patterns drawn from a binomial distribution. The procedure for testing is to check whether small deviations from these patterns are corrected as the network evolves. Storage of eight 100-dimensional patterns was investigated; the probe (initial pattern) presented to the HNN contained uniformly introduced errors. The result of the simulation is shown in Figure 4.6, with an expected trend. Large changes in the network do not reflect over a single bit (i.e. over a single iteration) but over several discrete steps. This is seen between steps $20-50$, which accounts for approximately 30 possible state changes with the error in memory recall approximately 25%, over that time.

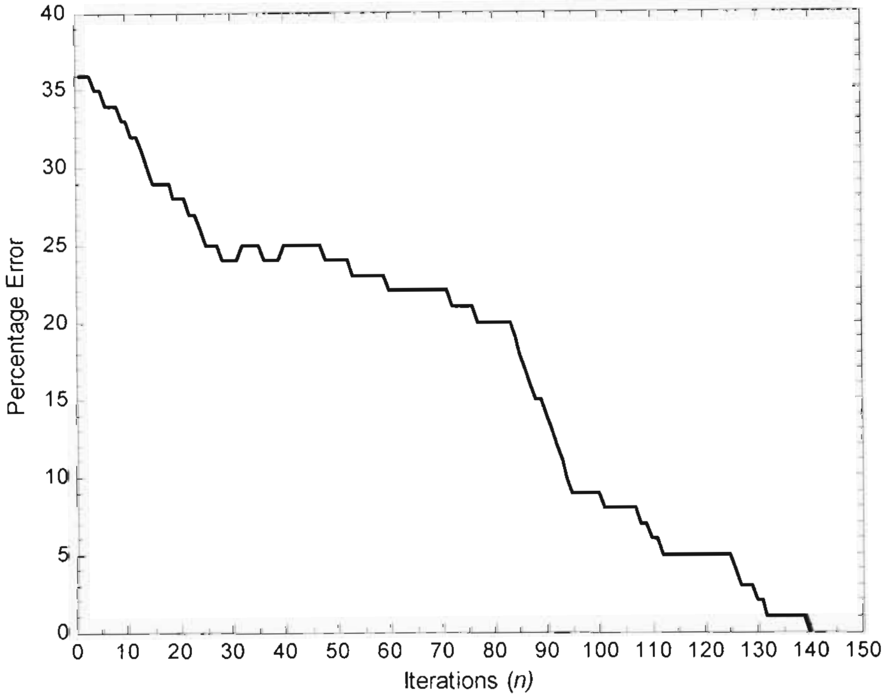

Figure 4.6 Pattern retrieval and error performance of the classical HNN model. $U=8, \hat{M}=100$.

Error performance of the HNN is largely dependent on capacity of the network. It is analyzed in the subsequent sections, but it is noted again that there is a limit to the level of noise that can be tolerated in the initial input pattern; the CAM is only insensitive to small errors. Convergence onto a specific state depends on the location of the initial state in the basin of attraction. This is usually quantified in terms of the radius of the basin, given by the Hamming distance between the pattern under test and the stored patterns, i.e. the initial error between the initial pattern and the stored pattern of interest. Correct recall is not always guaranteed and there is a point at which the memory is in error, as shown in Figure 4.7. However, an initial state that is relatively closer in the basin of attraction is associated with a fundamental pattern, within the same discrete-time. It is important to know what causes this effect. What is the probability of correct memory recall and what does this depend on? How noisy can the initial pattern be before memory recall deteriorates beyond an acceptable level? This is analyzed in the proceeding sections. It is shown in Section 4.3.2 that storage capacity plays a key role in memory recall and the imposing conditions are important when employing the HNN for tasks in other fields, such as MUD.

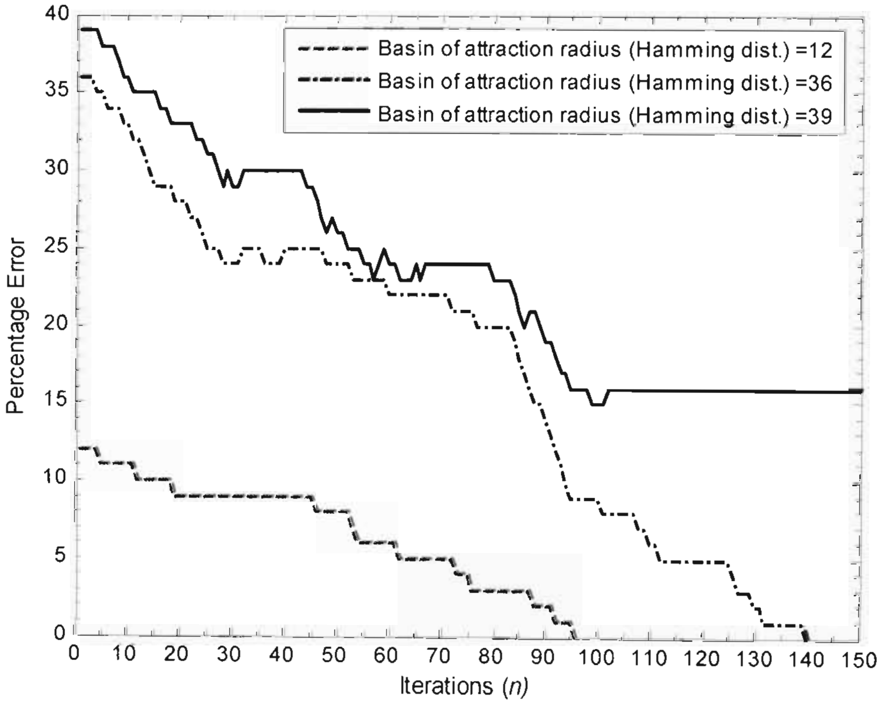

Figure 4.7 Effect of varying radius of the basin of attraction on the performance of the classical HNN. $U = 8, \hat{M} = 100$.

In the next section, we introduce the energy function of the HNN and investigate the role it plays in the dynamics of the network, in pattern association. It is of particular importance in MUD; it will be shown in Chapter 5 that the energy function shares a common structure with the objective function of the optimum MUD problem. Thereafter, pattern stability and network capacity is investigated in Section 4.3.2.

4.3.1 The Energy Function

The energy function, proposed by Hopfield, remains a very important contribution in neural network theory. The term comes from the analogy to spin (magnetic) systems of the sort familiar in physics. In [55], [58] the energy function is defined as a Lyapunov function for a continuous HNN. It supports the concept of stable states. Graphically, it has its own landscape with many minima that overlaps the configuration space with its stable states. For a discrete asynchronous model, the input-output relationships are redefined so that the energy function is given as:

$$E = -\frac{1}{2}\sum_{i=1}^{\hat{M}}\sum_{\substack{j=1 \\ i \neq j}}^{\hat{M}} w_{ij} x_i x_j \, . \tag{4.11}$$

The energy function is a monotonically decreasing, bounded function. As the system evolves according to the dynamical rule of (4.9), the energy function continues to decrease (Appendix C). Viewed in terms of pattern retrieval, the initial input represents a starting point in the energy landscape, which is an initial state in the configuration space. According to Lyapunov stability theory, state changes in the HNN will continue to occur until a local minimum of the energy landscape is reached, at which point information retrieval stops. The local minima of the energy landscape correspond to the attractors of the configuration space, which are the assigned fundamental memories of the network. This is an equilibrium (stable) state.

For a symmetric weight matrix, $\mathbf{W}$, that has zero diagonal elements, the state of the HNN always converges to a stable state i.e. a local minimum energy solution. Accordingly, the HNN is globally asymptotically stable; the attractor fixed-points are energy minima and vice versa [38]. When the local minimum is actually reached, the algorithm stays there because everywhere else in the close vicinity is an uphill climb.

In dynamical systems, the Lyapunov function, which in this case is the energy function, serves as a state function that must be minimized to find a stable or optimum (equilibrium) state. It is sufficient but not a necessary condition for stability. Furthermore, the conclusion is that the asymptotic behaviours of the asynchronous dynamics of a symmetrically connected network are fixed points (or attractors). The neurons must have no self-connections and in general the energy function exists if $w_{ij} = w_{ji}$. However, even the asymptotic behaviour (i.e. settling into a local minimum) can occur in asymmetric networks, thus symmetry is also not a necessary condition.

4.3.2 Stability and Capacity

The stability of a particular pattern can be examined using the stability condition that is implied in the dynamic rule. Consider the general Hopfield model. If the network is presented with a pattern ξ_u that is an attractor in the configuration space of the network then the stability condition is given by

$$\operatorname{sgn}(v_i) = \xi_{u,i}, \tag{4.12}$$

where v_i, in (4.1), is the net input to neuron *i* after the input of ξ_u. It is intuitive that when presented with input ξ_u, the next state of the network, which is calculated from (4.9), should result in the stored pattern. Without loss of generality the external biasing is assumed to be zero, and time dependency is removed. Then the sum of postsynaptic potentials delivered to all neurons may be written (in matrix form) as:

$$\mathbf{v} = \mathbf{wx} = \frac{1}{\hat{M}}\sum_{i=1}^{U} \xi_i (\xi_i)^T \mathbf{x} - \frac{U}{\hat{M}}\mathbf{Ix}, \tag{4.13}$$

where $\mathbf{W}$ is defined in (4.7) and since the initial state is ξ_u, (4.13) becomes

$$\begin{aligned}\mathbf{v} &= \frac{1}{\hat{M}}\sum_{i=1}^{U} \xi_i (\xi_i)^T \xi_u - \frac{U}{\hat{M}}\mathbf{I}\xi_u \\ &= \xi_u + \frac{1}{\hat{M}}\sum_{i=1, i\neq u}^{U} \xi_i (\xi_i)^T \xi_u - \frac{U}{\hat{M}}\mathbf{I}\xi_u .\end{aligned} \tag{4.14}$$

If the second term and third terms in (4.14) are zero then it can be concluded that ξ_u is stable, according to (4.12). (Appendix C extends on the proof of pattern stability and stable points). Multiplication by $1/\hat{M}$ is now clear, since $\xi_u(\xi_u)^T = \hat{M}$. Usually, for asynchronous systems, (4.13) and (4.14) are generalized for neuron i only. It is simpler to analyze the stability condition by assuming that there is self-feedback. In that case, by simplifying $\mathbf{W}$, the net (postsynaptic) input to all neurons is given by

$$\mathbf{v} = \xi_u + \frac{1}{\hat{M}} \sum_{t=1, t \neq u}^{U} \xi_t \left((\xi_t)^T \xi_u \right). \tag{4.15}$$

The second term is crosstalk between the elements of fundamental memory ξ_u and the other fundamental memories. It is regarded as the noise component. If the fundamental memories are orthogonal to each other i.e. $(\xi_t)^T \xi_u = 0$, then there is no noise, resulting in a stable pattern. This is still true if the crosstalk term is small enough so that it cannot change the sign of $\{\xi_{u,i}\}$, which is the case for a small set of patterns (Appendix C).

The stored patterns are stable in the sense that if the system is initiated from a stable state, it stays there. The network's error-correcting capability is evident since a fraction of incorrect bits in the input pattern is overwhelmed by the number of correct bits. A starting point in the vicinity of $\{\xi_{u,i}\}$, in terms of Hamming distance [40], relaxes to $\{\xi_{u,i}\}$. The concept is the same as that presented in Figure 4.4 earlier; it supports the idea of trajectories and basins of attraction.

An approximate upper limit on the storage capacity of the Hopfield (and Hebbian-based) neural networks can be obtained intuitively from (4.14). Assuming the crosstalk term is zero (in the case of orthogonal patterns and no self-feedback), then

$$\mathbf{v} = \xi_u - \frac{U}{\hat{M}} \mathbf{I} \xi_u . \tag{4.16}$$

To satisfy the stability condition, $\mathbf{v} \geq 0$ i.e. if the initial state corresponds to an attractor then the network should remain in that state. Thus, a pattern is stable if

$$U \leq \hat{M} \tag{4.17}$$

That is, the network can store, at most, the same number of patterns as there are neurons. However, this is on condition that the different patterns are completely orthogonal and usually the useful capacity is less than this.

A drawback of the HNN, when storing U patterns via the generalized Hebb learning rule, is the occurrence of spurious attractors (or states). These states represent stable states that are different from the fundamental memories of the network. Fixed points are located at certain corners of the $\hat{M}$-dimensional hypercube, which describes the energy space. However, other corners of the hypercube, in close proximity to the fixed points, may have possible spurious states which are also local minima of the energy function. This is seen by noting that the energy function is symmetric in the sense that its value remains unchanged if the states of the neurons are reversed, i.e.

$$E(-x_i) = -\frac{1}{2}\sum_{i=1}^{\hat{M}}\sum_{\substack{j=1 \\ i \neq j}}^{\hat{M}} w_{ij}(-x_i)-(x_j) = E(x_i). \tag{4.18}$$

This means that the network also stores negative images of its fundamental memories. Thus if the HNN was presented with a noisy version of a stored pattern ξ_u, with more than half its bits incorrect, then the retrieved pattern would be $-\xi_u$. In addition the network must contend with attractors that represent a linear combination of an odd number of patterns. Also, for a large number of fundamental memories, the energy landscape has local minima that are not correlated with any of the stored memories. This is analogous to spin-glass models of statistical mechanics.

The presence of the crosstalk terms leads to the probable instability of fundamental memories during retrieval. In addition, the possible existence of spurious states, tend to decrease the efficiency of a Hopfield network as a content-addressable memory.

The retrieval of a pattern in the presence of crosstalk (or noise), may be equated to the detection of an information signal in the presence of channel noise in communication theory.

The existence of spurious states increases with the number of fundamental memories that are stored in the network. Storage capacity in the HNN is therefore limited. Several expressions exist for the maximum storage capacity $U_{\max}$. First, the assumption is made that the patterns are random, generated from a sequence of $\hat{M}U$ Bernoulli trials, with $P(\xi_{u,t} = 1) = P(\xi_{u,t} = -1) = 1/2$. The noise is thus made up of $\hat{M}(U-1)$ independent random variables (since there is no self-feedback) with zero mean and variance of $1/\hat{M}^2$, due to the scaling factor of $1/\hat{M}$.

For $U\hat{M} >> 1$, the central limit theorem applies and the noise can be approximated by a Gaussian distribution with zero mean and variance of $(U-1)/\hat{M}$. Therefore the signal-to-noise ratio, for large $\hat{M}$ and U , is approximated as

$$SNR_{HNN} \approx \frac{\hat{M}}{U}. \tag{4.19}$$

To determine the storage capacity, a criterion for acceptable performance is defined in terms of error probability. The conditional probability of bit error is given by:

$$P(v_t > 0 | \xi_{u,1} = -1) = \frac{1}{2}\left[1 - \operatorname{erf}\left(\sqrt{\hat{M}/2U}\right)\right] \tag{4.20}$$

The error probability is illustrated in Figure 4.8. An important ratio is the load parameter η that is defined as the reciprocal of the signal-to-noise ratio in (4.19). As an example, if the performance criterion is $P(v_t > 0 | \xi_{u,t} = -1) < 0.01$ then from (4.20) $U_{\max} = 0.152\hat{M}$ and therefore $\eta = 0.152$. This is an upper bound. The quality of memory recalls deteriorates with increasing load parameter.

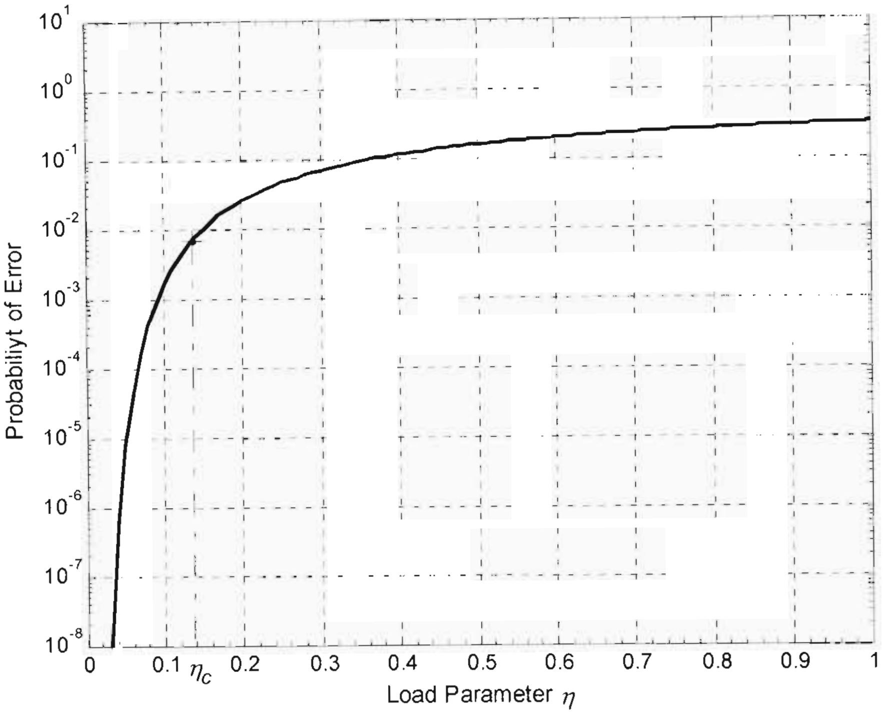

Figure 4.8 Probability of pattern bit error on memory recall. The point of critical loading is denoted by η_c.

The critical load parameter η_c, indicated in Figure 4.8, is defined as [39]:

$$U \leq \eta_c \hat{M} = 0.138\hat{M}. \tag{4.21}$$

An avalanche effect occurs if (4.21) is not observed, which causes bits (neuron states) to continuously flip until the network's collective state has no resemblance to a stable state. Then, memory recall becomes non-existent. The critical load parameter defines the storage capacity with errors on recall. Figure 4.8 shows that ideally $U << \hat{M}$. Thus the approximate upper bound is not a useful capacity measure unless the errors in some bits are tolerated.

Due to this trend, the capacity is redefined to recall most of the memories with minimum error. The storage capacity (almost without errors) is now the largest number of patterns that can be stored with most of them being recalled correctly [38], [40]. The problem here is determining what is meant by "most". Typically it is insisted that most patterns be recalled perfectly with some high probability, say with 99% [38]. However, some applications may sacrifice error probability for a greater number of stored patterns. For our intended application, it is necessary to recall all patterns perfectly. It can be shown [40] that this is achieved by taking:

$$U_{\max} < \frac{\hat{M}}{4\log_e \hat{M}}. \tag{4.22}$$

The above estimates refer to randomly generated fundamental memories. In practice, the fundamental memories will usually represent certain patterns (information). The storage capacity will depend on the degree of crosstalk among them and may be much smaller than stated. In general, the capacity is proportional to the number of neurons in the network, conditioned on (4.21), if errors in the retrieved pattern are acceptable. For perfect recollection the capacity is proportional to $\hat{M}/\ln\hat{M}$ [40]. A major limitation of the HNN is that the storage capacity must be maintained small for fundamental patterns to be recovered [38].

There are techniques to overcome the problems associated with spurious states. The Hebb's learning postulate is not the only way to obtain the weight matrix $\mathbf{W}$. Some learning modifications allow a network to retrieve any $\hat{M}$ linearly independent patterns perfectly $\forall U < \hat{M}$. Capacity increase may also result from the use of special or modified activation functions. This is beyond the scope of our work.

4.4 Summary

In this chapter an overview of neural networks was presented. Two basic network types were outlined and the operation of the basic processing unit, the neuron, was described. When applying neural networks to problems involving nonlinear dynamical or state dependent systems, neural networks with feedback can in some cases provide significant advantages over purely feedforward networks. The feedback connections allow for recursive computation and the ability to represent state information. The focus of this chapter was the RNN. In particular, the Hopfield neural network was investigated as it is the network of choice in this research.

The HNN is a well studied network, the theoretical operation of which can be understood in context of statistical concepts. The Hopfield model was considered in view of its application as CAM. The process of pattern association was discussed and the relevant mathematical equations, describing its operation, were provided. The concept of the HNN energy function was introduced.

The performance of the HNN is adversely affected by spurious states and crosstalk terms. However, it is shown in Chapter 5, via implementation in MUD, that the HNN can be improved by employing techniques analogous to spin glass models [39]. These techniques are intended to ultimately prevent local minima that results in incorrect pattern association. This depends on several factors. It was illustrated, via simulation, that the number of errors in the initial pattern is responsible for the poor performance of the HNN. Another important issue in feedback systems, such as the HNN, is stability. In some cases feedback can be harmful and can lead to propagation of activation values ad infinitum. Several requirements for stability exist, which must be met for acceptable error performance and hence successful pattern association. This limits the capacity of the network.

The most notable feature of this network is the ability to locate minima of the energy function during pattern association. The minimization of the energy function corresponds to locating a stable state in the state space of the dynamical system, which in turn corresponds to a fundamental pattern. The inherent minimization process lends the Hopfield network for use in the optimization problems of the combinatorial kind. One well known problem, in which the HNN has shown success, is the TSP. In Chapter 5, we expand on the idea of optimization, specifically in the context of the optimization of the optimum multiuser detector objective function.

5 Multiuser Detection Employing Neural Networks

5.1 Introduction

Many problems in science and engineering have been formulated in terms of neural networks. The idea is to construct less complex parallel algorithms with which solutions to the initial problem can be found. This is the basis for solving the optimal demodulation of multiple users. In the search for sub-optimal solutions to MUD in DS-CDMA systems, several techniques involving the use of neural networks have been proposed. The application of neural networks is seen as a viable alternative for MUD schemes due to their adaptability, non-linearity, and generalization; these characteristics are, in part, born out of the parallel distributed processing, which now is achievable at a much greater level in hardware. Furthermore, different neural networks are specified for, and have proven successful, in pattern classification and combinatorial optimization [55], [59].

In review of the two basic types of neural networks, multilayered feedforward networks are useful for pattern classification while recurrent networks are useful for optimization problems. They share a common function, which is usually to recognize a pattern either by classification or association. It is not surprising then, that both have been employed for MUD. In pattern classification the objective is to formulate decision boundaries to separate the different pattern classes. MUD is a computational problem that belongs to the class of non-deterministic polynomial (NP) complete problems; these are the hardest of all NP problems since there is no efficient algorithm to solve them (in time that increases polynomially with the problem size).

Hopfield and Tank [10] pioneered the use of neural networks to solve optimization problems with the continuous Hopfield model. The underlying process that occurs in the HNN is the optimization of an energy function; even when it is solely being used for pattern auto-association the network is expected to find a state space configuration that ultimately minimizes the energy function. Since the work in [10], RNN have been successfully employed for combinatorial optimization. If a combinatorial optimization problem is mapped to the Hopfield model, the cost function of the problem may be related to the energy function of the HNN and therefore the final state of the network is an optimum solution to the given problem.

Although RNN-based methods, like the HNN, are relatively new to the growing list of neural-based solutions, they are now a common choice in MUD. In many research circles, the multi-stage detector (MSD) defined by Varanasi and Aazhang [41] is regarded as the first multiuser receiver based on the concept of a RNN, although neither the term "neural networks" nor "Hopfield" was mentioned explicitly.

The MSD is based on a SIC scheme that improves the estimate of a desired information bit by using an iterative process (i.e. multiple stages), in which the MAI is subtracted out. The signals at each proceeding stage are a better estimate of the data, since the MAI obtained from the previous stage is removed. The strongest user is demodulated first and then its influence is subtracted from the signal during the next stage. The initial estimates are obtained using matched filters, thus the detector is susceptible to poor BER performance due to an increasing number of users, or due to relatively high cross-correlations. Power control is also a major concern since the order in which users are cancelled affects the performance. Computational complexity per symbol was shown to increase linearly with the number of users [41].

Aazhang *et al.* [11] were the first group of researchers to adopt neural networks, proper, for MUD. They introduced a two-layered perceptron for the demodulation of DS-SS signals. It was called the multi-layer perceptron (MLP) detector. Training of the network was achieved using the standard back-propagation (BP) algorithm and a modified BP rule in which the training is supervised by assuming that the bits of all users are known *a priori*. The MLP detector was shown to outperform the conventional detector. For synchronous transmission the decision boundary of the assisted BP network approximately overlaps the optimum boundary, showing that it is capable of near optimum performance. However, the two-layer feedforward design of the MLP is unfavourable in terms of complexity and *a priori* user information. Furthermore, convergence of the network was not proven [42]. Nevertheless, the results did display the gains that could be achieved using neural networks for MUD.

An extension to the work in [11] was provided by Mitra and Poor [42], who pioneered much work in the field of adaptive techniques. These authors proposed an adaptive detector based on a single-layered network and analyzed its convergence using Lyapunov's theorems. It was shown that the proposed network converged to an optimal set of weights. A radial basis function (RBF) network for adaptive MUD was also proposed [43]. In both feedforward implementations, the results were acceptable for a small number of users, but the hardware complexity grows exponentially with the number of users, i.e. the number of neurons increases exponentially. The RBF scheme, however, does not necessitate knowledge of other user's information.

Feedforward networks were employed by looking at MUD as a pattern classification problem to achieve the optimum non-linear boundary decisions. The initial results of these implementations led to research into RNN-based MUD schemes, established by authors such as Miyajima *et al.* [45], Nagaosa *et al.* [46], Kechriotis *et al.* [47] and Teich *et al.* [32]. Kechriotis *et al.* [47] was one of the first groups of authors to investigate the application of the HNN to demodulate information transmitted by synchronous or asynchronous users over an AWGN channel in a DS-CDMA system.

The NP-complete problem of optimal MUD can be solved by the maximization of an integer quadratic objective function. In [47], the authors proposed a solution to the optimization problem rather than in the context of pattern classification. It was shown that the maximization of the optimal objective function could be equated to minimizing the HNN energy function, and that it could be solved using dedicated analog VLSI, for a small number of users. The HNN-based detector was shown to be a generalization of the MSD. Under certain conditions this detector inherits the near-far resistance and BER performance of the MSD. Hence it is capable of achieving the near-optimal BER of the optimal detector. However, for larger practical systems, a hardware implementation of the proposed HNN-based detector was not realizable.

A pre-processing stage was later proposed, in [60], to reduce the dimensionality of the optimization problem. The simulation results of the reduced-detector showed improved performance over other suboptimal schemes (like the MSD), with lower computational cost. Another significant result of this work was the ability to provide real-time multiuser demodulation in a hardware implementation, achieved at low cost and complexity. The authors displayed this by combining digital microprocessors and neural network IC's for their HNN-based reduced-detection scheme.

Miyajima *et al.* [45] (cited in [46]) independently proposed a synchronous RNN-based multiuser detector using the discrete version of the HNN. In [46], Nagaosa *et al.* derived a model for M-ary SSMA communications, based on [45], and compared it to the continuous model. The discrete scheme offers improvements in near-far resistance and BER performance over the conventional detector, with a complexity that is linear in the number of users. However, its performance is sub-optimal. In contrast, the continuous model provides near-optimal BER performance. Results indicated that it has superior near-far resistance with a lower probability of spurious states for the same power of interfering users as compared to the discrete model.

The advantage of employing a HNN over a feedforward network is that there is no difficulty in determining the required number of layers of neurons, as there is only one layer. Moreover, the number of neurons and weight coefficients can be derived with relative ease from the parameters characterizing the communication system. This is due to the structural similarity between the Hopfield energy function and the log-likelihood function. This relationship was shown explicitly by Teich *et al.* [32], in their proposal of a multiuser receiver based on the RNN, known as the MU-RNN detector. Their work was an extension to the research by Miyajima *et al.* [45], in which a fading multipath channel was considered. In addition, the same authors later investigated the use of parallel updating methods in the MU-RNN [61].

There is one major drawback of the HNN; conceptually, the network converges to the first local minimum in the surface of the energy function since it is a gradient descent technique. As such, it suffers from localized optimization. In terms of pattern retrieval, this translates to converging to incorrect neuron states (as shown in Figure 4.7). Due to the number of local optima in the problem of optimum detection of multiple signals, the main difficulty in using the classical HNN is that it tends to become trapped in the local optima. Kechriotis and Manolakos [47] showed that, depending on the size of the problem (i.e. number of users) the HNN-based multiuser detector may not always provide near-optimal detection. They attempted to solve this problem using a reduced hybrid detector [60], which was described above.

The beneficial properties of neural networks, in view of the initial results of RNN-based schemes and their relatively good performance for a small number of CDMA users, has encouraged research into neural-based MUD strategies. In particular, a fair amount of work focuses on the development of modified (Hopfield) RNN structures and techniques for MUD. The work is aimed at improving receiver performance (in varying conditions) and ideally, to also achieve less complex cost-effective solutions.

Modified HNN schemes often introduce ways of avoiding getting stuck in local minima. Among these methods, stochastic simulated annealing[1] (SSA) and various deterministic simulated annealing approaches, such as hardware annealing and mean field approximate annealing, have been proposed. Yoon and Rao [48] proposed a neural-based multiuser receiver that employs simulated annealing (SA) which borrows techniques from statistical physics. Wang *et al.* [62] introduced a receiver based on a transiently chaotic NN using chaos theory. Jeney *et al.* [33], [34]

[1] The process of simulated annealing will be explained later in the chapter, for now it is merely stated for the purposes of the literature review.

proposed a stochastic Hopfield network (SHN), in which noise is added, in a controlled manner, to the Hopfield recursive algorithm, so as to help the model escape from local minima. This detector has shown to be superior to the classical Hopfield-based MUD scheme and in a perfectly coherent channel it achieves near-optimal performance. This result was extended in the investigation of a blind detection scheme using stochastic networks [63].

Stochastic models have shown great promise in achieving sub-optimal performance, however there is still an area for improvement. In this chapter, an HNN is proposed for MUD, based on a stochastic technique. We show how the problem of optimum MUD may be mapped to the problem of minimizing the HNN energy function. The statistical roots of the HNN are investigated and principle statistical techniques, which have been applied to neural networks to overcome local minima, are introduced. We discuss some stochastic methods and review the SHN detector [33]. Finally, the proposed model that incorporates SSA is introduced and its performance is quantified by comparing it to other sub-optimal MUD schemes, via simulations.

5.2 Problem Mapping

When neural networks are employed to solve a specific problem, the major task following the selection of an appropriate NN architecture is determining the network parameters. These parameters usually include the number of layers, number of neurons and biasing, for example. For use as a parallel algorithm in the external field (of MUD in CDMA systems), the parameters of the CDMA receiver must be clearly mapped to the defining parameters of the NN, to ensure that it operates as required.

Figure 5.1 is a block diagram of a typical neural-based multiuser receiver, in which the outputs from a SUMF detector is input into a NN. The problem is to determine what the matched filter outputs represent to the NN and, in general, which of the variables (signals) of the SUMF detector are required to specify the NN completely.

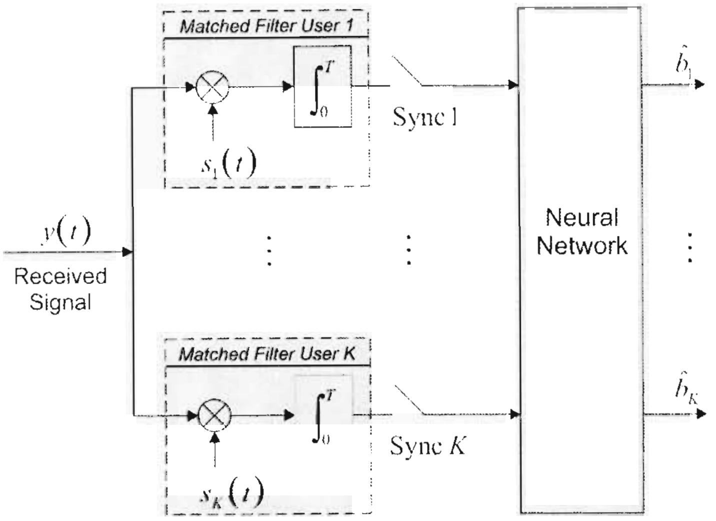

Figure 5.1 Multiuser detector model employing a neural network for post-processing of the matched filter outputs.

The HNN is employed for use in MUD by firstly relating the energy function to the log-likelihood function of the OMD [32], [46], [47]. The view taken is the same as in many other optimization problems that have been solved using neural networks, i.e. optimization in MUD can be translated to energy optimization in the HNN. It is relatively easier to map the parameters of the different systems if their objective functions are similar. To achieve this, we begin by accounting for the external inputs to the HNN (bias terms) by redefining (4.11) as:

$$E = -\frac{1}{2}\sum_{i=1}^{\hat{M}}\sum_{\substack{j=1 \\ i\neq j}}^{\hat{M}} w_{ij}x_i x_j - \sum_{i=1}^{\hat{M}} f_i x_i \,. \tag{5.1}$$

The energy is a function of the neuron states. By employing a vector-matrix notation, then during pattern retrieval the HNN maximizes the following quadratic form:

$$E(\mathbf{x}\ ) = -2\mathbf{f}^T\mathbf{x} - (\mathbf{x})^T\mathbf{W}\mathbf{x}, \tag{5.2}$$

where $\mathbf{x}(k) = \{x_i(k)\}$, $\mathrm{W} = \{w_{ij}\}$ is the weight matrix and $\mathbf{f} = \{f_j\}$ is the vector containing all external inputs.

For convenience, (3.54) is reproduced with $\mathbf{H} = \mathbf{R}$ [32], [46], [48], such that:

$$\Omega(\mathbf{b}) = 2(\mathbf{y})^T \mathbf{b} - \mathbf{b}^T \mathbf{H}\mathbf{b}. \tag{5.3}$$

There is high degree of similarity between the maximum likelihood function (5.3) and the energy function (5.2). It is possible to determine the parameters of the HNN from the parameters of the conventional DS-CDMA receiver by letting

$$E = -\Omega. \tag{5.4}$$

Under this premise, it is possible to acquire the most likely transmitted sequence by solving the optimum decision rule via the HNN energy function. The parameters of the HNN may now be specified. Firstly, the dimensions of the variables indicate the size of the network. For K users each transmitting M symbols, the network size is obtained by assigning a single neuron to a single symbol. Thus, the total number of neurons in the single-layered HNN is simply given by:

$$\hat{M} = K \times M. \tag{5.5}$$

Hopfield and Tank [10] showed that for convergence to a stable state, the weight matrix must be symmetric with zero diagonal elements. To equate the weight matrix to the packet channel matrix, (5.3) is modified so that $\mathbf{H}$ has zero diagonal elements. The weight matrix $\mathbf{W}$ is then defined as [46]:

$$\mathbf{W} = -(\mathbf{H} - \operatorname{diag} \mathbf{H}). \tag{5.6}$$

By making the substitution for the diagonal matrix $(\operatorname{diag} \mathbf{H})$ in (5.3), the term $\mathbf{b}^T(\operatorname{diag} \mathbf{H})\mathbf{b}$ is always positive and does not affect the decision rule [60]. The external inputs to the HNN are given by the matched filters, i.e. the biasing terms of the HNN (for unit amplitudes) is obtained from:

$$\mathbf{f} = \mathbf{y}. \tag{5.7}$$

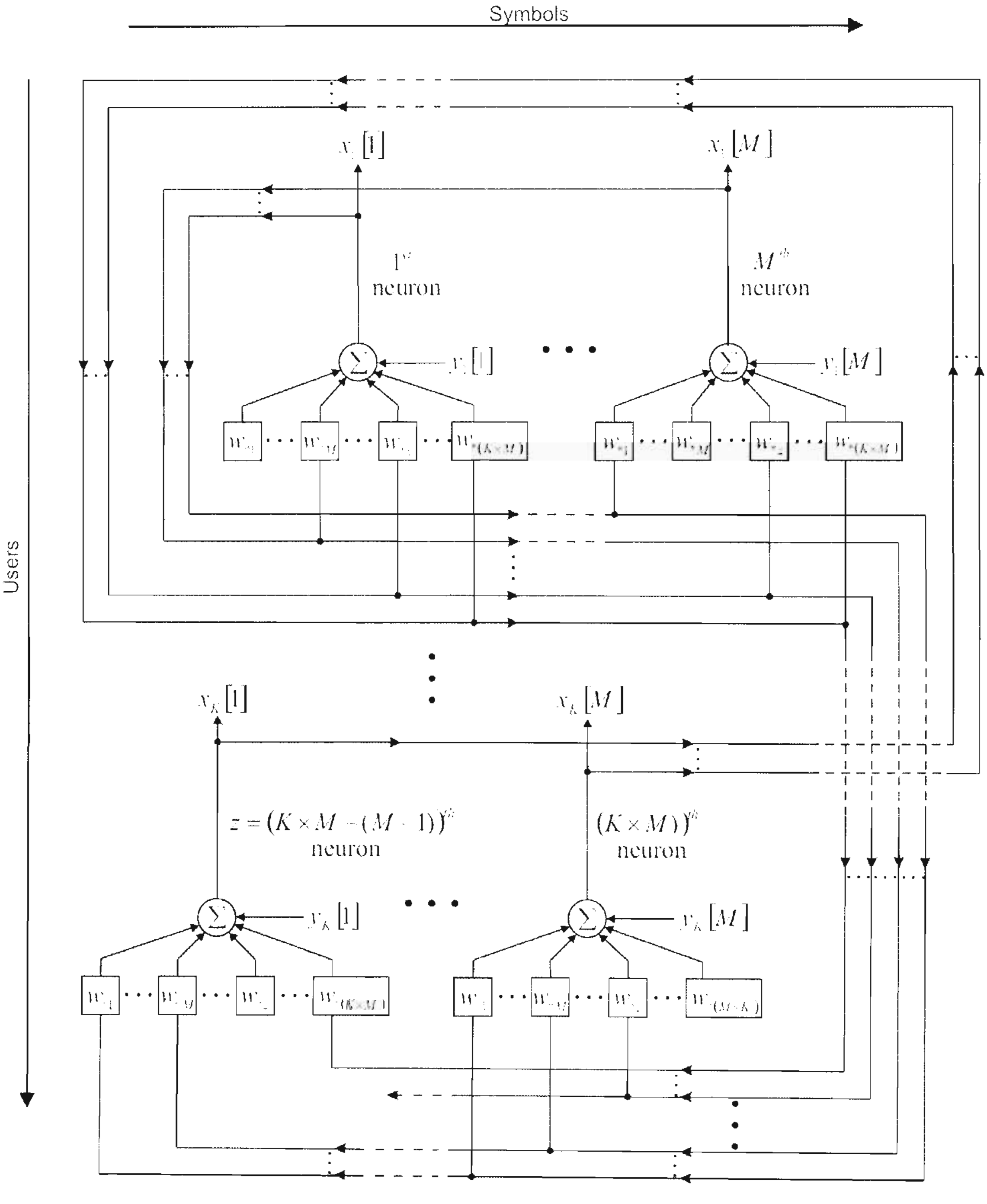

* = number of the current neuron in question

Figure 5.2 Schematic diagram of the Hopfield-based MUD, presented as a 2D array with rows and columns signifying users and symbols, respectively. Each symbol is allocated a single neuron [32].

Figure 5.2 shows an internal view of the neural network block depicted in Figure 5.1. For simplicity, the schematic presents the Hopfield-based MUD in two dimensions: symbol (time) and users. This scheme is only possible when the parameters are defined accordingly, using (5.5), (5.6) and (5.7). Under these conditions the (global) minimum of the energy function corresponds to the maximum of the likelihood function. Equation (5.5) ensures that there is no conflict in variable dimensions. Once the network parameters are obtained, the states of the neurons are iteratively updated. The initial state of the HNN is set to zero so that a jump to either of the two states $\{+1,-1\}$ occurs with equal probability; neither state is favoured.

The iterative process is typically sequential. Parallel updating is faster [38], [51] but convergence is not guaranteed and may result in unstable states. A combination of both techniques is also possible. In [61], a block technique was proposed in which there are randomly specified blocks of neurons and updating between blocks occurs sequentially but neurons within a block grouping are updated simultaneously. In the proposed model we employ sequential updating unless it is stated otherwise.

5.3 Statistical Mechanics

It has been shown how the HNN may be employed to perform MUD on the received DS-CDMA signal. In this section, we discuss the origin of the Hopfield model in the context of statistical mechanics and investigate some basic principles on which the HNN is modelled. The theory of statistical mechanics also lends itself to the development of many techniques, one of which is proposed herein, to improve the performance of the HNN and neural-based multiuser receivers in general.

Statistical mechanics is a field of condensed matter physics that investigates the macroscopic equilibrium properties of large systems (i.e. systems having many degrees of freedom). These properties are subject to microscopic changes that occur to the many particles that make up the system, and which adhere to the laws of mechanics [38]. Basically, this research field quantitatively describes the behaviour of physical systems, usually at or near thermal equilibrium. For the vast amount of constituent particles, the most probable behaviour of a system at thermal equilibrium can only be observed in experiments [56]. The overall properties are determined by the average behaviour of an ensemble of identical systems. In the context of this research, the theory of neural networks is closely linked to this field. Many neural models draw on statistical mechanics concepts and analogies to achieve varying functionality and which are inspired by the operation of physical systems.

Hopfield pointed out that the behaviour of some physical systems could be used as a form of CAM and this could be achieved using a type of RNN [55], [59], [64]. In the Hopfield model, the computation dynamics are characterized by the existence of stable states similar to a dynamical system. In particular, Hopfield drew analogies with the simple model of magnetic materials in the proposal of the HNN.

In a magnetic material each atom in the lattice has an associated spin that describes one of two states: up or down. The model of the magnet is based on the concept of these interacting spins, which may be represented in an Ising model [39], [40], An Ising model may simply be viewed as a 2-D configuration space that graphically shows the possible state of each spin at every lattice site. Possible assigned values are ± 1, i.e. a spin is either on ($\equiv$up) or off ($\equiv$down). Ising models are quite useful for describing two-valued variables. Their aim is to imitate the behaviour in which individual elements (e.g. atoms) respond to the behaviour of neighbouring elements surrounding them; the interaction and dynamics between elements are necessary to specify the complete Ising model [40].

It is clear to see that the states in an HNN are much like the states of magnetic spins. The Ising model is applicable to the neurons which constitute the network and which may be thought of as spins with firing and non-firing states. Many of the physical concepts, notably the process of annealing, are therefore also applicable. In statistical mechanics the question of importance is how the system behaves or what its properties are at the temperatures in which it settles. The Metropolis algorithm approximates the average behaviour of a many-particle system as a function of temperature, specifically at thermal equilibrium. It is an ideal tool for bringing methods in statistical mechanics to bear on optimization problems [56].

5.3.1 Metropolis Algorithm

Formally, the Metropolis algorithm provides an efficient simulation of the evolution of a solid in a heat bath to thermal equilibrium at a given temperature [65], using Monte Carlo techniques. In the context of optimization, a brief foray into the Metropolis algorithm is warranted so as to introduce the principles behind SA. The discussion is sufficient for the purposes of this study, but it is not an in-depth explanation of the physical concepts.

At thermal equilibrium, the states of a physical system obey the Gibbs distribution, which gives the probability of solid being in state i with energy E_i at temperature T. The Metropolis algorithm obtains samples from the Gibbs distribution [66] and as a result the final state evolves into this distribution. Consider a system in state i. The next state j is generated by subjecting the system to a small random perturbation or a randomly displaced atom. The change in the energy of the system is ΔE. If $\Delta E \leq 0$, state j becomes the new state, i.e. the change in the system is accepted. However, if $\Delta E > 0$, then state j is only accepted with some specified probability [56], [66], [67]. This is the basic operation of the Metropolis algorithm.

The probability that the configuration with the displaced atom is accepted is given as:

$$P(\Delta E) = \exp\left(-\frac{\Delta E}{k_B T}\right), \tag{5.8}$$

where T is the temperature and k_B is the Boltzmann constant. The probabilistic mechanism in the algorithm is implemented by drawing a random number from the uniform distribution $X \sim U(0,1)$ and comparing it to $P(\Delta E)$. If it is less than $P(\Delta E)$ then the next state is accepted otherwise the original state remains. Thus, during the search for the final (global) minimum energy state, the Metropolis algorithm may allow transitions to states which increase the energy temporarily to avoid local minima, unlike gradient descent methods. At equilibrium the Gibbs distribution prevails, indicating that at low temperatures only the minimum-energy states have a non-zero probability of occurring [68]. By repeating the Metropolis process the thermal motion of atoms in a solid, subject to temperature T, are simulated.

5.3.2 Simulated Annealing

Simulated annealing (SA) is a heuristic optimization technique that was introduced by Kirkpatrick *et al.* [56] as a method for finding optimal or near-optimal solutions to large scale optimization problems. It originates from the Metropolis algorithm and employs a thermodynamic metaphor from statistical mechanics, which likens the process of solving an optimization problem to finding the low temperature (energy) state of a physical system. The algorithm searches the set of solutions in a similar manner to how a thermodynamic system changes from one energy state to another. The fundamental idea is to avoid local minima by permitting fluctuations that may not always lower the cost function, while ultimately searching for a global minimum.

The thermodynamic metaphor is appropriate considering that the underlying process in an HNN is one of optimization and the cost function to be minimized is an energy function. SA is not unfamiliar to neural networks as it was first employed in the Boltzmann machine [65], thus some of the same concepts are applicable here.

The physical process of annealing is a method of obtaining low energy states of a solid [65], usually a metal (or glass) which is hardened by first heating it up and then cooling it down until it reaches a state of its crystalline lattice that is highly packed. The idea is to minimize the formation of defects resulting from locally optimal lattice structures. It is achieved by setting the initial temperature very high to get the atoms unstuck from sub-optimal states and then carefully lowering it. When cooled appropriately, the metal assumes a low energy configuration.

Kirkpatrick *et al.* [56] generalized the Metropolis algorithm to include a temperature schedule for efficient searching of the minimum energy states. It was shown that a process of annealing could be used to generate a sequence of solutions to a COP. This is achieved by minimizing a cost function in place of the energy function of a physical many-particle system. The solutions to the COP are equivalent to the states of the system. There is no equivalent for physical temperature in optimization; we denote T_p as a pseudo-temperature[2], which controls the process of finding the global minimum. Therefore, based on the physical concept, the simulation of the annealing process may be viewed as an iteration of a sequence of Metropolis algorithms executed over time-dependent (decreasing) temperatures.

The mathematical formalism of SA is based on the theory of finite Markov chains. The description herein is simple in comparison, but sufficient for our purposes. In practice, there are three specifications for SA. Firstly, a description of the problem representation is required. This consists of an expression for the cost function and the state space representation. Secondly, there must be a generation mechanism that creates a possible new solution (state), and an acceptance mechanism (exemplified by the Metropolis criterion) that decides if the new solution is acceptable based on some criteria. The criteria may vary depending on the problem. Finally, for an efficient annealing schedule, an initial value of the control parameter T_p, a method of decreasing T_p and a stopping criterion must be determined.

The following algorithm displays the simplicity and ease of application of SA. The algorithm starts by generating an initial solution (either randomly or heuristically constructed) and by initializing the pseudo-temperature. Depending on the problem

[2] The pseudo-temperature is also referred to as the control parameter [65].

at hand, this initial temperature, denoted by $T_{p,0}$, is estimated to be high enough so that all transitions are accepted with equal probability. At each successively lower temperature, the simulation must iterate long enough for equilibrium (steady state) to be reached, i.e. the "cooling" process must be sufficiently slow. This is achieved by using parameter C_{eq} which controls the length of run of the Metropolis algorithm at a single temperature. The basics of SA are shown below.

Algorithm 5.1: Basics of Simulated Annealing

```
1: Initialize
   1.1. Generate initial state $i$
   1.2. Calculate annealing schedule parameters:
        1.2.1. Initial temperature, $T_{p,0}$
        1.2.2. Time to thermal equilibrium, $C_{eq}$ ; $k = 0, c = 0$
        1.2.3. Cooling function/factor, $\lambda(k)$

2: Annealing
   2.1. Generate new state $j$
   2.2. Compute change in cost function $E$
   2.3. Apply acceptance mechanism, e.g. Metropolis criterion:

        while $c < C_{eq}$ {
            $c = c + 1$
            if $\Delta E \leq 0$ then $i = j$
            else {Generate $x \sim U(0,1)$
                if $\exp(-\Delta E/T_{p,k}) > x$ then $i = j$
                }
        }

   2.4. Apply annealing schedule:

        $k = k + 1$
        $T_{p,k+1} = \lambda(k) \cdot T_{p,k}$
        $c = 0$

3: Stopping Criteria
   3.1. Repeat 2 until $\Delta(\Delta E) = 0$ or $(\min T_p)$ reached
```

The technique of gradually lowering the temperature ensures that a local minimum can be avoided without having to spend an infinite amount of time waiting for a transition out of a local minimum. The sequence of pseudo-temperatures and the method of reaching equilibrium, at each temperature, define the *annealing schedule*.

5.3.3 Annealing Schedule

SA helps to escape the local minima by introducing fluctuations in the energy function. Provided the temperature is lowered slowly, the system will reach thermal equilibrium at each temperature. Geman and Geman (cited in [65]) were first to show the convergence of the SA algorithm; if the temperatures are decreased not faster than logarithmically, i.e. there is a lower bounded such that

$$T_{p,k} = \frac{T_{p,0}}{\ln k}, \tag{5.9}$$

for large $T_{p,0}$ and $k >> 1$, the algorithm will converge to a global optimum if started in an arbitrary state and given an suitable annealing schedule. Similar conditions for asymptotic convergence were derived by several other authors cited in [65], [66].

The SA algorithm converges onto the optimal solution set with probability one but this may occur over an infinite number of iterations [38], [65]]–[67], especially if the technique synonymous with the Boltzmann machine is used (i.e. with the Gibbs distribution). Even if the asymptotic behaviour is approximated, the amount of computation time that is required depends on the scale of the problem. There is a clear trade-off between the quality (optimality) of the solutions and the time required to compute them. Polynomial-time approximation of the SA algorithm maintains the practicality of using this algorithm while maintaining near-optimal performance.

For the intended application, it is useful to employ a finite-time approximation of the SA algorithm to limit the convergence time. While it may lower the possibility of finding a global minimum, it makes the algorithm practical to use (in the simulation for MUD) and in most cases a near-optimum solution is still guaranteed [38].

Finite-time approximation may be realized by employing an annealing (cooling) schedule with two distinguishing features. Firstly, it must have a finite sequence of pseudo-temperature values. These values are specified, in part, by an initial value $T_{p,0}$, a decrement function $\lambda(k)$ (or constant cooling factor λ) and a final value $T_{p,f} = T_{p,k\to\infty}$. The latter property depends on a stopping criterion that is used to halt the overall simulation. Secondly, for each $T_{p,k}$, a finite number of transitions must be allowed (e.g. transitions as determined by the Metropolis criterion). There are several techniques of decreasing T_p. Commonly, exponential scheduling (for the Gibbs distribution) is used (as in Algorithm 5.1), such that for $\lambda \in (0,1)$,

$$T_{p,k+1} = \lambda \cdot T_{p,k} \, , \tag{5.10}$$

A suitable initial temperature $T_{p,0}$ is one that results in an average increase of acceptance probability of about 0.8, i.e. there is an 80% possibility that a change which increases the objective function will be accepted [56]. The choice of $T_{p,0}$ is problem-specific. The time to thermal equilibrium is specified by C_{eq}. It satisfies the requirement of the second feature and limits the number of transitions. It may also denote the minimum number of accepted transitions for thermal equilibrium to occur at $T_{p,k}$. Irrespective of how C_{eq} is defined, its value depends on the size of the problem. For the proposed MUD scheme, we offer yet another definition. The SA process is terminated when a predefined final temperature $T_{p,f}$ is reached or when there are no further changes to report. Other stopping criteria, which dictate the value of $T_{p,f}$, include limiting the number of iterations k, or stopping when the number of accepted transitions is not achieved at three or more successive temperatures.

5.4 Stochastic Techniques for the HNN

What is the purpose of SA in the current application of neural networks for MUD? SA is a simple method of escaping local minima. Recall that the HNN suffers from localized optimization; when it evolves, the optimization process that defines pattern retrieval converges to the first local minimum found in the energy surface (since the approach is based on a gradient descent technique). This may not be the global minimum since there are also non-desirable local minima (often representing spurious states), which are a basic result of the network's non-linearity [68].

Several methods, categorized as either deterministic or stochastic, have been proposed to improve the performance of the Hopfield model for optimization. Developments in hardware implementation have also enabled local minima to be avoided [59]. Stochastic approaches address the problem of poor solution quality caused by local minima and SA is a stochastic search technique.

To employ SA, we must simulate the effects of temperature in the system, specifically the effects of the random perturbations which cause changes in the energy of the individual particles. We can simulate this behaviour in a NN by adding a stochastic element to its operation. There are a handful of methods, found in literature, with which stochasticity may be introduced into the HNN [59]. One way is to employ a stochastic decision-type activation function. Another is the introduction of noise to either the weights or to the external inputs (biasing) of the network, as it was done in [33]. A third way is to use a combination of these methods.

It is the general idea of stochastic techniques, and not just SA, to introduce randomness into the NN so that during convergence the energy is allowed to increase sometimes, thus allowing an 'uphill' move in the energy surface to escape local minima [38]. Such search methods are a widely used class of heuristics that are tailored to solve specific optimization problems. In comparison to iterative or gradient search methods, stochastic optimization algorithms are not restricted to ordinary iterative improvement i.e. taking only a "downhill" step (gradient descent). In addition, they may simultaneously explore many different regions of the search space. However, the objective is to obtain a near-optimal solution; a global optimum solution is not guaranteed but the probability of this occurring is generally assured for a relatively large number of iterations. The proceeding sections indicate how stochastic techniques may be employed in HNN-based multiuser detectors.

5.4.1 Stochastic Hopfield Network for MUD

In [33] a stochastic Hopfield network (SHN) was proposed to overcome local minima, for use in MUD. The state updating rule of (4.9) was modified by adding a random internal noise source $\upsilon(k)$, which resulted in a stochastic rule given by:

$$x_j(k+1) = F\left(\sum_{i=1}^{M} w_{ji} x_i(k) + f_j + \upsilon(k)\right), \tag{5.11}$$

where $\upsilon(k)$ is a zero mean random variable with logistic distribution function,

$$P[\upsilon(k) \leq x] = F(x,k) = \frac{1}{1+e^{-x\Lambda(k)}}, \tag{5.12}$$

and where

$$\Lambda(k) = \hat{\lambda} \cdot k \tag{5.13}$$

is a positively increasing function of k, $(\hat{\lambda} > 1)$, i.e. it is a control parameter that limits the level of noise. It should be noted that $\hat{\lambda}$ is also a cooling factor, but it is distinguished from λ. The range of possible values of $\Lambda(k)$ constitutes the annealing schedule. In standard form, $\Lambda^{-1}(k)$ is the scale parameter of the logistic distribution function [69] (Appendix D). The random variable $\upsilon(k)$ is used on condition that the $\lim\limits_{k\to\infty} E\left[(\upsilon(k))^2\right] = 0$, i.e. it must have a variance that is cooled with k. This is achieved by the SA schedule. Under this condition, and with the use of $F(x,k)$, the SHN model has been shown to asymptotically approach the classical HNN model [34]. It coincides with the state transitions and converges to the optimal state. It is interesting to note that the logistic function employed in this model describes thermal fluctuation in statistical physics. It is shown next that it also is appropriately used to model stochastic neurons.

5.4.2 Probabilistic HNN with SA

In neuroscience theory there are delays associated with individual transmissions between neurons. As a result of this, signals arriving at a specific neuron tend to spread. In addition, the neurons fire with variable strength and random fluctuations are bound to occur during synaptic transmission. These effects may be regarded as noise and are often accounted for by using stochastic neuron models. In these models the deterministic transition rule (4.9) is replaced with a probabilistic firing mechanism, which says that the jth neuron fires at time $(k+1)$ with some probability $P(v_j)$. Mathematically, the stochastic rule is given as:

$$x_j(k+1)=+1 \text{ with probability } P\left(\sum_{i=1}^{M} w_{ji}x_i(k)+f_j\right), \qquad (5.14)$$

with the jth neuron inhibited at time $(k+1)$ with probability $1-P(v_j)$, such that

$$x_j(k+1)=-1 \text{ with probability } 1-P\left(\sum_{i=1}^{M} w_{ji}x_i(k)+f_j\right), \qquad (5.15)$$

Returning to the analogy, the method of describing the effect of thermal fluctuations on spins in an Ising model is based on Glauber dynamics [39]. The Glauber choice for $P(v_j)$ is the logistic function, which is useful for employing concepts from statistical mechanics. However, since there is no physical temperature in the intended application, the Boltzmann constant is excluded. In that case, $P(v_j)$ is given as

$$P(v_j)=\frac{1}{1+e^{-2v_j/T_p}}, \qquad (5.16)$$

where T_p is the previously defined pseudo-temperature. At high temperatures all energy states are possible and the network can easily overcome local minima, since as the network is cooled, it becomes difficult to jump to higher energy states (which are possibly spurious states). Then, only the lower energy states will have a non-zero probability of occurring. Under these circumstances, the SA algorithm applies.

Algorithm 5.2: Modified Simulated Annealing for MUD

```
1: Initialize Network
    1.1. Set: $\mathbf{f} = \mathbf{y}$
    1.2. Set : $\mathbf{x}(0) = \mathbf{0}_{K \times M}$
    1.3. Calculate annealing schedule parameters:
        1.3.1. Initial temperature, $T_{p,0}$
        1.3.2. Accepted transitions, $C_{eq}$ ;$k = 0, c = 1$
        1.3.3. Cooling function, $\lambda(k)$

2: Simulated Annealing
    2.1. Calculate $v_j$ of (random) neuron $j$ $(j \neq i)$
    2.2. Sequentially update neuron states by applying (5.14) or
         (5.15), conditioned on (5.16)
    2.3. Accepted transitions?

         while $c < C_{eq}$ {
             if $\Delta E \leq 0$ then $c = c + 1$
             goto 2.2
             }
    2.4. Apply annealing schedule:

         $k = k + 1$
         $T_{p,k+1} = \lambda(k) \cdot T_{p,k}$
         $c = 0$

3: Stopping Criteria
    3.1. Repeat 2 until
        3.1.1. $k_{\max}$ iterations $(\min T_p)$ reached, or
        3.1.2. desired BER, or
        3.1.3. no states changes at three successive $T_{p,k}$
```

A modified SA algorithm for possible use in an HNN-based MUD is shown above (Algorithm 5.2). The generation mechanism is given by v_j in (4.1) and neurons are updated in consecutive order. The acceptance mechanism employs the stochastic transition rules described by (5.14) and (5.15).

From the discussion in Section 5.3.3, the (stopping) criterion that dictates whether equilibrium has been attained, given by C_{eq}, is now defined as the number of transitions that result in an energy decrease (i.e. the number of accepted transitions). Alternatively, it may represent the number of transitions that have occurred. These techniques constitute finite-time approximation methods, as discussed earlier. There are several ways of terminating the overall process. For MUD, steps 3.1.1 and 3.1.2 are most appropriate. They reduce simulation complexity and hence simulation time. Finally, the cooling function is left to be determined. In [33] and [34], $\hat{\lambda}(k)$ was determined empirically. To date, there is no formal mathematical result that illustrates the effect of the annealing schedule (or annealing constant) except from the viewpoint of statistical mechanics.

5.5 Results

In this section, the simulation results for the aforementioned proposed model and the sub-optimal detectors (SUMF, LDD and MMSE) are presented. Hereafter, the proposed stochastic HNN-based multiuser detector is denoted as the probabilistic HNN employing SA, or PHN-SA model. All simulations were performed in Matlab® and the results obtained are those for the transmission model described in Chapter 3, for the asynchronous uplink of a DS-CDMA system. Appendix E describes the setup of the simulation software.

The channel state information is known at the receiver. The channel is assumed to be affected by AWGN only $(h_k(t) = 1 \; \forall \; k \text{ and } t)$ and, unless otherwise stated, length-31

Gold codes $(N = 31)$ have been used. The frame length was set to $M = 100$ bits. The BER performance is compared, where appropriate, to the SUMF, LDD and MMSE detectors, as well as the HNN and SHN neural-based receivers. The single-user bound refers to the optimum error probability for a single BPSK user transmitting in an AWGN channel. For the PHN-SA model, the initial neuron states of the HNN were set to zero and updating was sequential.

The SA process is based on Algorithm 5.2. A limit on the maximum number of iterations was used as a stopping criterion, which is suitable considering the nature of the application and that the simulated systems vary in size. It was usually set to $k_{\max} = 20$, to reduce simulation time, but also depends on the system. For joint detection, the entire HNN is to be updated, so C_{eq} was set to the maximum number of possible transitions, which is the number of neurons. In that case, the instantaneous energy does not need to be computed. This reduces computational complexity, especially in the case of relatively large networks ($\geq 10^3$ neurons and with matrices of size $10^3 \times 10^3$, or greater). The cooling factor for the SHN model was set to $\hat{\lambda} = 1.5$ [33] and accordingly we set $\lambda = 1/1.5$ for the PHN-SA model, for the purposes of comparison. These parameters are assumed throughout, unless otherwise stipulated. Appendix E provides some of the basic simulation parameters.

First, the BER performance of the first user in a ten-user asynchronous system was investigated, with all users being received with equal powers. The relative delay of the kth user was calculated as $\theta_k = (k-1)T_c$, obtained from [33]. This deterministic approach was taken to investigate the effect of different delays assigned to each user and it assumes that user $k = 1$ is the first transmitting user, and so on. The results of the simulation are shown in Figure 5.3. The proposed PHN-SA model outperforms the SUMF and the linear sub-optimal detectors; at high SNR the performance gain is about 1.4 dB. Due to the enhancement of MAI, the LDD performs worse than the SUMF detector at low SNR, which is expected. As the SNR increases the MMSE approaches the performance of the LDD.

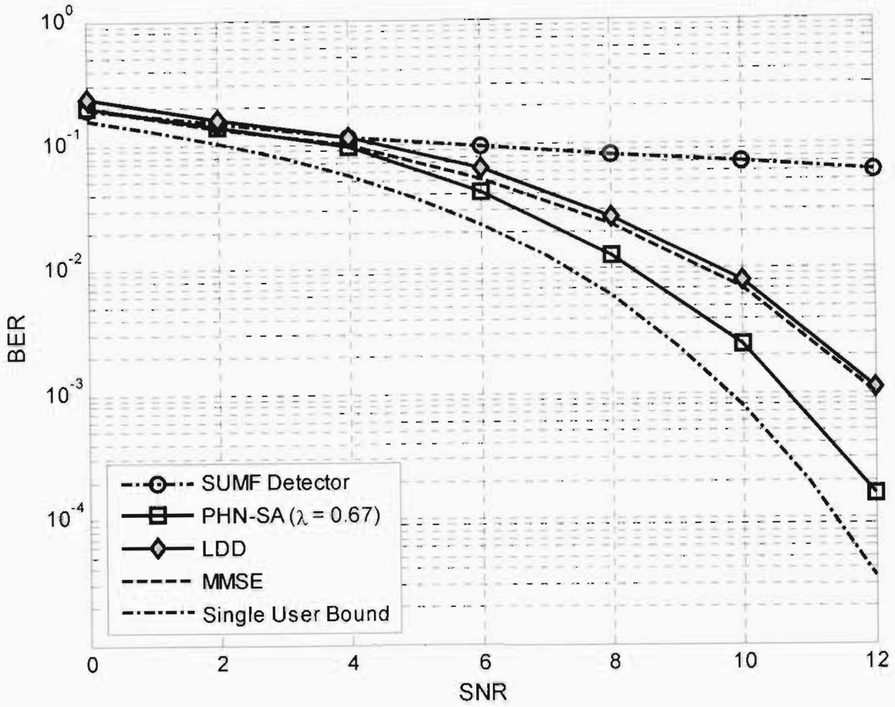

Figure 5.3 BER performance of user 1, for $K = 10$ equal-power asynchronous users.

Figure 5.4 shows the performance of the worst and best users (in terms of BER performance) [51] resulting from SUMF detection, in the system in Figure 5.3. For the same two users (user 4 and user 8), the PHN-SA model showed little difference in BER. The gain is at most 1 dB, indicating that the PHN-SA model is resistant to the errors in the conventional receiver.

Figure 5.5 investigated the BER performance of the (actual) best and worst users [51] in the PHN-SA detector, namely user 3 and user 10, respectively. These were the same for the LDD. As compared to the SUMF receiver (Figure 5.4), the performance difference in the PHN-SA, between its best and worst performing users is almost 1.3 dB only. Furthermore, the performance of the best user obtained using decorrelation detection coincided very closely to that of worst user in the PHN-SA detector. This clearly illustrates the performance improvement that the neural-based model can achieve.

8dB = 5.8×10^{-3}
(SUMF, LDD)
9dB = 2.4×10^{-3}
10dB. 7.8×10^{-4}

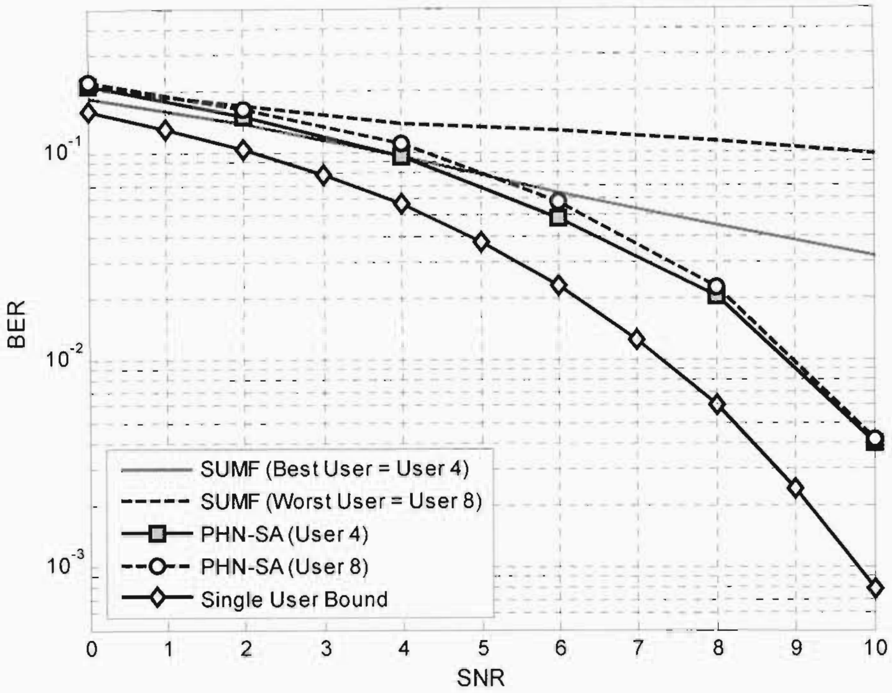

Figure 5.4 BER performance of the worst and best users (using SUMF detection) in the 10-user, asynchronous system.

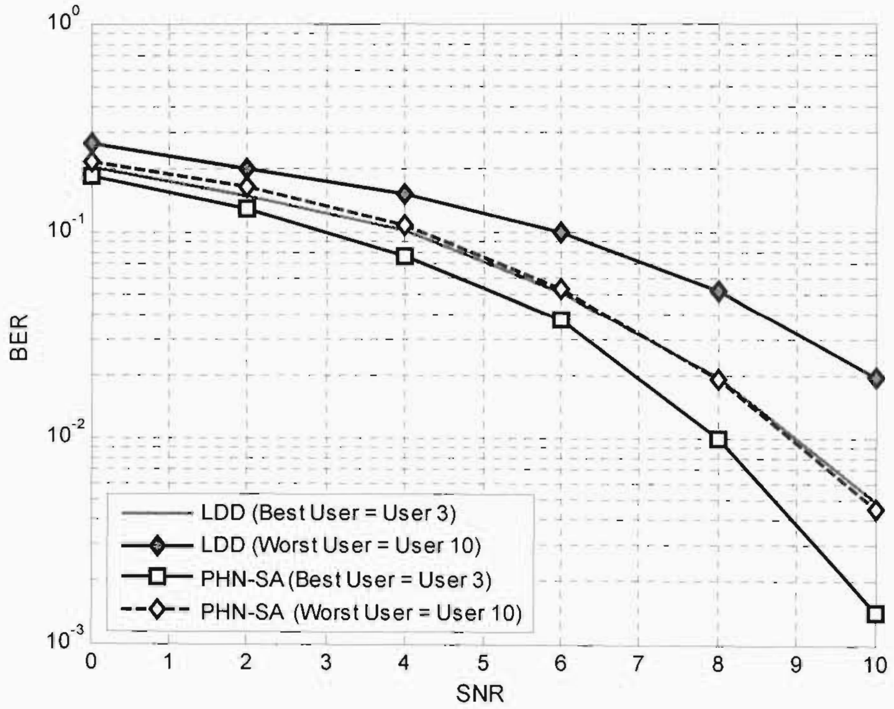

Figure 5.5 BER performance of the worst and best users (based on PHN-SA model) in the 10-user, asynchronous system.

The near-far resistance of the proposed PHN-SA scheme was investigated in the same manner as the SUMF detector (in Chapter 3). The case of two synchronous users was considered for three scenarios: $A_2 = A_1$, $A_2 = 2A_1$ and $A_2 = 6A_1$, with a constant cross-correlation of $\rho = 0.2$ [14]. The cross-correlation values were set so as to investigate the effects of higher (different) correlations, as carried out in [14]. A code length of $N = 31$ was still employed. The results of the SUMF detector (in Figure 3.3) are reproduced for the purpose of comparison. It can be seen from Figure 5.6 that the BER of user 1 is not significantly affected by the increasing amplitude of the interferer, in the PHN-SA model, i.e. it offers some level of near-far resistance.

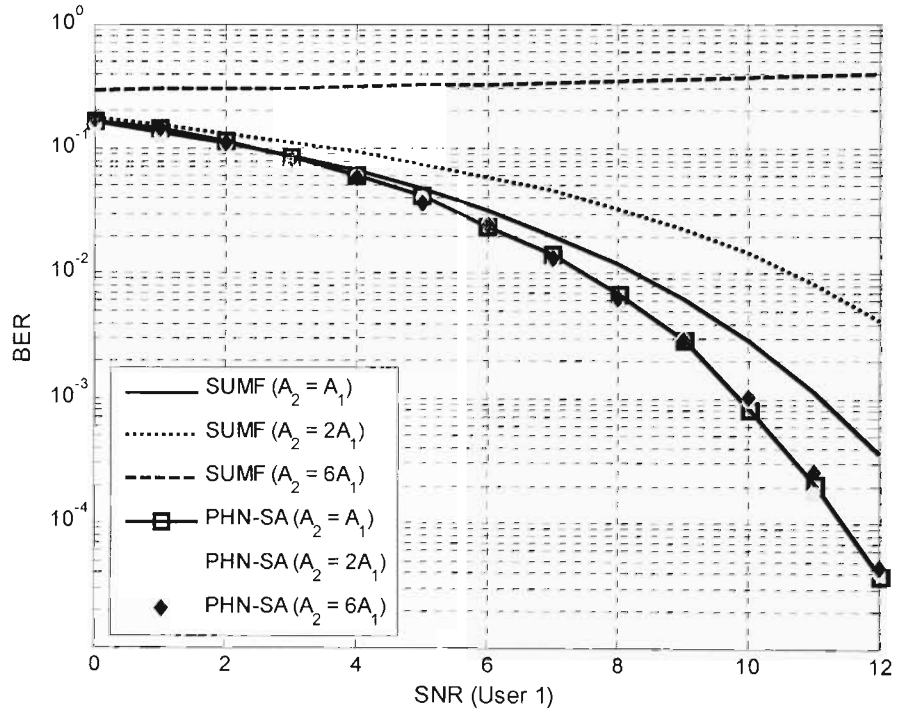

Figure 5.6 BER performance of user 1, for varying powers of the interfering user. $K = 2, \rho_{ij} = 0.2 \; \forall \, i, j$.

At first glance, the performance of the PHN-SA detector is similar to that exhibited by the LDD, in a near-far situation. This is investigated further in Figure 5.7, which illustrates the BER as a function of the ratio of the received amplitude of the interfering user to the received amplitude of the desired user, which is the near-far ratio. For the two-user system, the near-far ratio is given by $20\log_{10}(A_2/A_1)$. We have chosen the arbitrary SNR of 8 dB to evaluate the BER performance of the desired user (user 1).

Figure 5.7 shows that the performance of the PHN-SA does not deviate far from that of the LDD; it is near-far resistant to an acceptable degree. For a relatively high-powered interferer the PHN-SA outperforms the SUMF detector and is only slightly better than the LDD. However, its behaviour changes for sufficiently low interferer power. The performance of the SUMF detector degrades as the interfering signal becomes stronger. These results are comparable to and verified by the results in [41]. It was generally found that while the number of iterations was sufficient for the SUMF receiver, the random nature of the PHN-SA model required more iterations in the Monte Carlo simulation. A maximum of 20 000 iterations was processed.

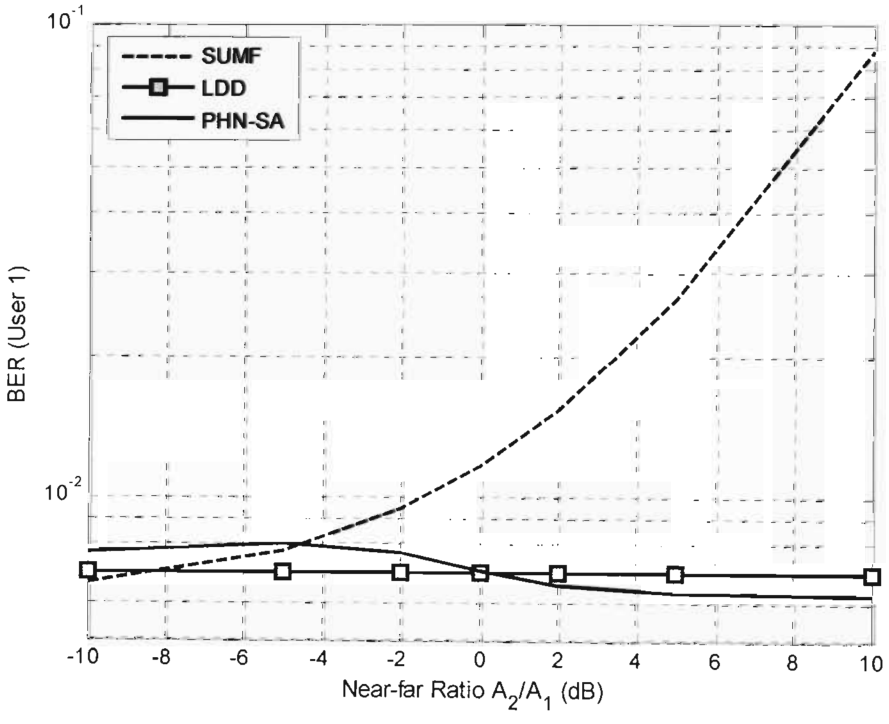

Figure 5.7 BER of user 1 as a function of the near-far ratio A_2/A_1, at 8 dB, for $K = 2$, with $\rho_{ij} = 0.2\ \forall\, i, j\ (i \neq j)$.

In [33], a single (empirically determined) annealing constant was employed. In Figure 5.8, the effect of the annealing constant (λ) on the BER performance was investigated, for several values of λ. Except at relatively high cooling factors (close to 1), the BER performance of the PHN-SA model does not differ very much for $\lambda \leq 0.7$ (approximately). This is expected, since as λ approaches 1, the cooling schedule ceases to exist. Although there are (high) values of λ for which the PHN-SA model performs worse than the SUMF receiver, the results show that, generally, there is a low dependency on the annealing schedule. The optimal range for λ, or an optimal cooling factor (if it exists), still needs to be determined. The analysis is left for possible future work.

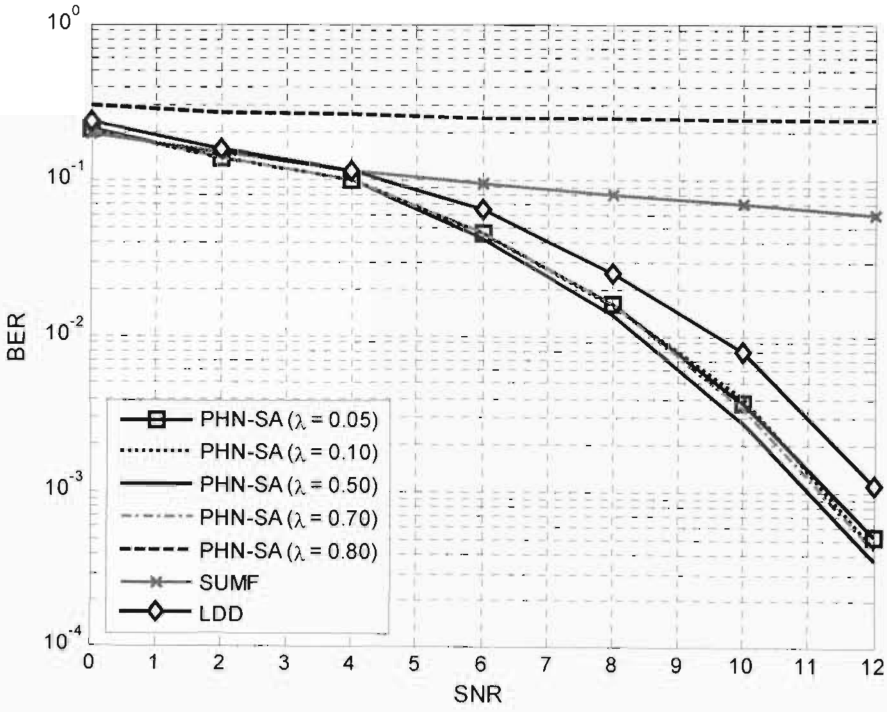

Figure 5.8 BER of user 1 in the presence of 9 equal-power users. $K = 10$, $\lambda \in \{0.05, 0.10, 0.5, 0.7, 0.8\}$, $\rho_{ij} = 0.2$.

The performance of a DS-CDMA system is severely affected by (high) cross-correlation properties of the spreading sequences assigned to the users. This depends on the family of PN sequences, as well as on the channel characteristics (or system).

The detection process, when the cross-correlations between the different users are increased beyond the theoretical cross-correlations (of length-31 Gold codes), was simulated. The system consisted of 5 synchronous users with $\rho_{ij} = 0.3$ $(\forall i, j\,; i \neq j)$, i.e. it is assumed to be constant for all pairs of sequences [14]. The problem associated with the classical HNN model can be seen in Figure 5.9 as it performs worse than both stochastic HNN-based receivers. However, in comparison, the LDD achieves the best performance, with a gain of almost 0.6 dB, relative to PHN-SA model. The reason for this is that the LDD is able to decouple the non-diagonal terms from the cross-correlation matrix irrespective of how large these terms are. Hence, it shows an improved BER performance over the neural-based receivers when the non-diagonal correlation terms become larger, which adversely affects their performance. At high SNR, the SHN only performs slightly better than the PHN-SA. However, both schemes outperform the SUMF receiver, with a gain of approximately 8 dB.

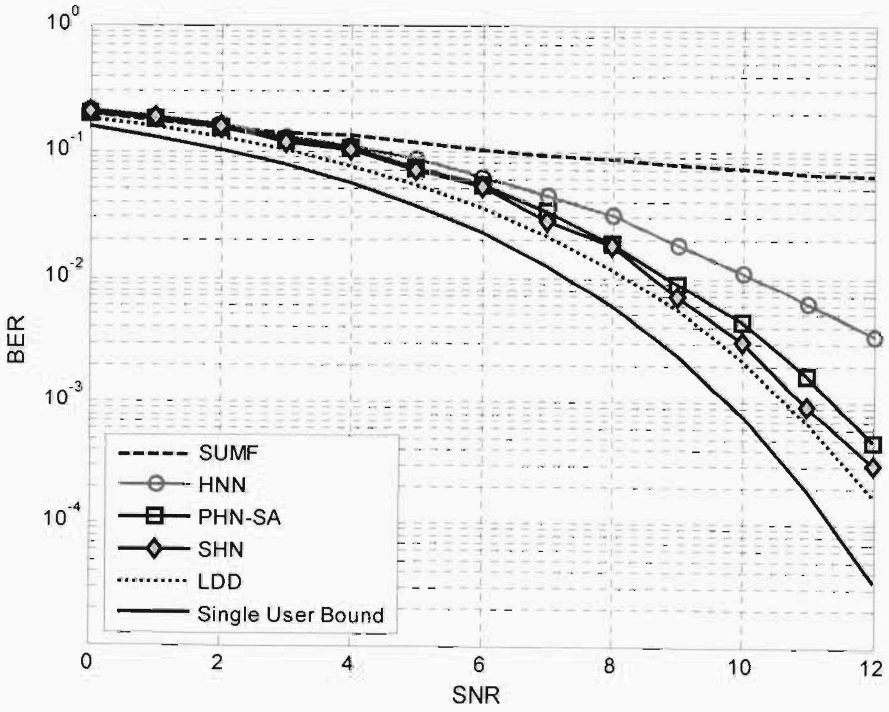

Figure 5.9 BER performance for a simulated cross-correlation of $\rho_{ij} = 0.3$, for $K = 5$ users.

The convergence characteristics of the SHN and PHN-SA were investigated, over 20 iterations, using a constant cross-correlation of $\rho_{ij} = 0.2\ (\forall i, j\,; i \neq j)$. The results are spread over two figures: Figure 5.10 (3 dB and 6 dB) and Figure 5.11 (9 dB and 12 dB). The SHN converges faster than the PHN-SA, but the BER of the PHN-SA is slightly better at higher SNR. This behaviour depends on the annealing schedule, i.e. the number of iterations required. It raises the issue of the generally slow convergence of SA, in which performance is often sacrificed for convergence time.

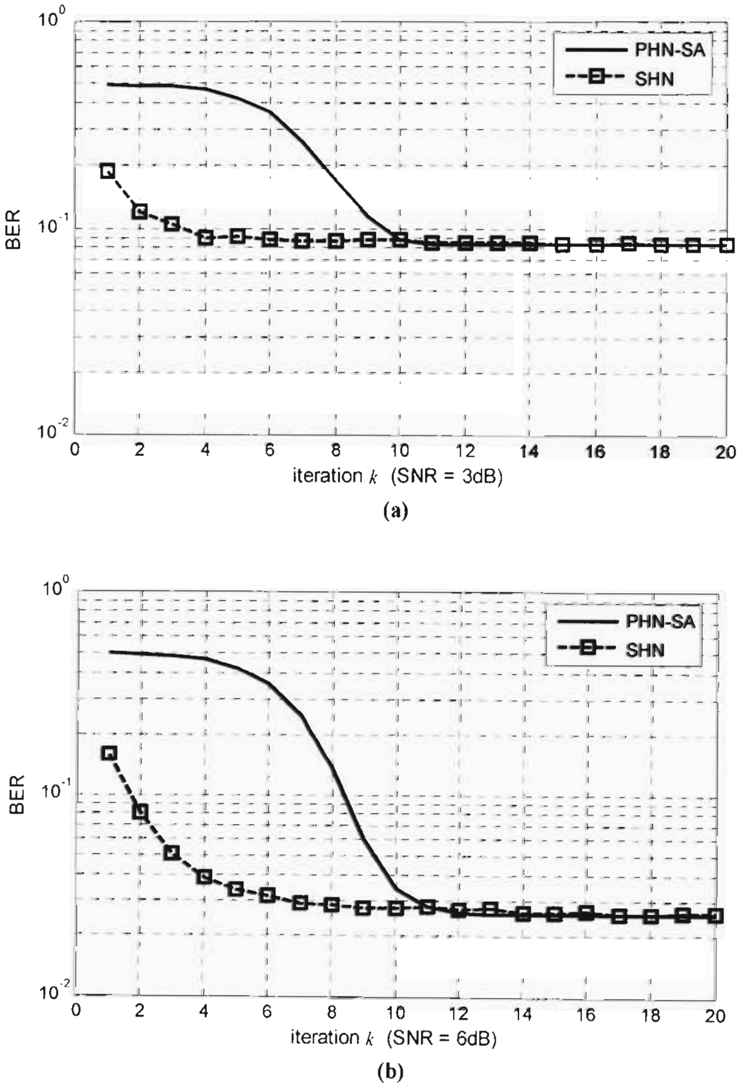

(a)

(b)

Figure 5.10 Convergence of the PHN-SA and SHN detectors over 20 iterations, shown by the BER performance of user 1 at intervals of (a) 3 dB, (b) 6 dB. $K = 5$, $\rho = 0.2\,\forall i, j\,(i \neq j)$.

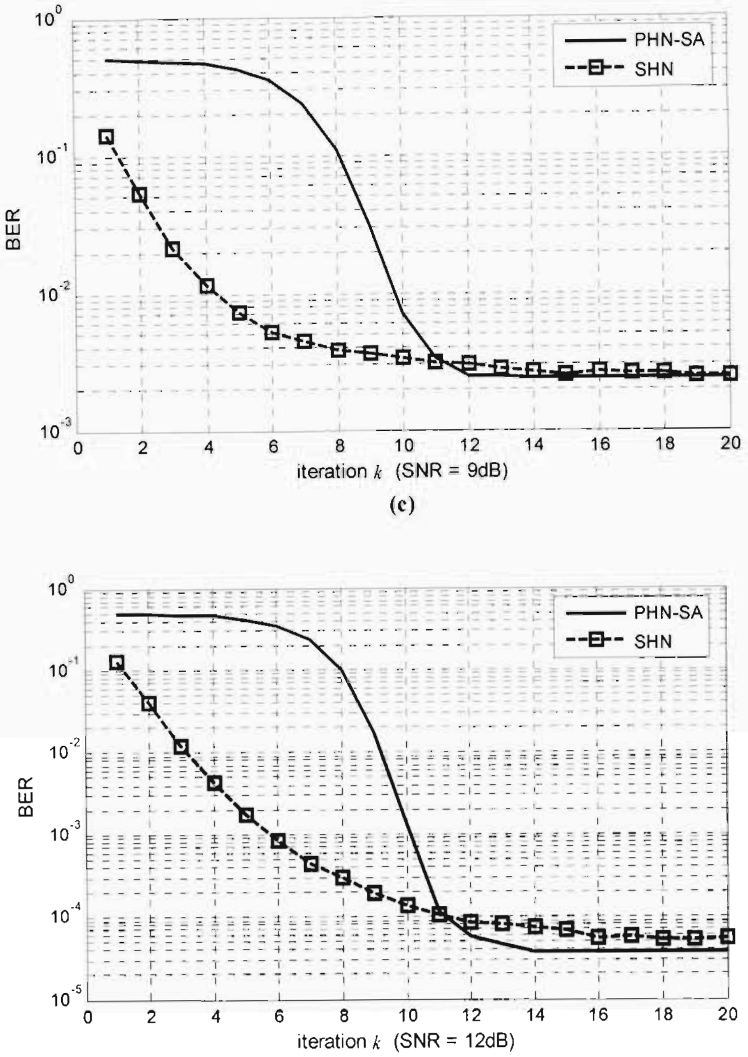

(c)

(d)

Figure 5.11 Convergence of the PHN-SA and SHN detectors over 20 iterations, shown by the BER performance of user 1 at intervals of (c) 9 dB, (d) 12 dB. $K = 5$, $\rho = 0.2\, \forall i, j\, (i \neq j)$.

In comparison, the convergence behaviour of the system in Figure 5.9, which is illustrated in Figure 5.12(a) for 30 iterations, shows that at 12 dB the BER of the SHN model is indeed better. This supports the results presented in Figure 5.9. With regards to the system simulated in Figure 5.10 and Figure 5.11, it may be concluded that the adverse effect of (high) cross-correlations is more pronounced in the PHN-SA model, which sees a greater loss in performance as compared to the SHN sub-optimal scheme. Furthermore, the PHN-SA requires a few more iterations to converge (at 12 dB).

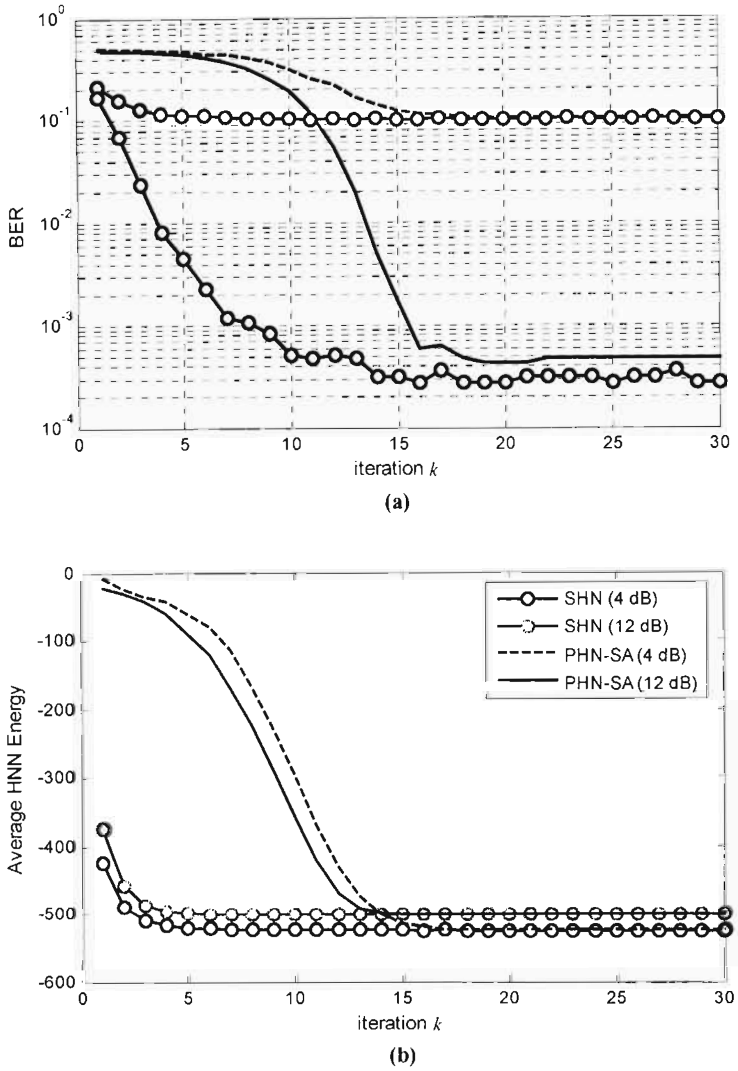

(a)

(b)

Figure 5.12 Convergence of the PHN-SA and SHN detectors over 30 iterations, shown by (a) the BER performance of user 1 and (b) the average HNN energy, at 4 dB and 12 dB. $K = 5$, $\rho = 0.3\,\forall i, j\,(i \neq j)$.

Figure 5.12(a) also illustrates the basic idea of stochastic techniques, which simply is to allow for the search (for a minimum solution) to 'move uphill' sometimes. In some steps the BER remains the same or increases, before it is reduced. These perturbations are visible in both models. Figure 5.12(b) shows the corresponding convergence of the energy function. The microscopic changes in BER are not visible in the energy function as it is not normalized. However, it enforces the point that pattern retrieval translates to finding a minimum energy (stable) state of the network.

The convergence behaviour of PHN-SA model for the 10-user asynchronous CDMA system (Figure 5.3) is investigated in Figure 5.13, which shows the performance of the best and worst user (Figure 5.5). The maximum number of iterations for the stopping criterion of the SA algorithm was set to $k_{\max} = 40$. Although that many iterations were not required, in comparison to the systems illustrated in Figure 5.10, Figure 5.11 and Figure 5.12, about 20 iterations were required for the SA process before the state of the network settled. This is expected, and may be explained in terms of a physical system. As the number of particles increase, more possible transitions may occur before equilibrium can be reached.

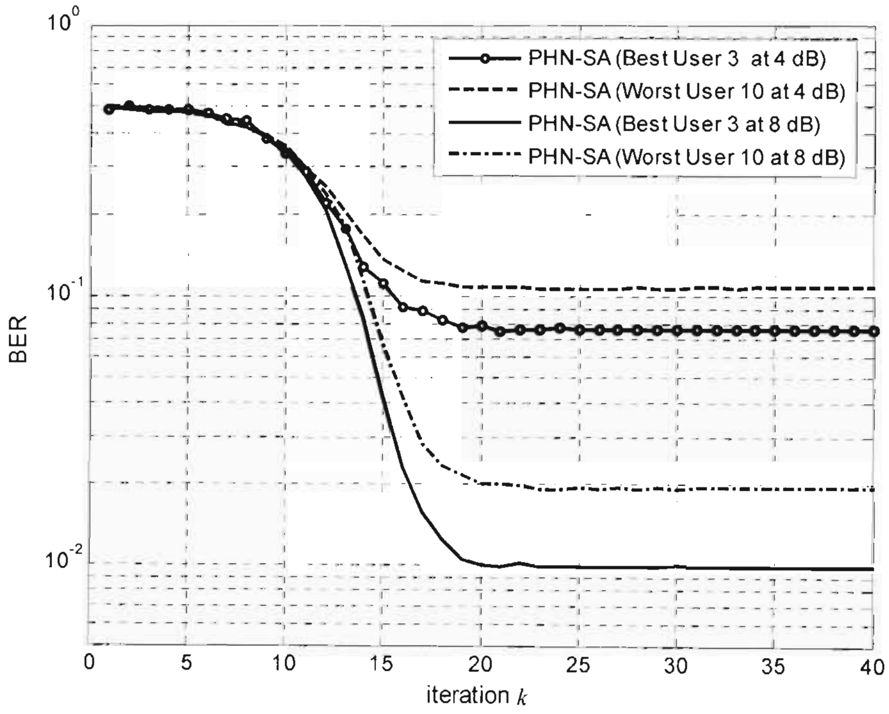

Figure 5.13 Convergence of the PHN-SA model over 40 iterations, for the 10-user asynchronous system.

A loaded (synchronous) DS-CDMA system was investigated in Figure 5.14. In the case of length-31 Gold codes this corresponds to a maximum of $K = 33$ active users. The problem of the classical HNN-based receiver is illustrated further as its performance deteriorates relative to that of the PNH-SA multiuser detector. It also indicates the additional performance gains that are possible when semi-orthogonal spreading sequences are employed as opposed to the system illustrated in Figure 5.9.

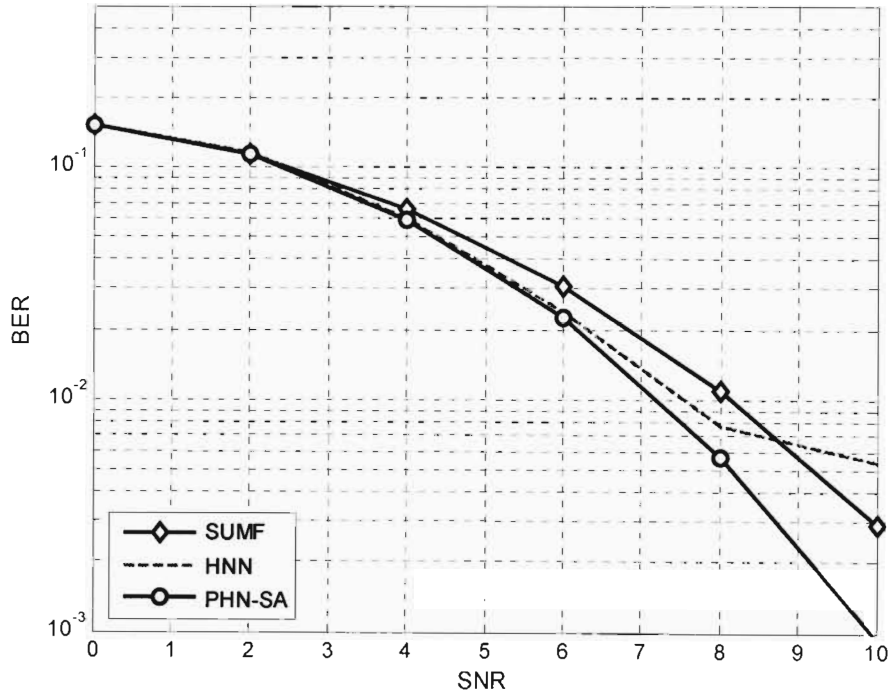

Figure 5.14 BER performance of a synchronous DS-CDMA system employing length-31 Gold codes, with $K = 33$ users.

Lastly, the BER performance of the PHN-SA model (in comparison to the SUMF detector) was investigated for a varying number of DS-CDMA users, K. Figure 5.15 illustrates the approximate BER trend (at 12 dB) as K increases. For these results, a maximum number of 10000 frames were processed, due to processing time constraints. The SUMF receiver is affected to greater degree by the increasing MAI. The results indicate that, for relatively low cross-correlations (such as those of the

Gold codes), the PHN-SA multiuser receiver is not interference limited to the extent that the SUMF receiver is limited, due to (increasing) MAI.

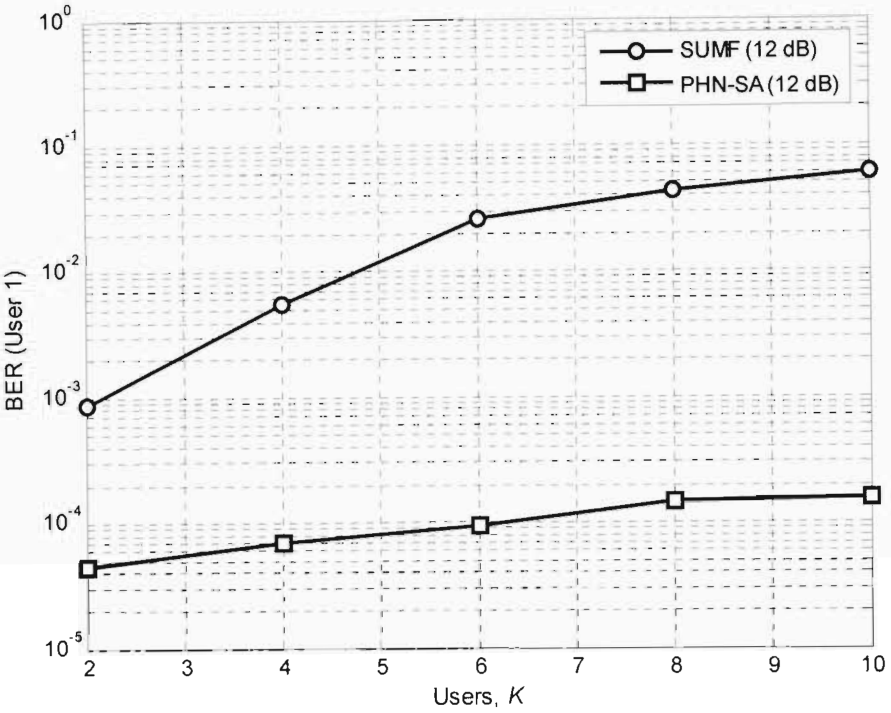

Figure 5.15 BER performance, at 12 dB, as a function of the number of users (K) in a DS-CDMA system, employing length-31 Gold codes.

5.6 Summary

In this chapter the classical HNN-based MUD architecture for the AWGN channel was presented. The mapping between the Hopfield model and the conventional receiver was given. The classical Hopfield model was investigated again, in view of statistical mechanics, and some basic principles and techniques associated with physical systems were introduced. Specifically the Metropolis algorithm and the process of annealing were discussed. These methods combine formidably to solve combinatorial optimization problems [56].

The Hopfield model suffers from localized optimization and therefore it becomes necessary to employ optimization techniques such as a stochastic global search. In neural networks that are composed of stochastic neurons, such as the popular Boltzmann machine, state transitions occur by probabilistic mechanisms. The Boltzmann machine can be thought of as a generalization of the Hopfield model with the exception of having hidden layers and being composed of stochastic neurons. The use of stochastic neurons allows for application of the simulated annealing algorithm to search for near-optimal solutions.

The approach of simulated annealing and other stochastic techniques is to deal with the problem of local minima in the HNN. The assumption that the final NN state follows a Gibbs distribution is motivated by the fact that the Gibbs distribution provides a mechanism for the characterization of the global minima [67]. The stochastic Hopfield model [33] was presented. A new strategy for multiuser detection was presented, which employs stochastic neurons and simulated annealing in order to sub-optimally detect multiple signals in an AWGN environment. It is based on the HNN-based multiuser detector and it importantly addresses the problem of local optimization in the classical HNN.

The results indicate that the proposed PHN-SA model is capable of achieving near-optimal performance in terms of the optimal single-user bound, in both synchronous and asynchronous systems. It performed better than the LDD and achieved an even higher performance gain over the SUMF detector. An interesting observation was that, although the proposed detector utilizes the outputs of the bank of matched filters, its performance is not severely compromised, unlike in the MSD. This was indicated by results for the worst and best user, in the case of SUMF detection.

The PHN-SA model was also shown to exhibit near-far resistance to a degree comparable to that of the LDD, for a range of interferer powers. With regards to addressing the issues of the classical HNN, the PHN-SA performs better than the HNN detector for high cross-correlation values (between the spreading sequences), although not as well as the SHN detector. However, while the PHN-SA offers improved performance, convergence of the simulated annealing process is typically slow and the performance of the PHN-SA is seen to be affected to a greater extent by the correlation properties of the spreading sequences, as compared to the other sub-optimal schemes.

For the larger systems $(K \geq 10)$, the PHN-SA detector outperformed the SUMF receiver and achieved near-optimal performance, in the synchronous case. Furthermore, it was shown that, for the semi-orthogonal Gold codes, the performance of the PHN-SA gradually degrades with an increasing number of users. This degradation is minimal in comparison to the performance of the SUMF detector.

6 Conclusion

Wideband DS-CDMA, alongside OFDM, is establishing itself as the one of air interfaces of choice for future generation networks. In 3G communications, it is achieving the objectives set out in IMT-2000, which is collectively aimed at enhancing the mobile user experience and providing a new level of value-added cellular services. The provision of higher data rates, greater capacity and spectrally efficient (multimedia) services is possible through advanced signal processing techniques. It is expected that future generation networks will require even faster rates and increased system capacity. Joint detection techniques such as optimum multiuser detection therefore are paramount to the success of multiuser communication systems.

6.1 Dissertation Summary

The area of this research is in the field of wireless multiuser communications, In view of the practical importance of CDMA in mobile radio networks, Chapter 1 provided an overview of 3G standards (IMT-2000) and the demands facing current and future generation networks. It provided motivation for research in the field of CDMA and the need for near-optimum joint detection techniques.

An overview of the multiple access techniques that are employed in existing (2G and 3G) networks, were discussed in Chapter 2, with emphasis on spread spectrum systems and CDMA. We discuss the advantages of spread spectrum systems (CDMA) over FDMA and TDMA systems, by investigating the basic process of transmission and reception using the different access techniques. We illustrated the process of spreading the information bandwidth using pseudorandom sequences, in DS-CDMA, via simple mathematical equations. The success of DS-CDMA relies on the use of semi-orthogonal or orthogonal spreading sequences with good (out-of-phase) auto and cross-correlation properties. Spreading sequences affects the theoretical number of users (upper limit) that can be supported, the processing gain and the amount of multiple access interference in the CDMA system. An overview of spreading sequences was provided, wherein the issue of orthogonality was discussed and a simple measure of correlation in a synchronous channel.

In Chapter 3, the topic of MUD and its associated advantages over single-user detection techniques was discussed. A vector transmission model of a DS-CDMA system was presented, for synchronous and asynchronous transmission. It is a generalized model which is applicable to fading channels as well. The conventional matched filter detector was discussed and its performance was evaluated via simulations. The poor performance in a near-far situation was illustrated. The structures of two popular sub-optimal MUD schemes, namely the LDD and the MMSE detectors were also illustrated. Their performance was compared to the conventional receiver. The performance improvement, in terms of MAI suppression and near-far resistance, is evident in the linear sub-optimal schemes and it emphasizes the need for joint detection in multiuser communications. The linear schemes are important as they constitute the benchmark to which many new sub-optimal (hybrid) schemes are compared to and in this research they are employed to determine the feasibility of the proposed neural-based MUD scheme.

The optimal multiuser detector was also described. While it achieves optimal performance and near-far resistance, the optimal objective function cannot be solved for practical DS-CDMA systems; it is an NP-hard optimization problem. However, the objective function can be mapped onto a simpler combinatorial problem, which is the basic idea behind the derivation of the Hopfield MUD scheme.

Chapter 4 introduced the topic of neural networks. It provided a historical overview of the combined field of artificial intelligence and neural networks. The basic processing unit that constitutes both feedforward and feedback networks was described. Different networks vary in functionality as a result of the various arrangements, interconnections and activation functions of the processing units that make up the networks. Networks with feedback are able to perform recursive computation and represent state information, thus they can provide considerable advantages over feedforward networks in problems which involve nonlinear state dependent systems. The Hopfield recurrent neural network is one such dynamical system which operates in an unsupervised manner. It is well suited as a platform for solving combinatorial optimization problems or as content addressable memory and has been successfully employed to solve the TSP and is commonly applied for pattern association. Notably, it has found application in several neural-based detectors. In fact, the most common neural approach to MUD uses the Hopfield model which was the emphasis of Chapter 4.

The basic Hopfield model was illustrated and its operation was described mathematically by a dynamic state transition rule. There are two basic stages to its operation, namely pattern storage, which is one-shot, and pattern retrieval. During retrieval, state updating is sequential (for the aforementioned tasks). A simple simulation was carried out for pattern retrieval where the performance of the HNN was indicated. It was also shown that the performance depends on the initial input to the network. This is a downfall of an implementation in MUD, as the network must utilize the outputs of conventional receiver.

The theory of the HNN operation is rooted in the field of statistical physics. Pattern retrieval is an optimization problem, in which the objective function is the Hopfield energy function. The search in state space results in the minimization of the energy function. Research has shown that minimization of the energy function can be mapped to the maximization of the optimal MUD object function. The chapter concluded with a discussion on stability and the capacity of the Hopfield network. Sequential updating ensures that the model converges to a stable state and the fundamental memories are retrieved under the conditions that there is no self-feedback and that the bound on the network capacity is satisfied.

Chapter 5 is the focal point of this dissertation, which combines the concepts in the previous chapters and is concerned with MUD schemes that employ neural networks, specifically the Hopfield network. A literature review of some important neural-based multiuser receivers was provided and it indicated how current research direction has evolved towards recurrent networks and the use of stochastic techniques, for MUD. The recurrent neural network serves as a post-processing stage following the conventional receiver, which is very similar to the linear detection methods. The idea behind the application of the Hopfield model is to perform the problem of optimization in an alternative and simpler manner. The parameters of the HNN were defined by finding an appropriate mapping of variables from the optimal MUD problem to the energy optimization problem in the HNN. It was shown by simple matrix manipulation that the mapping is achieved by equating the optimal objective function to the HNN energy function. The neural-based detector that is the result of this mapping suffers from localized optimization.

A detour into some basic statistical concepts was provided. Stochastic techniques help prevent local minima by perturbing the energy function. It was shown that simulated annealing, which is a stochastic search technique that is based on the Metropolis algorithm, may be employed to search for near-optimal solutions. A HNN composed of stochastic neurons was defined. These neurons simulate the effects of a pseudo-temperature in the HNN i.e. the effects of the random displacements which cause energy changes in the individual particles. The method of SA was employed to reduce the pseudo-temperature, in an efficient manner. A modified SA algorithm was proposed for the stochastic HNN-based multiuser receiver.

The simulation results for the proposed model showed that it is capable of near-optimal performance and that it is near-far resistant. In some cases it was found to outperform the linear sub-optimal detectors. Although SA can be a slow process, for the systems simulated, the PHN-SA has shown to achieve the objective of obtaining a sub-optimal MUD solution using a Hopfield RNN. By operating directly on the optimal objective function, the proposed model offers a feasible alternative to optimum MUD, through the use of stochastic techniques.

6.2 Future Work

Future work in this area of research includes the hardware implementation of the neural-based receiver, either by FPGA or VLSI implementation, so as to investigate the real-time application and feasibility of using recurrent neural networks for MUD. Analysis of the results, shown herein, could be undertaken and performance of the proposed scheme could be analyzed in fading channels.

The use of antenna arrays in 3G systems improves system capacity, quality and coverage. The research could be extended to incorporate space-time signal processing techniques. There are also issues concerning the PHN-SA model which need to be addressed first. A topic of importance is time-to-converge. This is especially a problem when the system operates in an adverse channel environment, resulting in bad cross-correlation (non-diagonal) matrices, and considering that the SA process can be very slow. In that regard, mean-field annealing techniques could be investigated to improve convergence time.

Appendix A: Spreading Sequences

Multiple access communications in a DS-CDMA system depends, to some degree, on the auto-correlation and cross-correlation properties of the noise-like spreading sequences which are employed. Spreading codes are deterministic, since they must be known to the transmitter and the intended receiver; however, they share many characteristics of random binary (antipodal) sequences. Due to their noise-like properties, they appear as random noise to non-intended receivers. Hence they referred to as pseudorandom or pseudonoise (PN) sequences.

A1. Maximal-length Sequences

PN sequences may be generated using linear feedback shift registers, which are described by generator polynomials. For a shift register composed of m stages, the maximum period of the generated sequence is $2^m - 1$. Sequences derived using primitive generator polynomials are sequences having the maximum period that can be achieved in m-stage shift register. They are known as maximal-length sequences or m-sequences, with length $N = 2^m - 1$ and are repeated periodically with period N.

If the output of the shift register is defined as $a[i] \in [0,1], i = 1,2,\ldots,N$, then for $c[i] = (-1)^{a[i]}$, a typical spreading waveform may be given by

$$s(t) = \sum_{i=1}^{N} c[i] e(t - iT_c). \tag{A1.1}$$

The properties of m-sequences give rise to a two-valued discrete normalized periodic auto-correlation defined as:

$$\rho^m(n) = \begin{cases} 1 & n = lN \\ -1/N & n \neq lN \end{cases} \tag{A1.2}$$

where l is an integer and N is the period. This is obtained from the discrete periodic auto-correlation, which is derived from the set of sequences $\{c_k[i]\}$ $\forall i \in \{1, 2, \ldots, N\}$ and $\forall k \in \{1, 2, \ldots, K\}$, given by

$$\rho_{kk}^{m}(n) = \frac{1}{N}\sum_{i=1}^{N} c_k[i]c_k[i+n], \tag{A1.3}$$

with the discrete periodic cross-correlation denoted by

$$\rho_{jk}^{m}(n) = \frac{1}{N}\sum_{i=1}^{N} c_j[i]c_k[i+n]. \tag{A1.4}$$

A quantity of measure is the peak correlation defined as the maximum of either R_a, the maximum out-of-phase auto-correlation $(n \neq 0)$, or R_c, the maximum periodic cross-correlation. It is defined as:

$$R_{\max} = \max\{R_a, R_c\} \tag{A1.5}$$

where

$$\begin{aligned} R_a &= \max\left\{\left|\rho_{kk}^{m}(n)\right|,\ \forall\ 1 \le n \le N-1\right\} \\ R_c &= \max\left\{\left|\rho_{jk}^{m}(n)\right|,\ \forall\ 0 \le n \le N-1,\ j \neq k\right\} \end{aligned} \tag{A1.6}$$

Low out-of-phase auto-correlation allows for easier sequence synchronization, while low periodic cross-correlation reduces MAI. The "goodness" of a set of K sequences with period N is obtained by comparing the optimal cross-correlation to the Welch lower bound, which is given by

$$R_{\max} \ge N\left(\frac{K-1}{NK-1}\right)^{1/2} \tag{A1.7}$$

There are a limited number of generator polynomials that result in maximal-length sequences of constant length N. The number of sequences of the same length is bounded. This bound is defined to be:

$$K \leq \frac{N-1}{m} \tag{A1.8}$$

When N is prime the number of possible sequences that may be constructed from a generator polynomial of degree m is equal to the bound.

A2. Gold Sequences

Certain pairs of m-sequences, of length N, exhibit a three-valued cross-correlation function and are known as preferred pairs. Gold codes are generated by linearly combining two preferred pairs (constructed from different generator polynomials) with different offsets. That is, given a pair of preferred sequences $\mathbf{a}_1$ and $\mathbf{a}_2$, a set of Gold sequences is obtained by taking the modulo-2 sum of $\mathbf{a}_1$ with N cyclically shifted versions of $\mathbf{a}_2$. By including the sequences $\mathbf{a}_1$ and $\mathbf{a}_2$, a set consisting of a total $N+2$ sequences results.

Gold codes have better cross-correlation properties than m-sequences and they constitute a larger set size, i.e. in comparison, the size of an m-sequence set is typically smaller than the length of the m-sequences in the set. The three-valued cross-correlation function takes on the values

$$\rho^{g}(k) \in \{-1,\ -t(m),\ t(m)-2\}\ \forall k, \tag{A1.9}$$

where

$$t(m) = \begin{cases} 2^{(m+1)/2}+1 & (\text{for odd } m) \\ 2^{(m+2)/2}+1 & (\text{for even } m) \end{cases} \tag{A1.10}$$

This also holds true for the off-peak auto-correlation function i.e. $(k \neq 0)$. Gold sequences are non-maximal length sequences; however, the peak cross-correlation magnitude is the same as that of a maximal connected set of m-sequences; a collection of m-sequences which has the property that each pair is a preferred pair is a *connected set* and the largest possible connected set is a *maximal connected set*. Besides, the comparatively large number of codes that can be generated, for a given generator polynomial these codes have constant and bounded correlation values. Although they do not have the same auto-correlation properties for phase offsets, Gold codes are a popular choice of sequences in CDMA applications for their low cross-correlation. In practical systems they are used in conjunction with orthogonal codes as scrambling sequences.

Kasami sequences constitute another family of sequences, which are constructed from preferred polynomials. Several sizes of Kasami sequence sets exist, ranging from small, large to very large set size. However, the cross-correlation values increase with the number of codes, which is unsuitable for large systems, from a performance point of view. Kasami sequences are near-optimum with respect to the Welch bound. They are also employed as scrambling codes. Orthogonal codes which have zero cross-correlation for zero delay between sequences are also employed. However, their properties deteriorate when there are offsets between the sequences. Thus they are best employed for synchronous transmission. Walsh codes are orthogonal codes which are employed in the forward link of DS-CDMA systems.

Appendix B: Gaussian Approximation in DS-CDMA Systems

Consider the derivation of the probability of bit error for a single user in the presence of $K-1$ interferers, in an asynchronous DS-CDMA system. From the central limit theorem, the summation of $K-1$ independent random variables can be modelled by the Gaussian distribution. By assuming that the MAI, due to the $K-1$ other users, is a Gaussian random variable, the probability of error (Figure B1.1) is given by

$$P_{e,k} = Q\left(\left[\frac{N_0}{E_b} + \frac{K-1}{3N}\right]^{-0.5}\right), \tag{B1.1}$$

where E_b is the bit energy, N is the processing gain, K is the number of users and N_0 is the power spectral density of zero mean AWGN with variance equal to σ^2. A Gaussian approximation such as this becomes inaccurate at relatively high SNR [14].

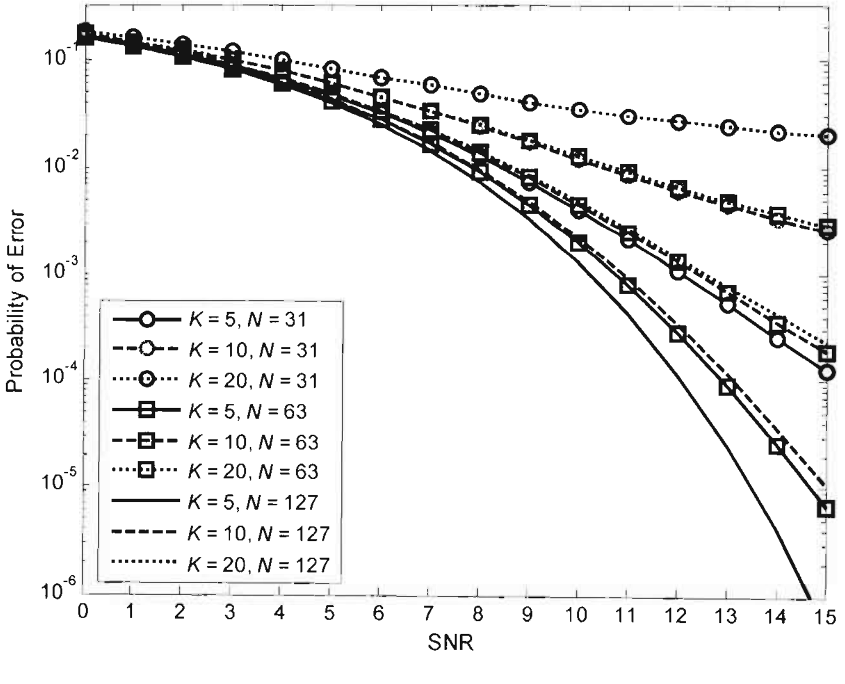

Figure B1.1 Gaussian approximations of BER achieved in a DS-CDMA system, for varying N and K.

Appendix C: The Hopfield Network

C1. Pattern Stability and Stable Points

Stability of all patterns is determined by examining the stability of a particular pattern $\xi_{u,i}$ from the set $\{\xi_{u,i}, \forall\, i = 1, 2, \ldots, \hat{M};\ u = 1, 2, \ldots, U\}$. The stability condition, generalized for the net input to neuron i and assuming no biasing, indicates that when the network converges to a stable point then

$$\operatorname{sgn}\left(\sum_{j} w_{ij}\xi_{u,j}\right) = \xi_{u,i} \tag{C1.1}$$

To prove that this is the case, consider the left term within the brackets in (C1.1). By expanding it, we arrive at

$$\begin{aligned}
\sum_{j=1} w_{ij}\xi_{u,j} &= \frac{1}{\hat{M}}\sum_{j=1}^{\hat{M}}\sum_{v=1}^{U}\xi_{v,i}\xi_{v,j}\xi_{u,j} \\
&= \xi_{u,i} + \frac{1}{\hat{M}}\sum_{j=1}^{\hat{M}}\sum_{v,v\neq u}^{U}\xi_{v,i}\xi_{v,j}\xi_{u,j} \\
&= \xi_{u,i}\left(1 + \frac{1}{\hat{M}}\sum_{j=1}^{\hat{M}}\sum_{v,v\neq u}^{U}\xi_{v,i}\xi_{u,i}\xi_{v,j}\xi_{u,j}\right)
\end{aligned} \tag{C1.2}$$

By defining the crosstalk as the second term in (C1.2), then the stability condition (C1.1) is satisfied for

$$\frac{1}{\hat{M}}\sum_{j=1}^{\hat{M}}\sum_{v,v\neq u}^{U}\xi_{v,i}\xi_{u,i}\xi_{v,j}\xi_{u,j} > -1 \tag{C1.3}$$

In that event, for all i, pattern u is stable and (C1.1) holds true. However pattern stability is also dependent on the capacity of the network, as discussed in the text.

Looking at convergence, a recurrent network with $w_{ji} = w_{ij}$, in which updating proceeds according to (C1.4) below, has stable limit points.

$$x_j(k+1) = \begin{cases} +1 & , \sum_{i=1}^{\hat{M}} w_{ji} x_i(k) + f_j > 0 \\ -1 & , \sum_{i=1}^{\hat{M}} w_{ji} x_i(k) + f_j < 0 \\ x_j(k) & , \sum_{i=1}^{\hat{M}} w_{ji} x_i(k) + f_j = 0 \end{cases} \tag{C1.4}$$

It is noted that with $w_{ji} = w_{ij}$, the energy function can be expressed as

$$E = -\frac{1}{2} \sum_{i=1}^{\hat{M}} \sum_{\substack{j=1 \\ i \neq j}}^{\hat{M}} w_{ij} x_i x_j - \sum_{j=1}^{\hat{M}} f_j x_j \tag{C1.5}$$

The existence of stable points is proven by first considering that the energy function is bounded below by x_j, with w_{ij} and f_j being constants. Secondly, the energy E is a monotonically decreasing function. This is shown by expressing the energy change ΔE due to a state change Δx_j. Since the net potential of neuron j may be written as

$$v_j = \left(\sum_{i=1, i \neq j}^{\hat{M}} w_{ij} x_i + f_j \right), \tag{C1.6}$$

the energy change is therefore given by

$$\Delta E = -\Delta x_j \left(\sum_{i=1, i \neq j}^{\hat{M}} w_{ij} x_i + f_j \right), \tag{C1.7}$$

$$\Rightarrow \Delta E = -\Delta x_j v_j . \tag{C1.8}$$

By analyzing (C1.8), it is evident that if the state of neuron j changes from $-1 \rightarrow +1 \Rightarrow v_j > 0$, then $\Delta E < 0$. This is also true if the state of neuron j changes from $+1 \rightarrow -1 \Rightarrow v_j < 0$. Otherwise, if the state of neuron j remains unchanged i.e. $\Delta x_j = 0$ then $\Delta E = 0$. This means that E is a monotonically decreasing function.

C2. Trivial Sample Calculation: Auto-association

The process of auto-association is illustrated in the HNN with the use of the relevant equations. Consider the trivial case of storing three randomly generated patterns $(U = 3)$ of dimension $\hat{M} = 7$. The fundamental memories/patterns for storage are:

$$\xi_1 = [1 \quad -1 \quad -1 \quad -1 \quad 1 \quad 1 \quad -1]$$
$$\xi_2 = [1 \quad 1 \quad -1 \quad -1 \quad -1 \quad -1 \quad -1]$$
$$\xi_3 = [1 \quad 1 \quad 1 \quad -1 \quad -1 \quad -1 \quad 1]$$

Storage of patterns is achieved by distributing the all pattern information across the synaptic weights of the weight matrix $\mathbf{W}$, which is determined by

$$\mathbf{W} = \frac{1}{\hat{M}} \sum_{u=1}^{U} \xi_u (\xi_u)^T - \frac{U}{\hat{M}} \mathbf{I}. \tag{C1.9}$$

Therefore,

$$\mathbf{W} = \frac{1}{7}\left[\xi_1(\xi_1)^T + \xi_2(\xi_2)^T + \xi_3(\xi_3)^T\right] - \frac{3}{7}\mathbf{I}_{7\times 7}$$

$$\Rightarrow \mathbf{W} = \frac{1}{7}\begin{bmatrix} 0 & 1 & -1 & -3 & -1 & -1 & -1 \\ 1 & 0 & 1 & -1 & -3 & -3 & 1 \\ -1 & 1 & 0 & 1 & -1 & -1 & 3 \\ -3 & -1 & 1 & 0 & 1 & 1 & 1 \\ -1 & -3 & -1 & 1 & 0 & 3 & -1 \\ -1 & -3 & -1 & 1 & 3 & 0 & -1 \\ -1 & 1 & 3 & 1 & -1 & -1 & 0 \end{bmatrix}$$

Assume that ξ_2 is the pattern to be retrieved. Given a noisy version of ξ_2, denoted as $\xi_{initial}$, we wish to make an association to ξ_2. Assume that $\operatorname{sgn}(\xi_{initial})$ is given by:

$$\xi_{initial} = [1 \quad -1 \quad 1 \quad -1 \quad -1 \quad 1 \quad -1]$$

The initial state of the HNN is therefore $\mathbf{x}''(0) = \xi_{initial}$. Using the update procedure:

$$x_j(k+1) = \operatorname{sgn}\left(\sum_{i=1}^{\hat{M}} w_{ji} x_i(k)\right), \qquad \text{(C1.10)}$$

each neuron $\{j = 1, 2, \ldots, 5\}$ is chosen to be updated. For simplicity, updating is done consecutively, although normally, neurons are chosen randomly. In this case only two iterations in the procedure are required. The states of the neurons per iteration are tabulated below:

Table C1.1 Neuron State Table, derived using (C1.10).

	$k=0$	$k=1$	$k=2$
x_1''	1	1	1
x_2''	−1	1	1
x_3''	1	−1	−1
x_4''	−1	−1	−1
x_5''	−1	1	−1
x_6''	1	−1	−1
x_7''	−1	−1	−1

Appendix D: The Logistic Distribution

The logistic distribution function is defined as

$$F(x)=\frac{1}{1+\exp\left(-\frac{x-a}{b}\right)} \qquad \text{(D1.1)}$$

where $-\infty < x < \infty$, a is the location parameter (which is also the mean) and b is the scale parameter. a defines the abscissa of a location point (midpoint) of the range, while b is the scale of measurement of the quantile x [69]. The variance is given by $\pi^2 b^2/3$. The standard logistic function may be denoted by $\boldsymbol{X}:0,1$. The distribution function is shown in Figure D1.1, for different scale parameter values. In the case of the stochastic neuron model, which utilizes the logistic function, the trend in the graph (function) is as a result of the value of the pseudo-temperature.

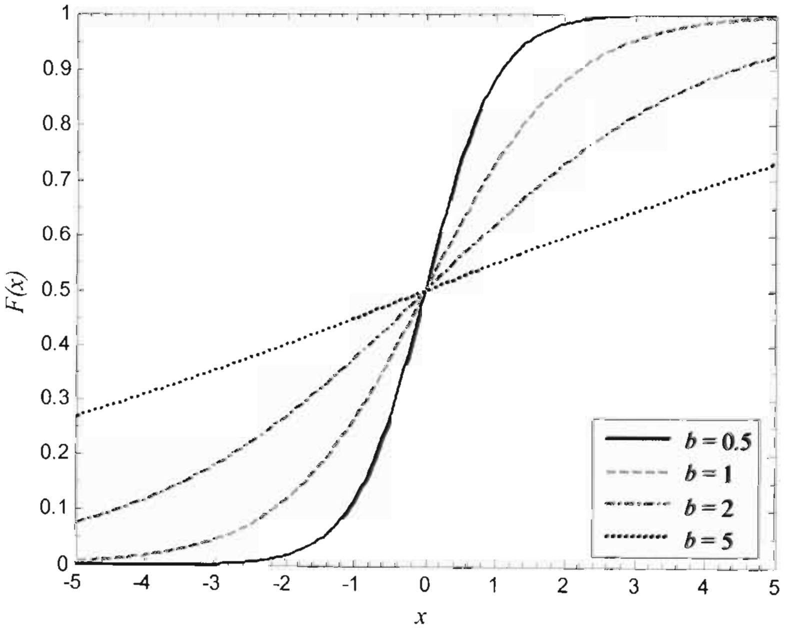

Figure D1.1 Logistic distribution function $(a=0)$.

The probability density function (Figure D1.2) of the logistic distribution is given by:

$$f(x) = \frac{\exp\left(-\frac{x-a}{b}\right)}{b\left[1+\exp\left(-\frac{x-a}{b}\right)\right]^2} \tag{D1.2}$$

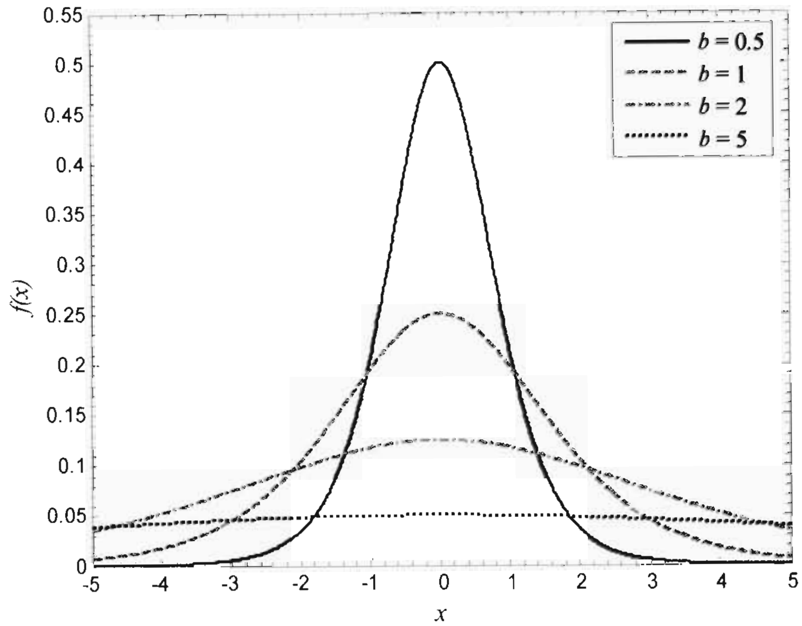

Figure D1.2 Logistic probability density function $(a = 0)$.

For simulation purposes, a transformation from the rectangular (uniform) variate is often useful for obtaining random numbers of a variate X. By generating random numbers of the standard rectangular variate $\boldsymbol{R}$ with distribution $F_R(x) = x$ [69], then random numbers of the logistic variate X: a, b may be generated using the relation

$$X : a, b \sim a + b\log\left[\frac{\boldsymbol{R}}{1-\boldsymbol{R}}\right] \tag{D1.3}$$

In the Matlab® environment random numbers from $\boldsymbol{R}$ are generated using the *rand* function, so the generation of random numbers from X is a straightforward task.

Appendix E: Software Documentation

The DS-CDMA system, in terms of transmission and reception (including single user and multiuser detection) was simulated in Matlab®, for performing matrix computations. Basic built-in functions were used for random number generation, matrix inversion (and other matrix functions), and convolution. User-defined functions were used to perform certain tasks in the DS-CDMA model, such as PN sequence generation and computation of the correlation matrix. All user-defined functions are briefly outlined in the proceeding sections of this appendix.

E1. Simulation Parameters

The simulation environment utilized length-31 Gold codes, constructed from a pair of preferred sequences [16]. For the calculation of one data point (i.e. a single SNR value), a Monte Carlo type simulation was employed to obtain a statistical average. For the DS-CDMA system, a constant frame length of 100 bits was employed with constant error-checking criterion, however the number of frames that was transmitted per SNR was limited to 20000 due to the overhead incurred in the processing time.

E2. Simulation Files

Four m-files were employed. The first m-file, "CDMA_MUD.m", simulates the DS-CDMA system and performs linear sub-optimal MUD. The second group of three m-files, "NN_MUDP.m", "NN_MUDS.m", "NN_MUDH.m", collectively simulates the three neural-based MUD (PHN-SA, SHN and HNN) schemes. Except for the model, the three neural-based m-files have the same structure. Thus only "NN_MUDP.m" will be discussed. The user-defined functions that are employed in each file are briefly described, in the order that they are used. The actual usage of these functions is provided in the software. The main parameters (variables) required for the simulation are also listed (as they appear in the m-files).

E2.1 CDMA_MUD.m

This file simulates the DS-CDMA model (described in Chapter 3), encapsulating the transmission and reception of *K* DS-CDMA signals. It performs SUMF detection, and implements the LDD and MMSE schemes. The workspace, which contains all the defined variables, is saved in a MAT-file©. The transmitted data and the outputs of the bank of matched filters, for a single iteration, are saved to text files. The stored data is required for the simulation of the neural-based schemes.

The main variables and primary user-defined functions are listed below. Variables K, M and N are defined globally since they are used in several functions. Hence they do not need to be passed during a call to a function. Other user-defined functions which are not used directly in "CDMA_MUD.m" are explained in the code.

Defining Variables

`K`	Number of users
`M`	Frame length (number of transmitted bits)
`N`	Processing gain $(\mathrm{N} = 31)$
`minSNR`	Minimum signal-to-noise ratio
`maxSNR`	Minimum signal-to-noise ratio
`interval`	Interval (in dB) between each successive SNR
`nIterations`	Maximum number of iterations that may be processed at a single SNR value.
`minError`	A vector containing the minimum number of errors that must occur at each SNR.

User-defined Functions

`NewDirName()`	Creates a name string for the directory that the workspace and text files are saved to.
`GoldCodeGeneration()`	Generates K length-N Gold codes $(K \leq N+2)$.
`CodesToTransmit()`	Normalizes the spreading codes and incorporates the delays of each user, for (asynchronous) simulated transmission.
`CorrelationMatrix()`	Generates a $KM \times KM$ (Toeplitz) matrix of auto and cross-correlations between pairs of users, for each bit interval.
`TheoreticalBounds()`	Computes some of the theoretical error probability bounds for comparison purposes.
`ConvertTime()`*	Processes the elapsed time to determine the length of time for the simulation to run.
`DateStamp()`*	Creates a string of date and time, for the name of the MAT-file that the workspace is saved to.

E2.2 NN_MUDP.m

This file contains the code for the simulation of the PHN-SA detection scheme. It is representative of the post-processing block in a typical neural-based multiuser detector (Figure 5.1) because it processes the information from the matched filter receiver of the DS-CDMA system. Since two separate files are employed, this file cannot run without first running "CDMA_MUD.m". It requires the simulation results of the DS-CDMA system to perform the appropriate mapping of variables (in Section 5.2) to define the HNN; this includes knowing the size of the DS-CDMA system, the soft outputs of the bank of matched filters, all users amplitudes and the

* These are general functions which are also employed in "NN_MUDP.m".

correlation matrix. In addition, it also uses some of the variables defined in "CDMA_MUD.m". The required data is loaded (automatically) from the MAT-file containing the CDMA workspace and the text files containing the transmitted and demodulated data, directly after "CDMA_MUD.m" is run or the required directory and MAT-file can be entered manually. The results of the neural network simulation are saved to a separate MAT-file.

The key parameters and user-defined functions are listed below, as they appear in the m-file. Parameters which are defined as a result of the mapping to the DS-CDMA system are listed as predefined variables, as there is no direct input by the user. All NN models are located in this one m-file; there are no function calls to these models.

Defining Variables	
`nnIt`	Number of iterations for updating the HNN
`Ynn`	$KM \times 1$ column vector of current neuron states of the HNN (initialized to a zero vector)
`lambda`	Annealing/Cooling constant
`T0`	Initial pseudo-temperature

Predefined Variables	
`nNeurons`	Number of neurons (equal to $K \times M$)
`W`	Weight matrix, given by $\mathbf{W} = -(\mathbf{R} - \text{diag}\mathbf{R})$
`Vnn`	Vector of bias terms of the HNN (equal to the $KM \times 1$ vector of matched filter outputs, $\mathbf{y}$)
`Frames`	A vector containing the number of iterations processed at each SNR in the DS-CDMA simulation

User-defined Variables	
`Logistic()`	Generates random numbers from the logistic distribution.

References

[1] ITU (2005, Dec.). *ICT Statistics*. [Online]. Available:
http://www.itu.int/ITU-D/ict/statistics/ict/
(Last Accessed 2006/01/09)

[2] GSMA/Wireless Intelligence. (2005, Dec.). *GSM Association Statistics Q3 2005*. [Online]. Available:
http://www.gsmworld.com/news/statistics/pdf/gsma_stats_q3_05.pdf
(Last Accessed 2006/01/09)

[3] CDMA Development Group. (2005, Sept.). *CDG: Worldwide: 3Q 2005 CDMA Subscribers Statistics*. [Online]. Available:
http://www.cdg.org/worldwide/cdma_world_subscriber.asp
(Last Accessed 2006/01/09)

[4] UMTS Forum. (2004, June). *Benefits of Mobile Communications for the Society*. UMTS Forum Report 36. [Online]. Available:
http://www.umts-forum.org/servlet/dycon/ztumts/umts/Live/en/umts/Resources
_ Reports_36_index
(Last Accessed 2006/01/09)

[5] T. Ojanperä and R. Prasad, "An overview of air interface multiple access for IMT-2000/UMTS," *IEEE Communications Magazine*, vol. 36, no. 9, pp. 82–86, Sept. 1998.

[6] L. B. Milstein, "Wideband code division multiple access," *IEEE Journal on Selected Areas in Communications*, vol. 18, no. 8, pp. 1344–1354, Aug. 2000.

[7] S. Verdú, "Minimum probability of error for asynchronous Gaussian multiple-access channels," *IEEE Transactions on Information Theory*, vol. 32, no. 1, pp 85–96, Jan. 1986.

[8] S. Haykin, "Adaptive Systems for Signal Process," in *Advanced Signal Processing* Handbook, S. Stergiopoulos, Ed. Boca Raton, Fl. : CRC Press LLC, 2001, ch. 2.

[9] G. I. Kechriotis, E. Zervas, and E. S. Manolakos, "Using recurrent neural networks for adaptive communication channel equalization," *IEEE Transactions on Neural Networks*, vol. 5, no. 2, pp. 267–278, March 1994.

[10] J. J. Hopfield and D. W. Tank, "Neural computation of decisions in optimization problems," *Biological Cybernetics*, vol. 52, no. 3, pp. 141–152, July 1985.

[11] B. Aazhang, B. -P. Paris, and G. C. Orsak, "Neural networks for code-division multiple-access communications," *IEEE Transactions on Communications*, vol. 40, no. 7, pp. 1212–1222, July 1992.

[12] P. Nicopolotidis, M. S. Obaidat, G. I. Papadimitriou, and A. S. Pomportsis, *Wireless Networks*. Chichester, UK: John Wiley & Sons, 2003.

[13] H. Sari, F. Vanhverbeke, and M. Moeneclaey, "Extending the capacity of multiple access channels," *IEEE Communications Magazine,* vol. 38, no. 1, pp. 74–82, Jan. 2000.

[14] S. Verdú, *Multiuser Detection.* New York, NY: Cambridge University Press, 1998.

[15] T. Ojanperä and R. Prasad, *Wideband CDMA for Third Generation Mobile Communications*. Norwood, MA: Artech House, 1998.

[16] J. G. Proakis, *Digital Communications*, 4th ed., New York, NY: McGraw-Hill, 2001.

[17] M. D. Yacoub, *Foundations of Mobile Radio Engineering.* Boca Raton, Florida: CRC Press, 1993.

[18] S. Verdú, "Optimum multiuser asymptotic efficiency," *IEEE Transactions on Communications*, vol. 34, no. 9, pp. 890–897, Sept. 1986.

[19] S. Verdú, "Wireless bandwidth in the making," *IEEE Communications Magazine*, vol. 38, no. 7, pp. 53–58, July 2000.

[20] S. Moshavi, "Multi-user detection for DS-CDMA communications," *IEEE Communications Magazine*, vol. 34, no. 10, pp. 126–133, October 1996.

[21] D. Koulakiotis and A. H. Aghvami, "Data detection techniques for DS/CDMA mobile systems: A review," *IEEE Personal Communications*, vol. 7, no. 3, pp. 24–30, June 2000.

[22] S. Verdú, "Adaptive multiuser detection," in Proc. *IEEE International Symposium on Spread Spectrum Techniques and Applications (*ISSSTA'94), Oulu, Finland, July 1994, vol. 1, pp. 43–50.

[23] U. Madhow, "Blind adaptive interference suppression for direct-sequence CDMA", *Proc. of the IEEE,* vol. 86, no. 10, pp. 2049–2069, Oct. 1998

[24] M. Honig, U. Madhow and S. Verdù, "Blind adaptive multiuser detection," *IEEE Transactions on Information Theory*, Vol. 41, No. 4, pp. 944–960, July 1995.

[25] A. Dua, "MPOE based multiuser detection for DS-CDMA communications," M.Tech. Thesis, Department of Electrical Engineering, Indian Institute of Technology, Powai, Mumbai, India, 2002.

[26] J. B. Whitehead, "Space-time multiuser detection of multi-carrier DS-CDMA systems," M.Sc. Thesis, School of Electrical and Electronic Eng., University of Natal, Durban, KZN, SA, 2001.

[27] P. van Rooyen, M. Lötter, and D. van Wyk, *Space-Time Processing for CDMA Mobile Communications*. Norwell, MA: Kluwer Academic Publishers, 2000.

[28] R. Lupas and S. Verdú, "Linear multiuser detectors for synchronous code-division multiple-access channels," *IEEE Trans. Inform. Theory*, vol. 35, no, 1, pp. 123–136, Jan. 1989.

[29] H. V. Poor and S. Verdú, "Single-user detectors for multiuser channels," *IEEE Transactions on Communications*, vol. 36, no. 1, pp. 50–60, Jan. 1988.

[30] J. Lindner, "MC-CDMA and its relation to general multiuser/multi-subchannel transmission systems," in *Proc. IEEE 4th International Symposium on Spread Spectrum Techniques and Applications Proceedings (ISSSTA'96)*, Mainz, Germany, Sept. 1996, vol. 1, pp. 115–121.

[31] J. Lindner, "MC-CDMA in the context of general multiuser/multi-subchannel transmission methods," *European Transactions on Telecommunications*, vol. 10, no. 4, pp. 351-367, July/August 1999.

[32] W. G. Teich and M. Seidl, "Code division multiple access communications: multiuser detection based on a recurrent neural network structure," in *Proc.*

IEEE 4th International Symposium on Spread Spectrum Techniques and Applications (ISSSTA'96), Mainz, Germany, Sept. 1996, vol. 3, pp. 979–984.

[33] G. Jeney, S. Imre, L. Pap, A. Engelhart, T. Dogan, and W. G. Teich, "Comparison of different multiuser detectors based on recurrent neural networks," in *Proc. COST 262 Workshop on Multiuser Detection in Spread Spectrum Communications*, Reisensburg, Germany, Jan. 2001, pp. 61–70.

[34] G. Jeney, J. Levendovszky, S. Imre, and L. Pap, "Comparison of different neural network based multi-user detectors," presented at EUNICE 2000 (Open European Summer School), Enschede, Netherlands, Sept. 13–15, 2000.

[35] A. Duel-Hallen, J. Holtzman, and Z. Zvonar, "Multiuser detection for CDMA systems," *IEEE Personal Communications*, vol. 2, no. 2, pp. 46–58, Apr. 1995.

[36] R. Lupas and S. Verdú, "Near-far resistance of multiuser detectors in asynchronous channels," *IEEE Transactions on Communications*, vol. 38, no, 4, pp. 496–508, April 1990.

[37] H. V. Poor and S. Verdú, "Probability of error in MMSE multiuser detection," *IEEE Trans. Inform. Theory*, vol. 43, no. 3, pp. 858–871, May 1997.

[38] S. Haykin, *Neural Networks: A Comprehensive Foundation*, 2nd ed., Upper Saddle River, New Jersey: Prentice-Hall, 1999.

[39] P. Peretto, *An Introduction to the Modeling of Neural Networks*. Cambridge, UK: Cambridge University Press, 1992.

[40] J. Hertz, A. Krogh, and R.G. Palmer, *Introduction to the Theory of Neural Computation*. Redwood City, CA: Addison-Wesley, 1991.

[41] M. K. Varanasi and B. Aazhang, "Multistage detection in asynchronous code-division multiple-access communications," *IEEE Transactions on Communications*, vol. 38, no. 4, pp. 509–518, April 1990.

[42] U. Mitra and H. V. Poor, "Neural network techniques for multi-user demodulation," in *Proc. IEEE International Conference on Neural Networks*, San Francisco, CA, March/April 1993, vol. 3, no. 9, pp. 1538–1543.

[43] U. Mitra and H. V. Poor, "Neural network techniques for adaptive multiuser demodulation," *IEEE Journal on Selected Areas in Communications*, vol. 12, no. 9, pp. 1460–1470, Dec. 1994.

[44] U. Mitra and H. V. Poor, "Adaptive receiver algorithms for near-far resistant CDMA," *IEEE Transactions on Communications*, vol. 43, no. 234, pp. 1713–1724, Feb./Mar./Apr. 1995.

[45] T. Miyajima, T. Hasegawa, and M. Haneishi, "On the multiuser detection using a neural network in code-division multiple-access communications," *IEICE Trans. Communications*, vol. E76-B, no. 8, pp. 961–968, Aug. 1993.

[46] T. Nagaosa, T. Miyajima and T.Hasegawa, "On the multiuser detection using a Hopfield network in M-ary/SSMA communications," in *Proc. PIMRC '94,* The Hague, Netherlands, Sept. 1994, vol. 2, pp. 420–424.

[47] G. I. Kechriotis and E. S. Manolakos, "Hopfield neural network implementation of the optimal CDMA multiuser detector," *IEEE Transactions on Neural Networks*, vol. 7, no. 1, pp. 131–141, Jan. 1996.

[48] S. H. Yoon and S. S. Rao, "Multiuser detection in CDMA based on the annealed neural network," presented at IEEE International Conference on Neural Networks, Washington DC, USA, June 3–6, 1996.

[49] S. S. Yoon and S. S Rao, "High performance neural network based multiuser detector in CDMA," in *Proc. IEEE International Conference on Acoustics, Speech, and Signal Processing (ICASSP'97),* Munich, Germany, April 1997 vol. 4, pp. 3357–3360.

[50] S. H. Yoon and S. S. Rao, "Annealed neural network based multiuser detector in code division multiple access communications", *IEE Proceedings on Communications*, vol. 147, no. 1, pp. 57–62, Feb. 2000.

[51] A. Engelhart, W. G. Teich, J. Lindner, G. Jeney, S. Imre, and L. Pap, "A survey of multiuser/multi-subchannel detection schemes based on recurrent neural networks," *Wireless Communications and Mobile Computing*, vol. 2, no. 3, pp. 269–284, May 2002.

[52] F. Carlier, F. Nouvel, and J. Citerne, "Multi-user Detection for CDMA Communications Based on Self Organized neural network structures," in *Proc. First IEEE International Workshop on Electronic Design, Test and Applications (DELTA'02)*, Christchurch, NZ, Jan. 2002, pp. 52–56.

[53] A. Hottinen, "Self-organizing multiuser detection," in *Proc. IEEE International Symposium on Spread Spectrum Techniques and Applications (ISSSTA '94)*, Oulu, Finland, July 1994, vol. 1, pp. 152–156.

[54] N. Moodley and S. H. Mneney, "Recurrent neural network techniques for multiuser detection," in *Proc. IEEE AFRICON 2004*, Gaborone, Botswana, Sept. 2004, vol. 1, pp. 89–94.

[55] J. J. Hopfield, "Neural networks and physical systems with emergent collective computational abilities," *Proceedings of the National Academy of Sciences of the United States of America*, vol. 79, no. 8, pp. 2554–2558, April 1982.

[56] S. Kirkpatrick, C. D. Gelatt, Jr., and M. P. Vecchi, "Optimization by simulated annealing," *Science*, vol. 220, no. 4598, pp. 671–680, May 1983.

[57] J. J. Steil, "Input-output stability of recurrent neural networks," Ph.D. Thesis, The Technical Faculty, University of Bielefeld, Bielefeld, Germany, 1999.

[58] J. J. Hopfield, "Neurons with graded response have collective computational properties like those of two-state neurons," *Proceedings of the National Academy of Sciences*, vol. 81, no. 10, pp. 3088–3092, May 1984.

[59] K. A. Smith, "Neural network for combinatorial optimization: a review of more than a decade of research," *INFORMS Journal on Computing*, vol. 11, no. 1, pp. 15–34, (Winter) 1999.

[60] G. I. Kechriotis and E. S. Manolakos, "A hybrid digital signal processing-neural network CDMA multiuser detection scheme," *IEEE Transactions on Circuits and Systems II: Analog and Digital Signal Processing*, vol. 43, no. 2, pp. 96–104, Feb. 1996.

[61] W. G. Teich, M. Seidl and M. Nold, "Multiuser detection for DS-CDMA communication systems based on recurrent neural network structures," in *Proc. IEEE 4th International Symposium on Spread Spectrum Techniques and Applications (ISSSTA '98)*, Sun City, South Africa, Sept. 1998, vol. 3, pp. 863–867.

[62] B. Wang, J. Nie, and Z. He, "A transiently chaotic neural-network implementation of the CDMA multiuser detector," *IEEE Transactions on Neural Networks*, vol. 10, no. 5, pp. 1257–1259, Sept. 1999.

[63] G. Jeney, J. Levendovszky, and L. Kovács, "Blind adaptive stochastic neural network for multiuser detection," in *Proc. Vehicular Technology Conference 2001*, Rhodes Island, Greece, May 2001, vol. 3, pp. 1868–1872.

[64] J. J. Hopfield, "Artificial neural networks," *IEEE Circuits and Devices Magazine*, vol. 4, no. 5, pp. 3–10, Sept. 1988.

[65] E. Aarts and J. Korst, Simulated Annealing and Boltzmann Machines: A Stochastic Approach to Combinatorial Optimization and Neural Computing. Chichester, UK: John Wiley & Sons, 1990.

[66] S. B. Gelfand and S. K. Mitter, "Simulated annealing," in *Stochastics in Combinatorial Optimization*, G. Andreatta, F. Mason, P. Serafini, Ed. Singapore: World Scientific, 1987, pp. 2–51.

[67] L. Ingber, "Simulated annealing: Practice versus theory," *J. Math. Comput. Modelling*, vol. 18, no. 11, pp. 29–57, Dec. 1993.

[68] V. Pavlović, D. Schonfeld and G. Friedman, "Enhancement of Hopfield neural networks using stochastic noise processes," presented at IEEE Signal Processing Society Workshop on Neural Network for Signal Processing (NNSP), Falmouth, MA, September 10–12, 2001.

[69] M. Evans, N. Hastings, and B. Peacock, *Statistical Distributions*, 2nd ed., New York, NY: John Wiley & Sons, 1993.

Bibliography

[1] R. C. de Lamare and R. Sampaio-Neto, "An approximate minimum BER approach to multiuser detection using recurrent neural networks," in *Proc. 13th IEEE International Symposium on Personal, Indoor and Mobile Radio Communications (PIRMC'02)*, Lisbon, Portugal, Sept. 2002, vol. 3, pp. 1295–1299.

[2] A. Ephremides, "The use of neural networks in optimization problems in communication networks," in *Proc. IEEE Colloquium in South America*, Argentina/Brazil/Chile, Aug./Sept. 1990, pp. 66–70.

[3] W. C. Y. Lee, "Overview of cellular CDMA," *IEEE Transactions on Vehicular Technology,* vol. 40, no. 2, pp. 291–302, May 1991.

[4] T. K. Sarkar, H. Schwarzlander, S. Choi, M. S. Palma, and M. C. Wicks, "Stochastic versus deterministic models in the analysis of communication systems," *IEEE Antennas and Propagation Magazine*, vol. 44, no. 4, pp. 40–50, Aug. 2002.

[5] X. -S. Zhang, *Neural Networks in Optimization.* Dordrecht, Netherlands: Kluwer Academic Publishers, 2000.